The 1st Setouchi Neutrino Workshop

Teshima, Japan
August 20th – 21st

Exploring the Fate of Massive Stars with Diffuse Supernova Neutrino Background

Yosuke Ashida[1], Ken'ichiro Nakazato[2], Takuji Tsujimoto[3]

[1]Department of Physics and Astronomy, University of Utah
[2]Faculty of Arts and Science, Kyushu University
[3]National Astronomical Observatory of Japan

Introduction

Stellar Core Collapse

- Massive stars (>8M_{Sun}) cause **gravitational collapse of the core** at the end of their life.
  - One of the most dynamic phenomena in the Universe (energy ~10^{53} erg).
  - Play an important role in cosmic chemical evolution.
- Multiple patterns are possible after core collapse.
  - In a successful case, a neutron star is produced afterwards, and the explosion is optically observable.
  - Otherwise, a black hole is produced and not possible to be optically observed (failed SN).
  - **Neutrinos** are emitted from both cases and play an important role in the mechanism.

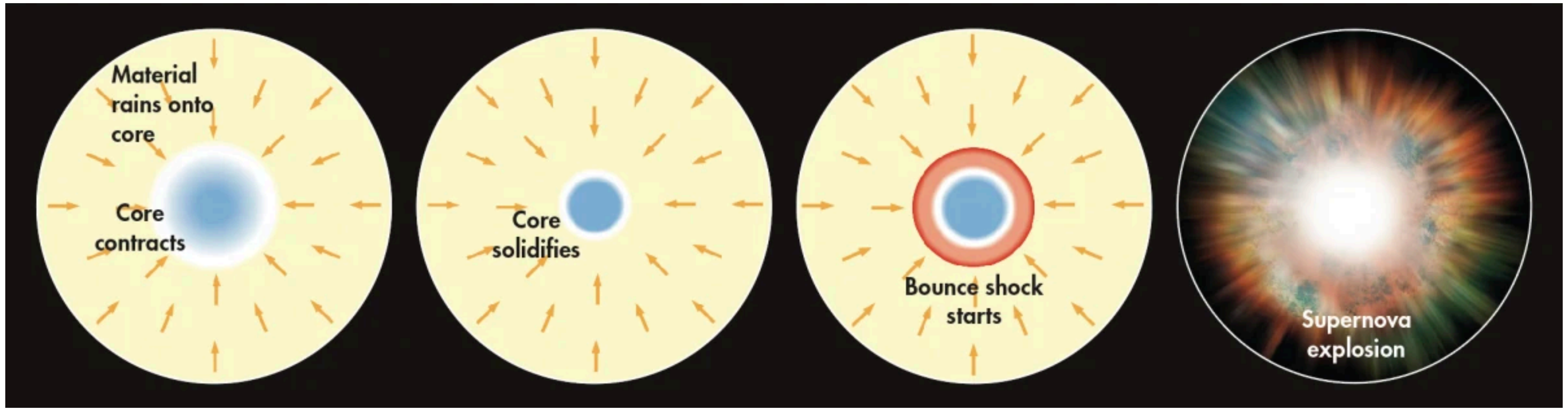

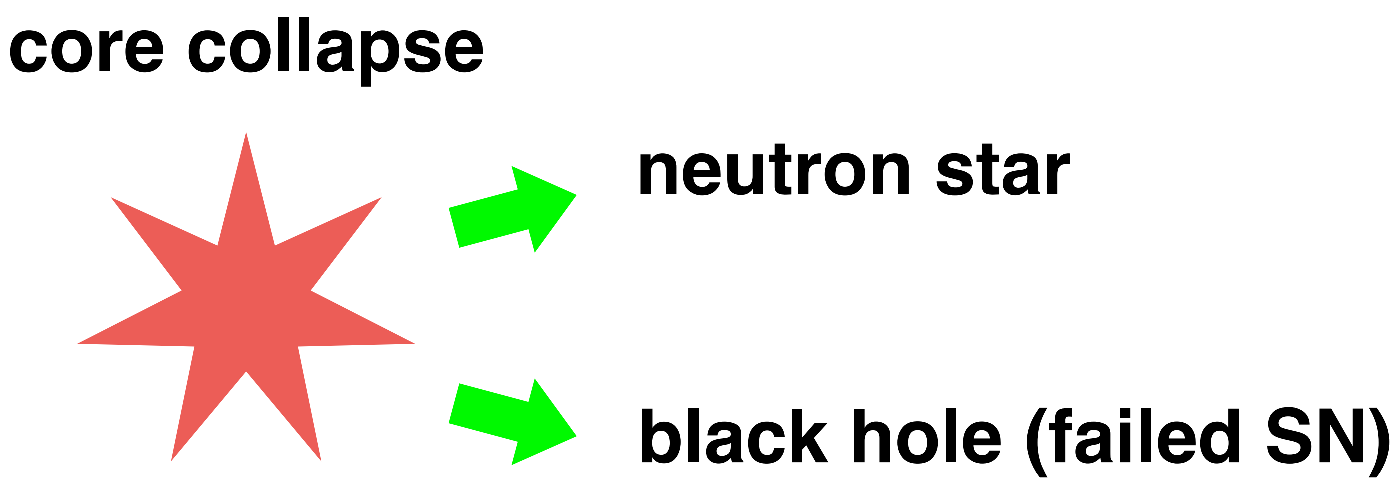

Neutrino Emission in Collapse Process

K. Nakazato et al., ApJ Suppl. 205, 2 (2013)

accretion phase

- Both **NS** and **BH** cases
- Longer accretion for BH case
- Mainly ν_e and anti-ν_e
- Higher energy

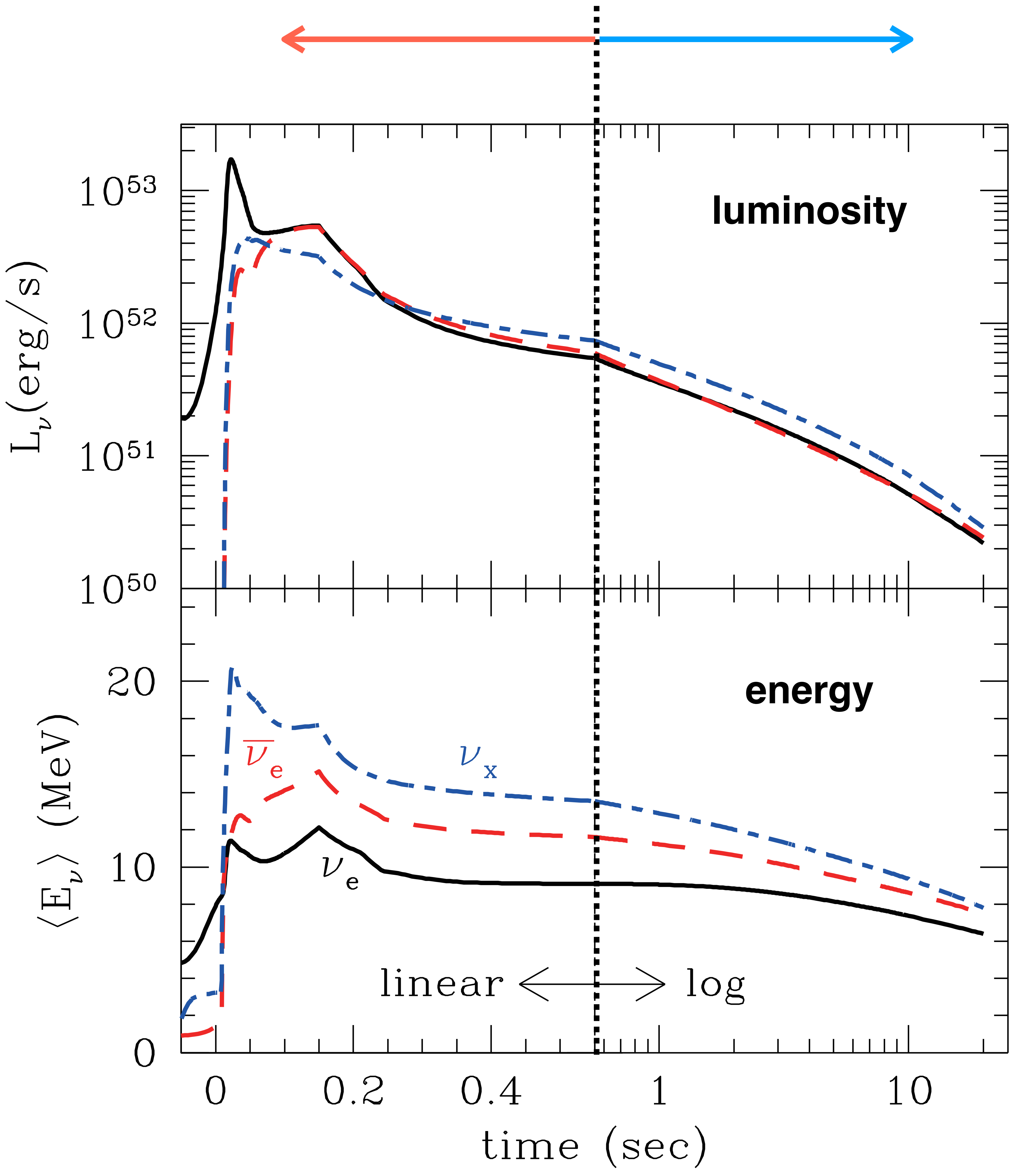

cooling phase

- Only **NS** case
- Large integrated flux
- All flavors
- Lower energy

Observation of Supernova Neutrinos

So far only *one* observation of supernova neutrinos (**SN1987A**).

- Low supernova rate (~a few times/century/galaxy)
- Small neutrino cross section
- *~10 neutrino* events expected, for a *Mpc* far SN, even at a *Mton*-size detector.

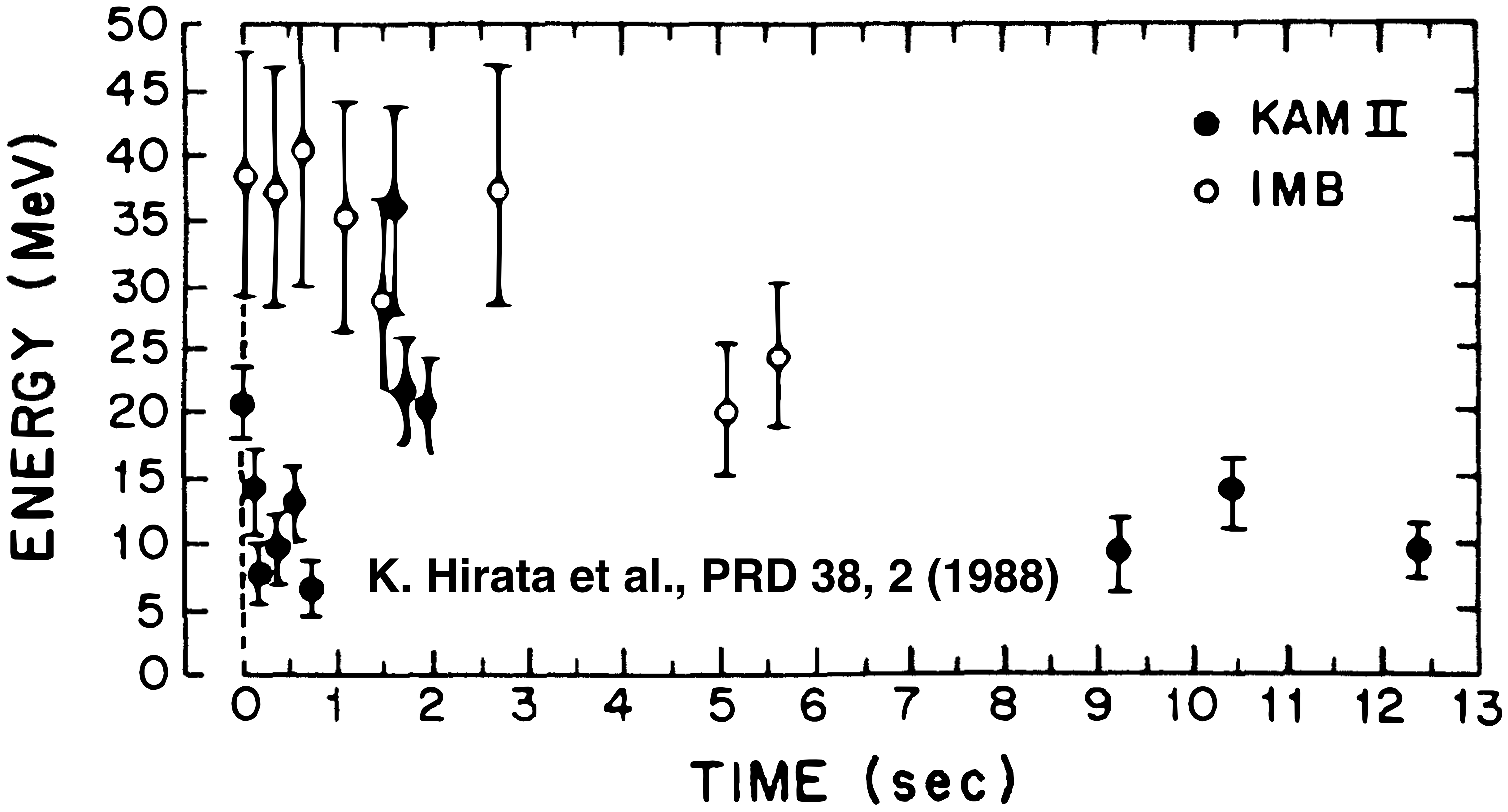

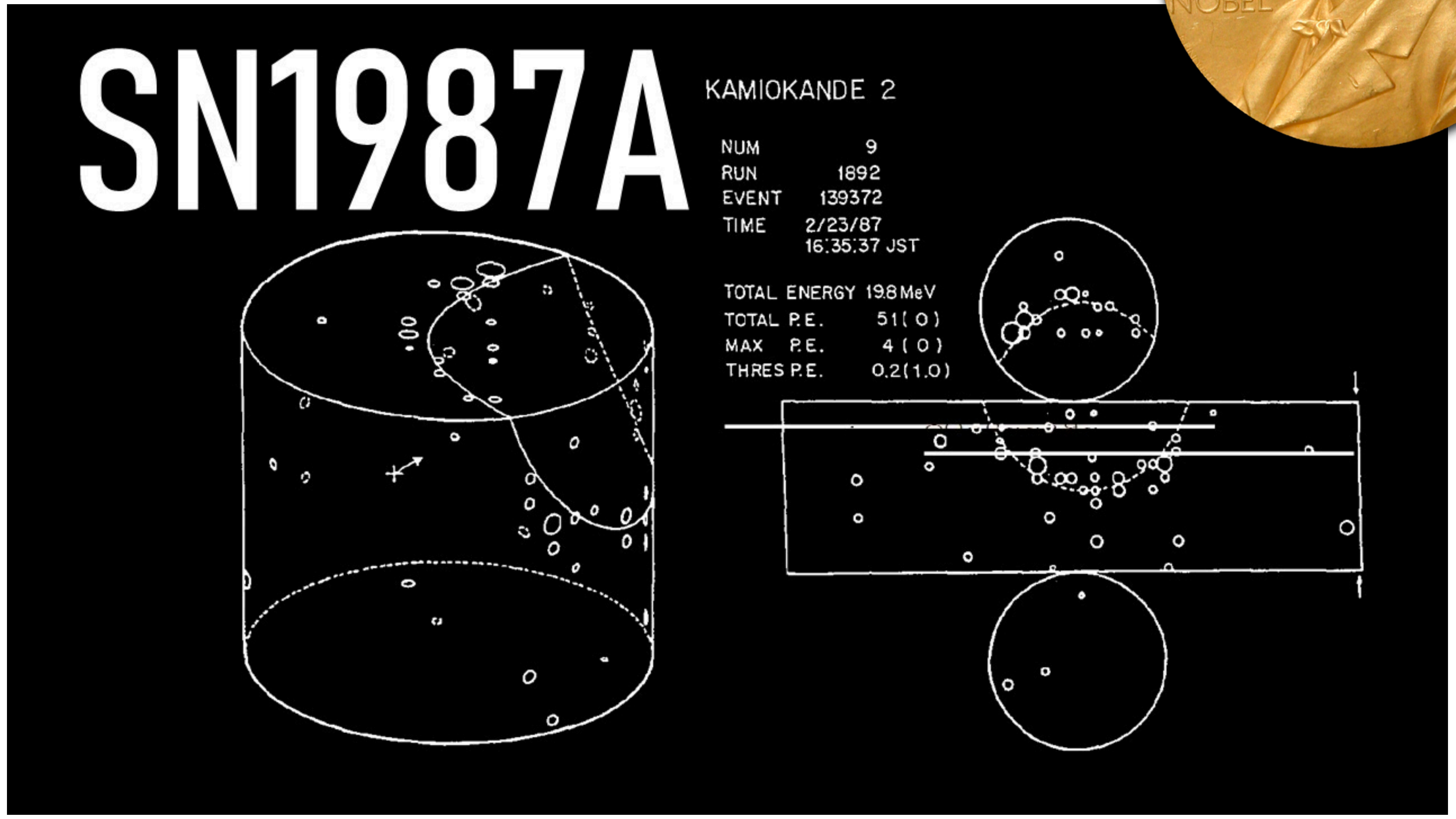

Diffuse Supernova Neutrino Background

The accumulated flux of neutrinos from all past core collapses over the cosmic history

= **Diffuse Supernova Neutrino Background** (DSNB)

- Many factors affecting DSNB (SFR, nuclear EOS, BH formation, neutrino oscillation, etc).
- Experimental detection is challenging because of small flux & huge backgrounds.

$$\Phi = \int [\nu \text{ emission}] \otimes [\text{Star formation}] \otimes [\text{Universe expansion}]$$

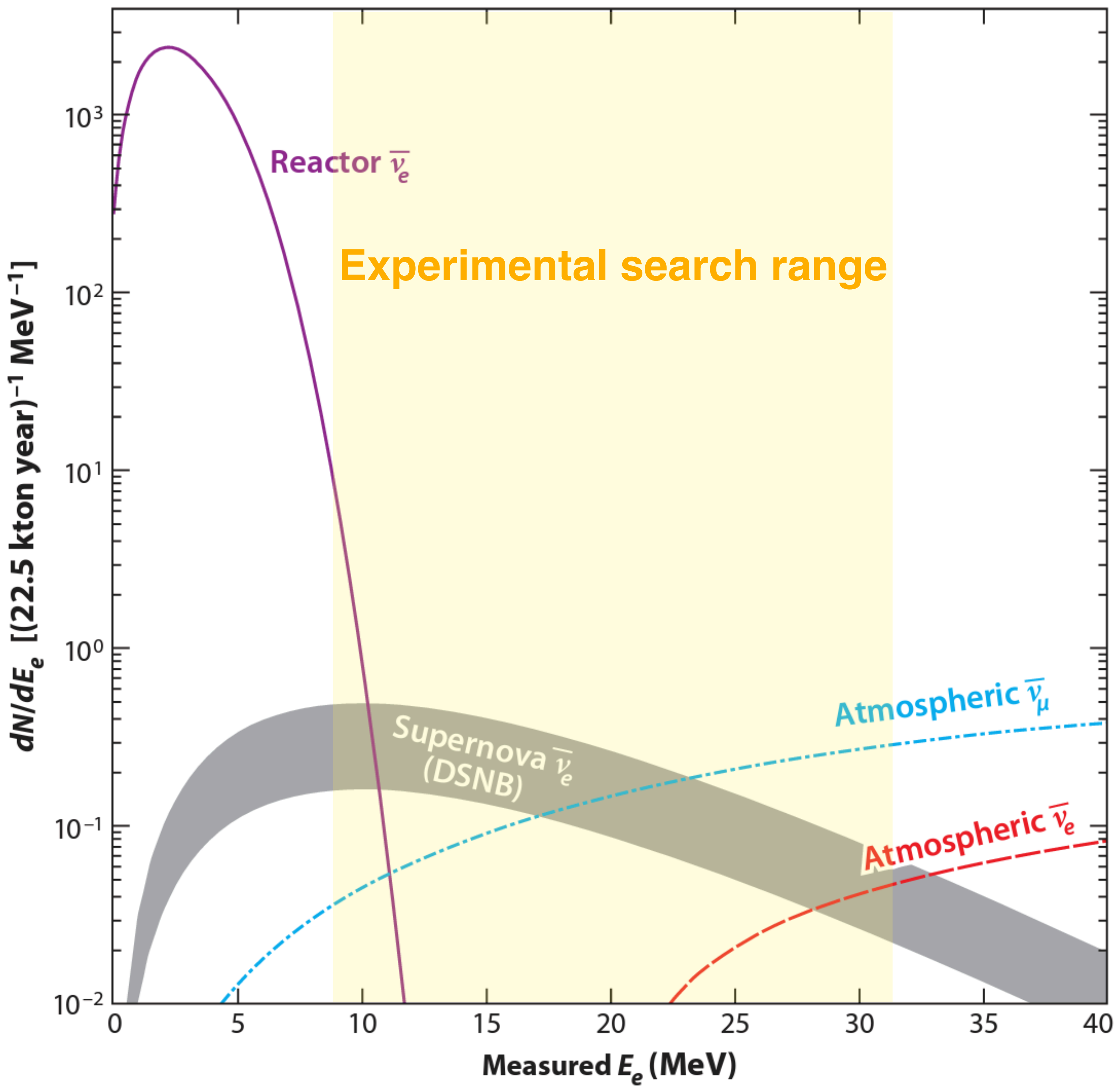

J. F. Beacom, ARNPS 60, 439 (2010)

DSNB Flux Predictions

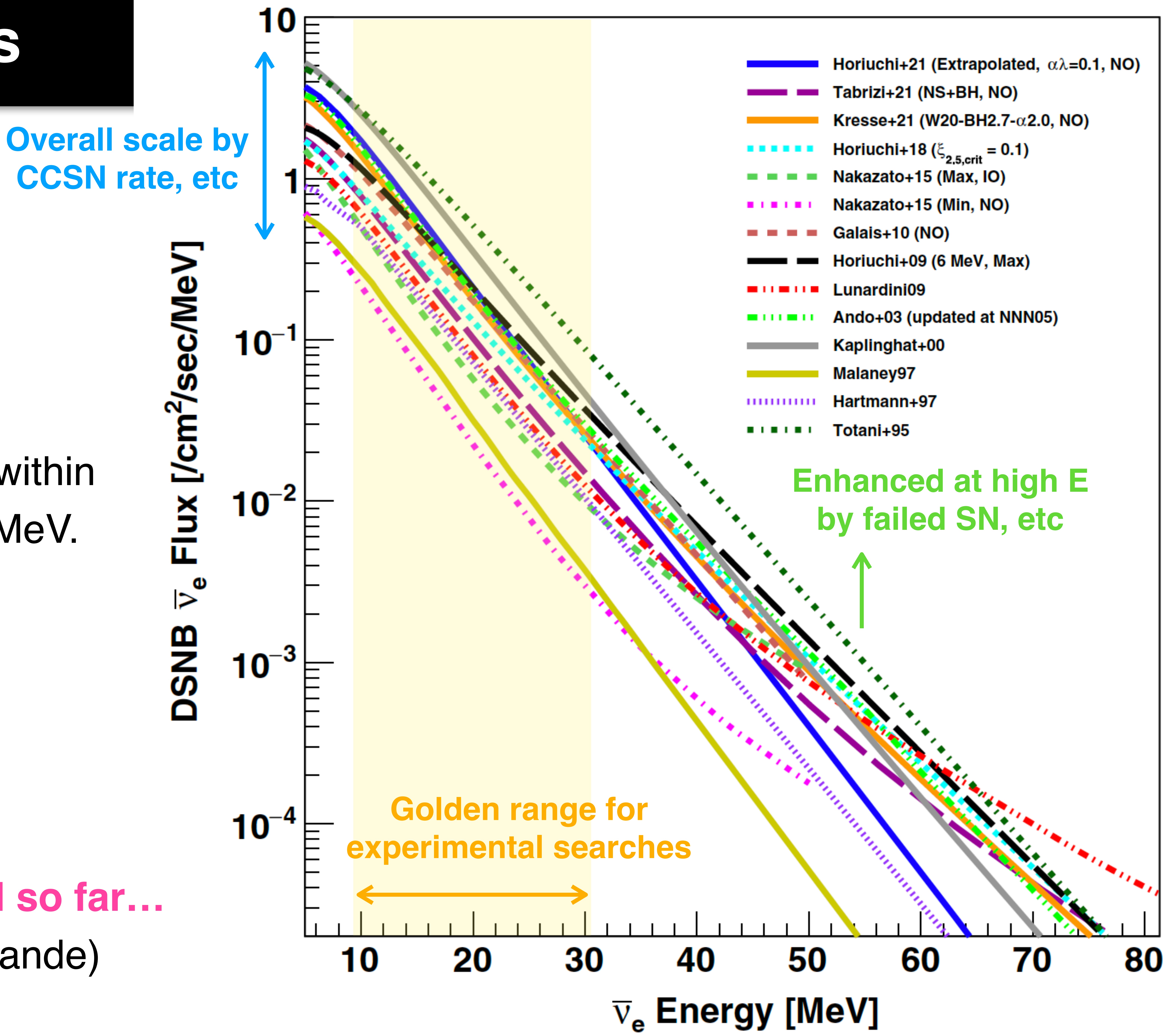

Most theoretical predictions exist within ~1 order of magnitude at 10~30 MeV.

Not experimentally discovered so far…

(best limits by Super-Kamiokande)

Experimental Search at Water Cherenkov Detectors

- Signal = **inverse beta decay (IBD)**, $\bar{\nu}_e + p \rightarrow e^+ + n$ (largest cross section)
  - e^+ = "*prompt*" signal (main signal range: **10~30 MeV**)
  - **n** = "*delayed*" signal via **γ-ray(s)** from thermal capture on hydrogen or gadolinium

- Many types of backgrounds mimicking this signature.
  - Atmospheric neutrinos
  - Radioactive isotopes produced by atmospheric muons
  - Solar neutrinos
  - Reactor neutrinos

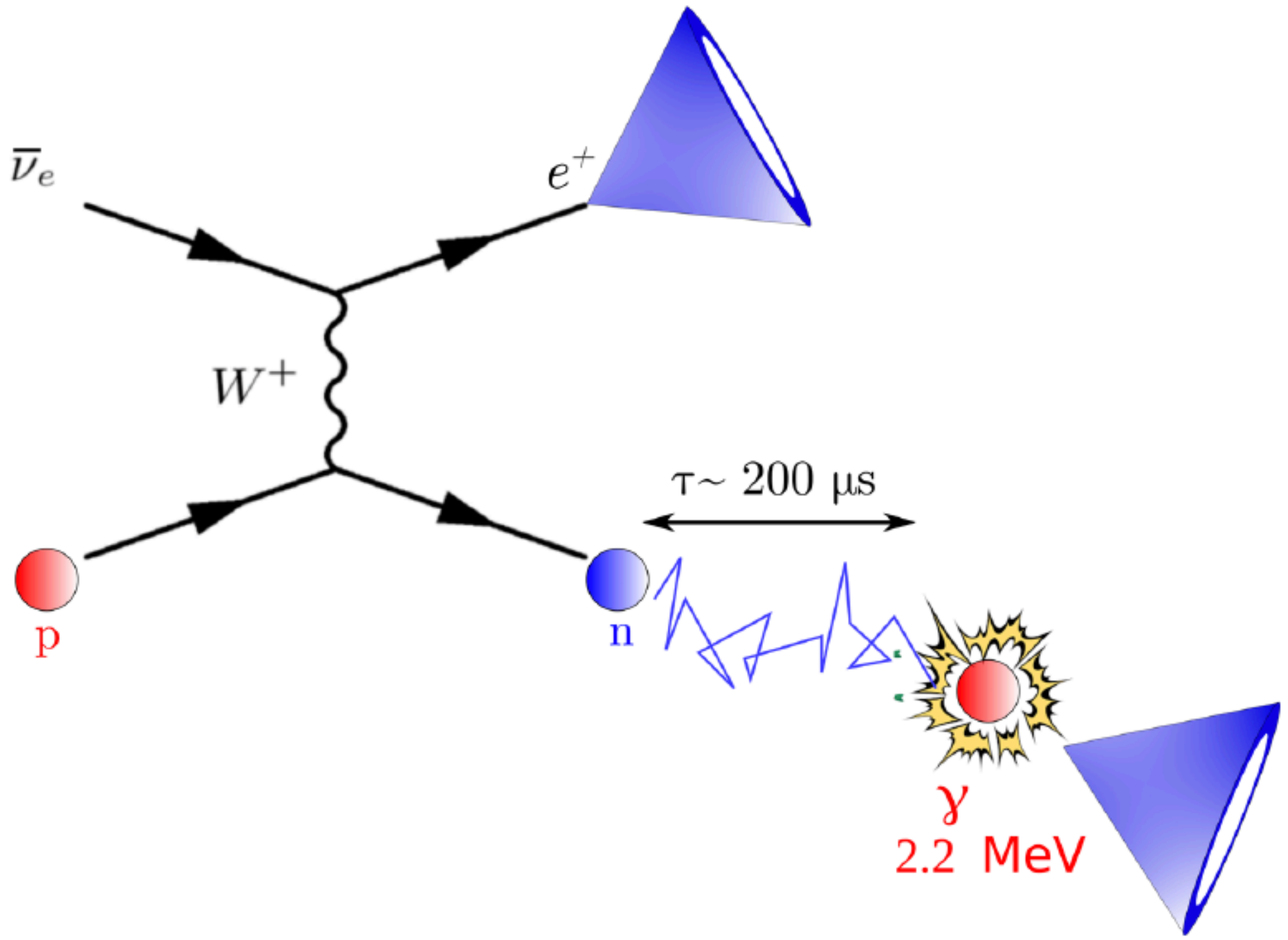

Focus in This Study: “Fate” of Stellar Collapse

- A lot of DSNB models are proposed for recent years.
  - Many of them end up serving flux.
  - Most lacking precise bkg estimation in their sensitivity discussion.

- Focus on **stellar core collapse fate** (NS or BH), which is accessible by other observations, making multi-messenger studies possible.
  - Pulsars
  - Monitoring luminous stars for failed SNe
  - Gravitational wave observations for binaries

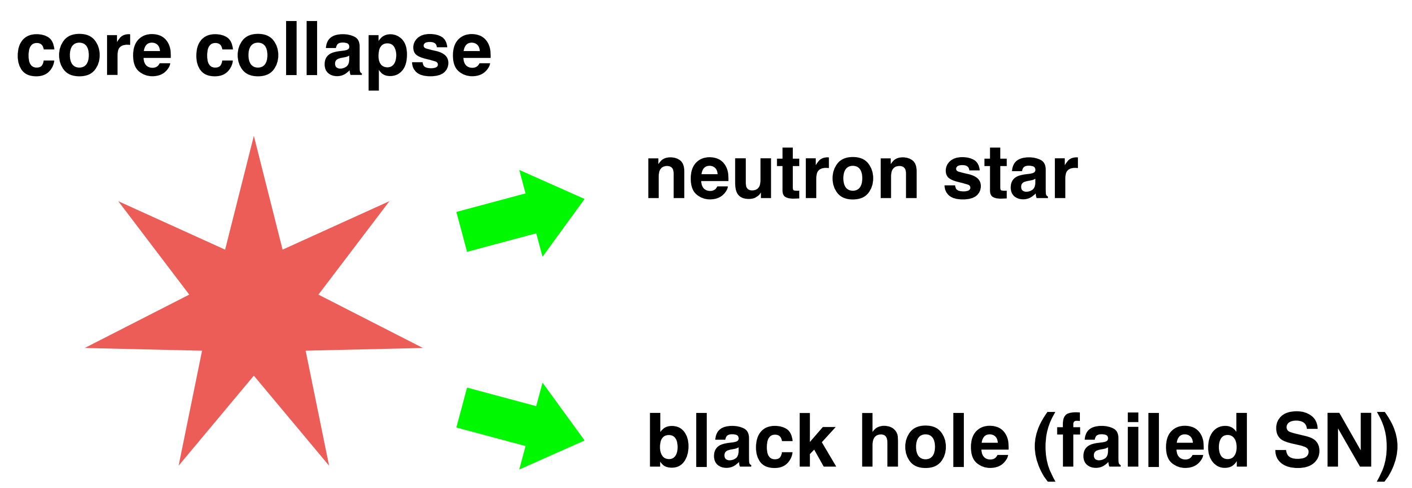

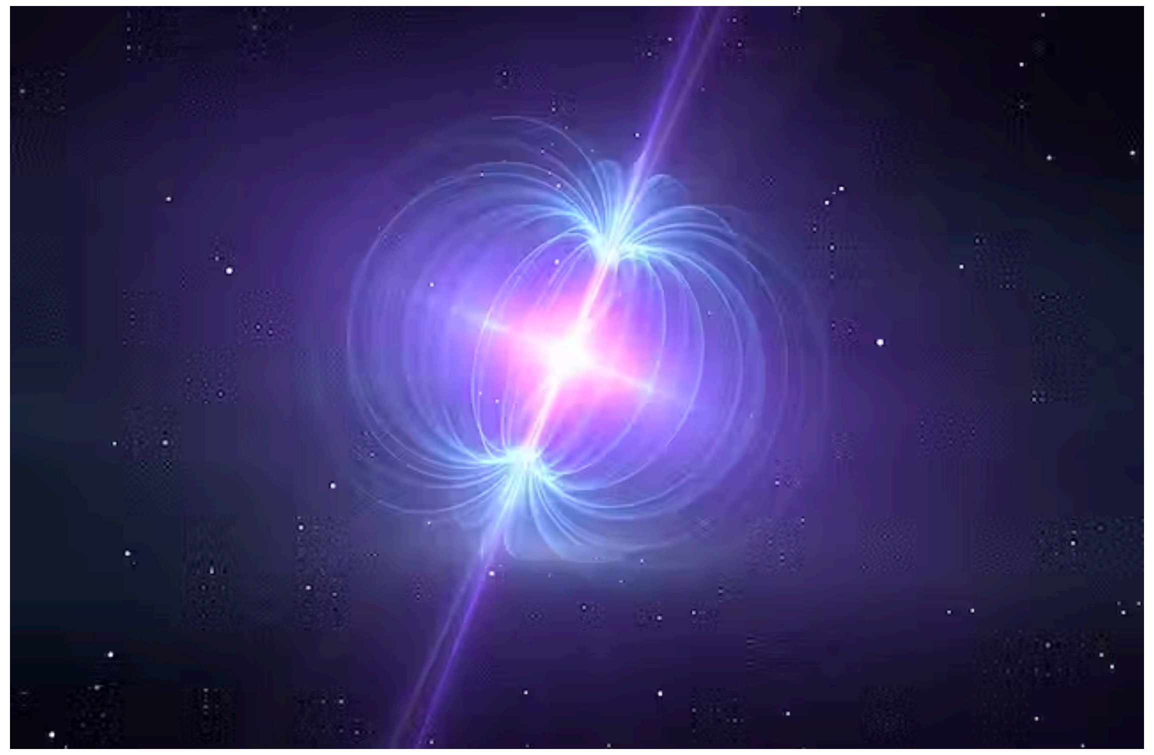

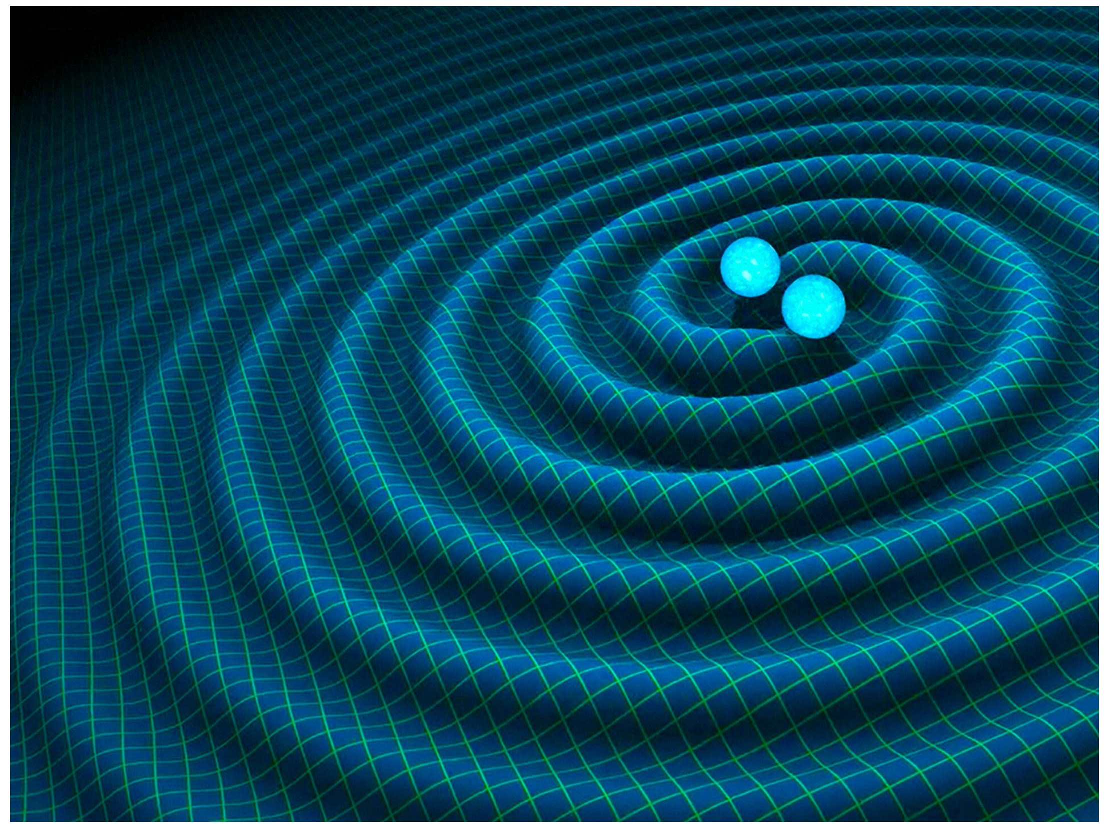

Ref: Observed Neutron Star Mass

- Neutron mass distribution from optical observations of the binary system shows a peak and higher tail.
- Natural born heavy, *or* gained mass through accretion from companion stars.

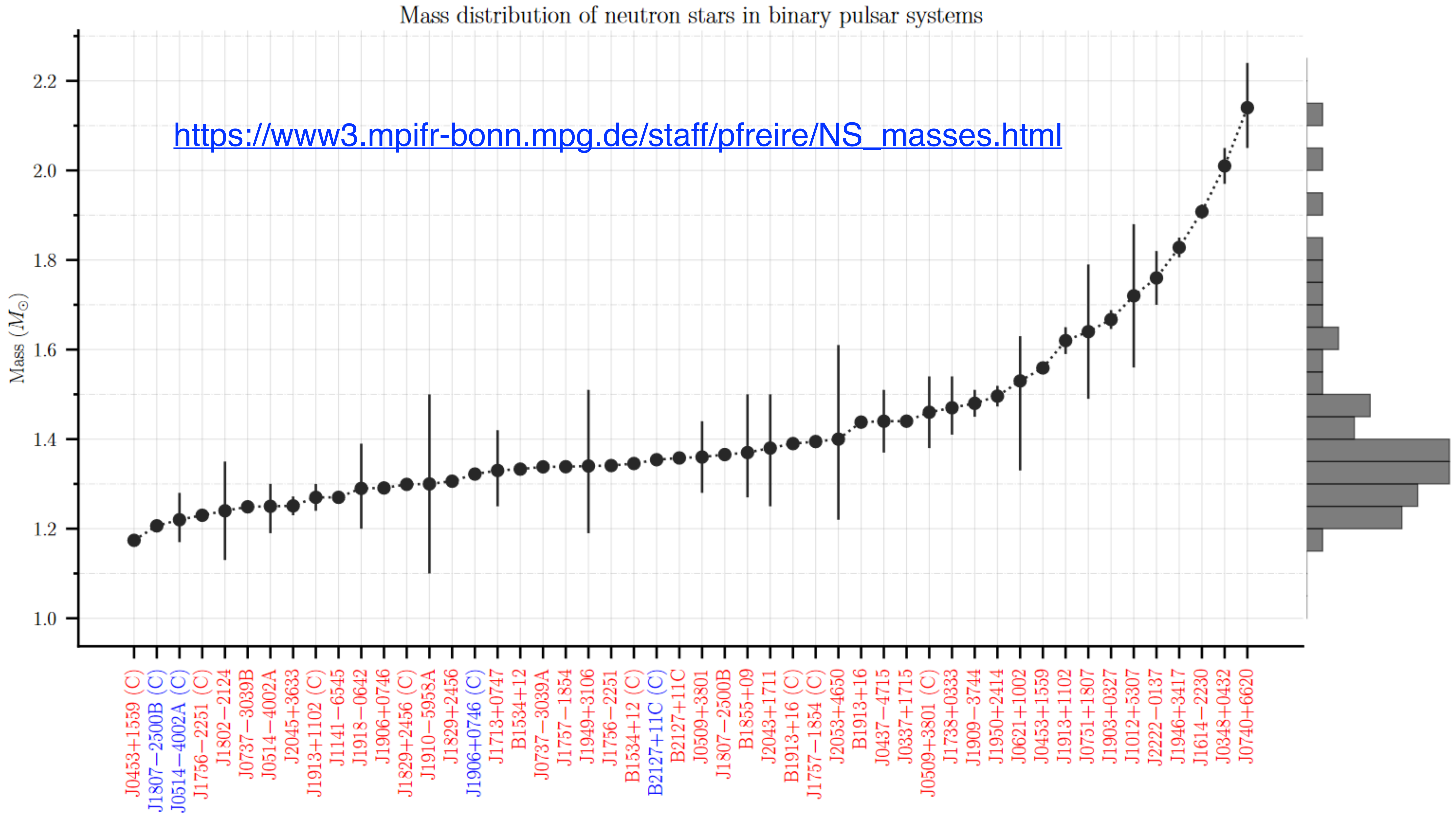

J. Antoniadis et al., arXiv:1605.01665

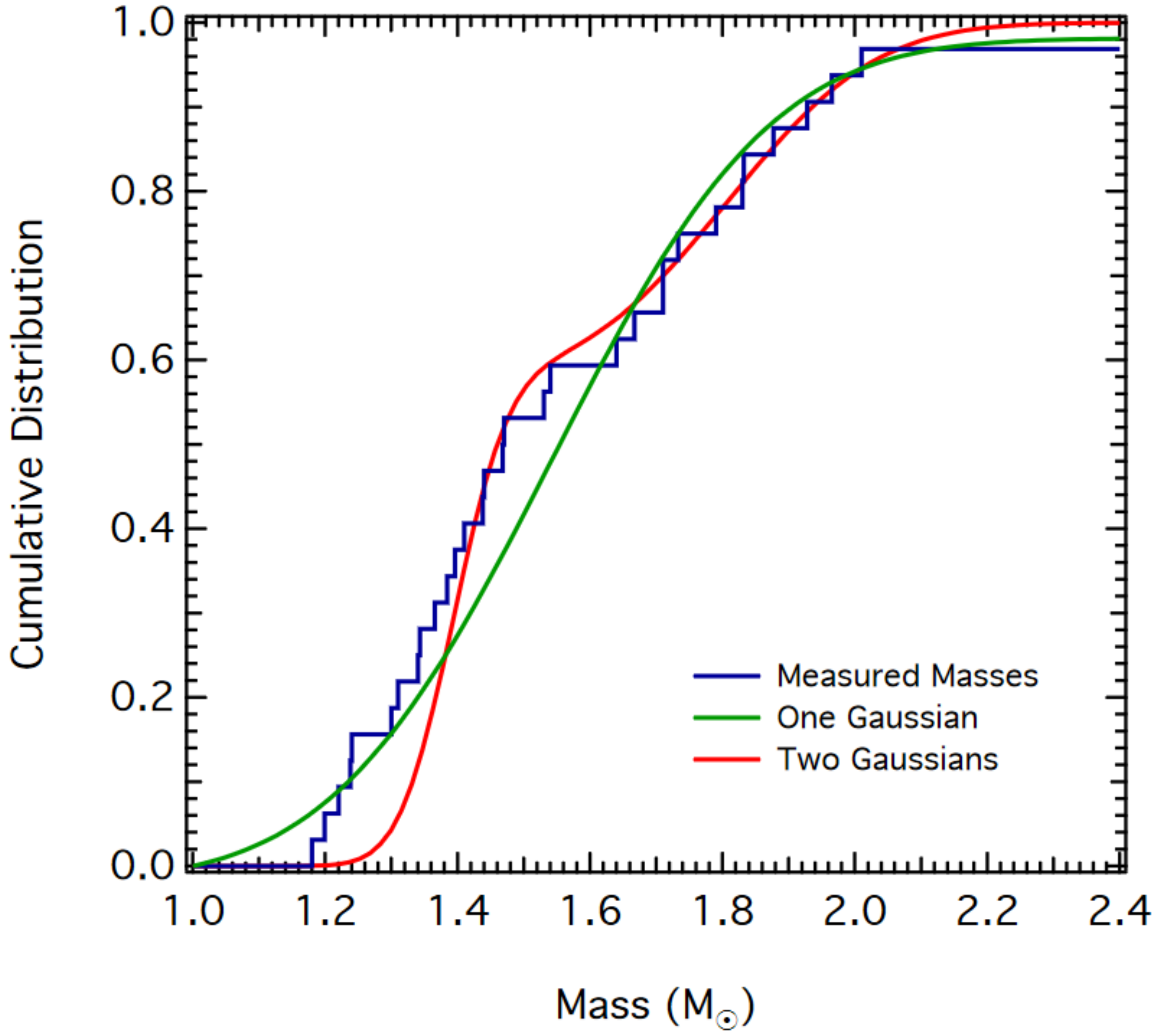

Ref: Failed SN Fraction

- Monitoring luminous stars gave constraints on a failed SN fraction.
- 2 failed SN candidates (N6946-BH1, M101-OC1) out of 8 SNe.
  - Failed SN fraction ~ **4–39% (90% C.L.)**, assuming N_{FSN} = 1 and N_{SN} = 8.

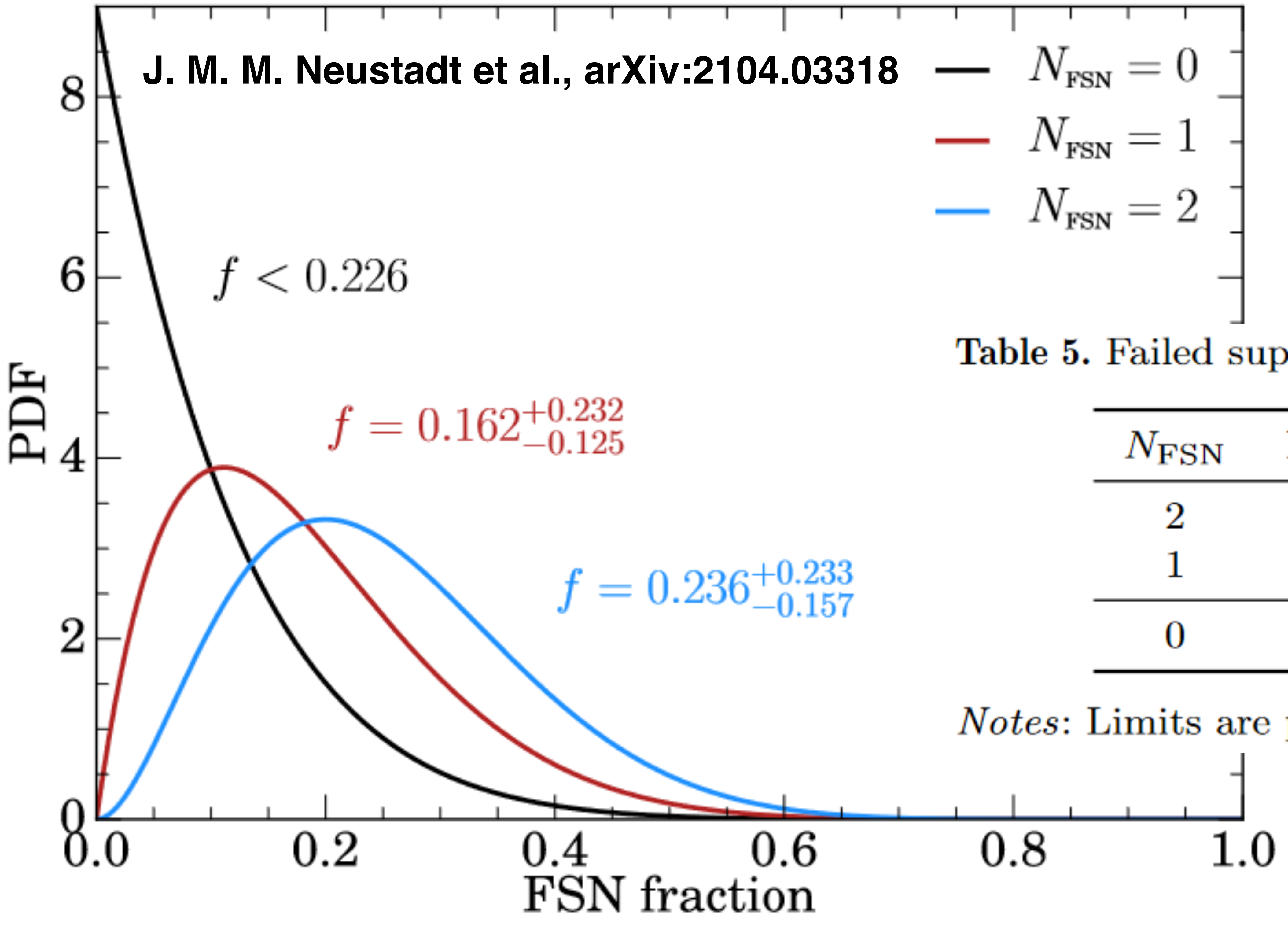

Table 5. Failed supernova/core-collapse fraction

N_{FSN}	Lower limit	Median	Upper limit
2	0.079	0.236	0.470
1	0.037	0.162	0.394
0	–	–	0.226

Notes: Limits are presented at the 90 per cent confidence level.

C. M. Basinger et al., arXiv:2007.15658

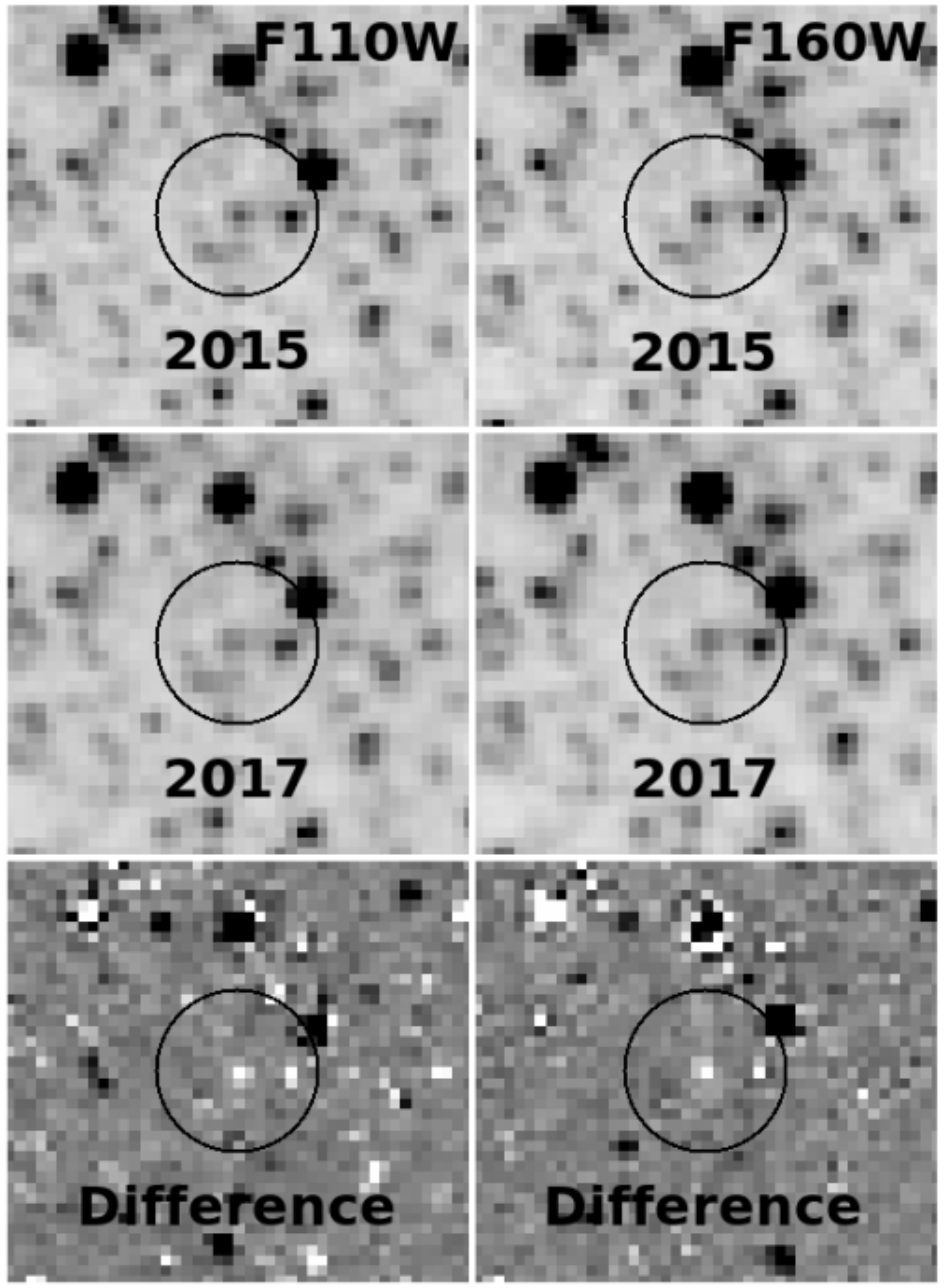

Ref: Nuclear Equation-of-State Impact

- In the NS case, neutrino emission amount depends on ***radius*** of proto-NS.
- In the BH case, neutrino emission amount depends on ***maximum mass*** of proto-NS.

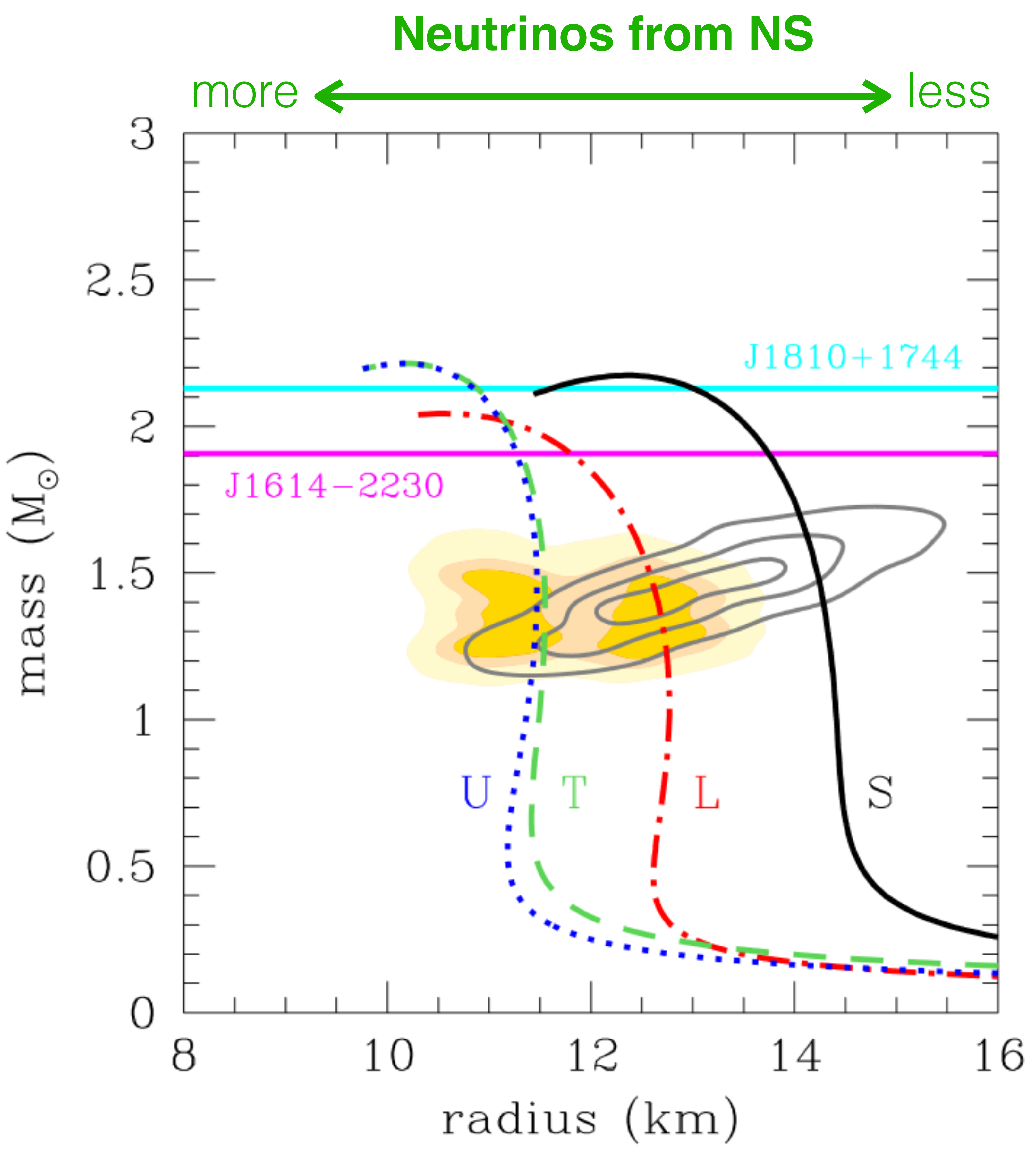

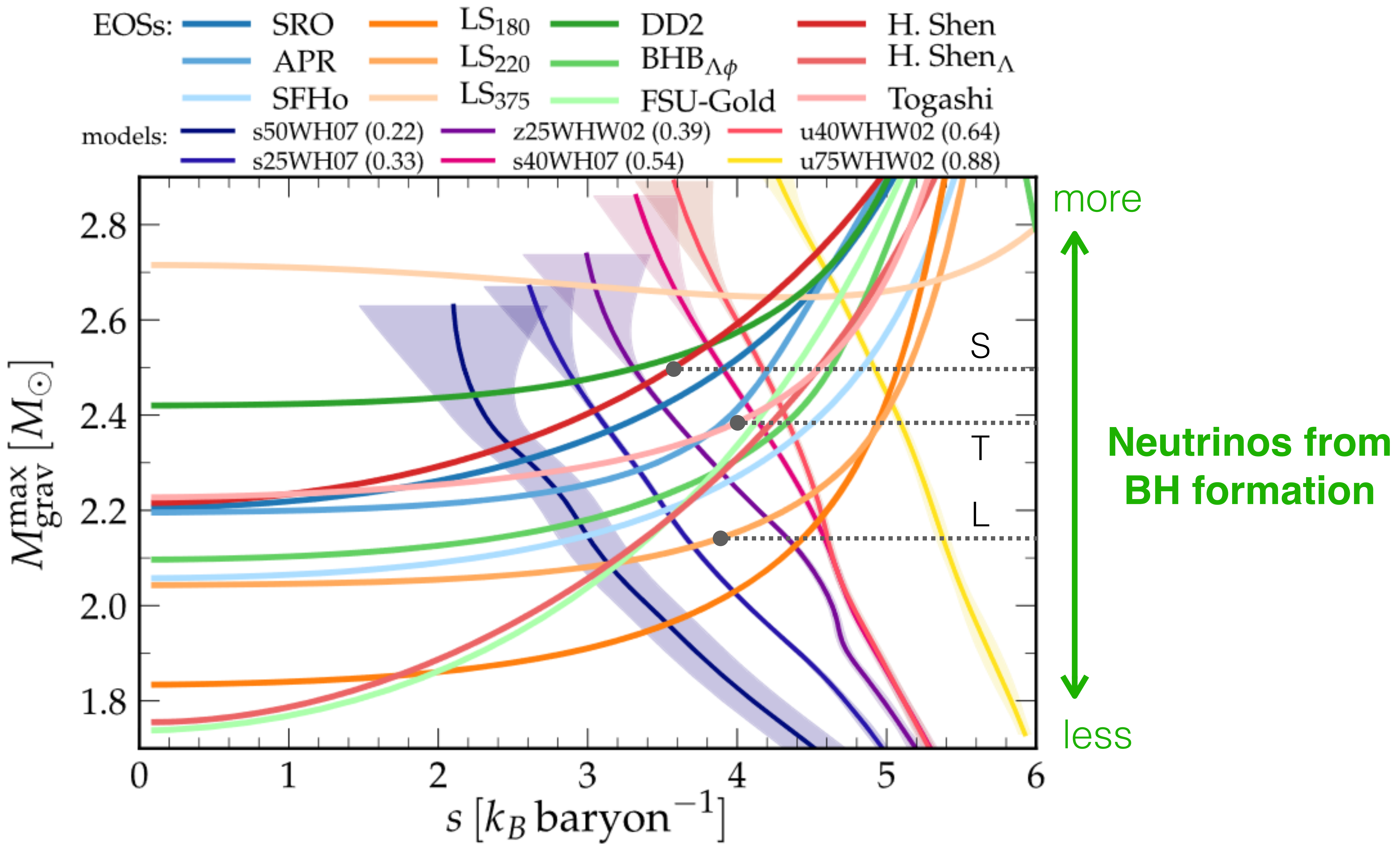

THE ASTROPHYSICAL JOURNAL, 937:30 (11pp), 2022 September 20 https://doi.org/10.3847/1538-4357/ac8a46

Exploring the Fate of Stellar Core Collapse with Supernova Relic Neutrinos

Yosuke Ashida[1] and Ken'ichiro Nakazato[2]
[1] Dept. of Physics and Wisconsin IceCube Particle Astrophysics Center, University of Wisconsin–Madison, Madison, WI 53706, USA
assy.8594.1207.physics@gmail.com
[2] Faculty of Arts and Science, Kyushu University, Fukuoka 819-0395, Japan
Received 2022 April 15; revised 2022 August 11; accepted 2022 August 15; published 2022 September 21

Abstract

Core collapse of massive stars leads to different fates for various physical factors, which gives different spectra of the emitted neutrinos. We focus on the supernova relic neutrinos (SRNs) as a probe to investigate the stellar collapse fate. We present the SRN fluxes and event rate spectra at a detector for three resultant states after stellar core collapse, the typical mass neutron star, the higher mass neutron star, or the failed supernova forming a black hole, based on different nuclear equations of state. Then possible SRN fluxes are formed as mixtures of the three components. We also show the expected sensitivities at the next-generation water-based Cherenkov detectors, SK-Gd and Hyper-Kamiokande, as constraining the mixture fractions. This study provides a practical example of extracting astrophysical constraints through SRN measurement.

Unified Astronomy Thesaurus concepts: Neutrino astronomy (1100); Supernova neutrinos (1666); Core-collapse supernovae (304); Massive stars (732); Neutron stars (1108); Black holes (162)

Modeling

- Emitted neutrino spectrum is expected to depend on the remnant after core collapse ("*fate*").
- Consider three major cases as a fate.
  - Canonical mass neutron stars ($1.47M_{\mathrm{Sun}}$)
  - High mass neutron stars ($1.86M_{\mathrm{Sun}}$)
  - Black holes (failed SNe)
- Use numerical simulations results for neutrino spectrum for each case from K. Nakazato et al., ApJ Suppl. 205, 2 (2013) & K. Nakazato et al., ApJ 925, 98 (2022).
- Calculate DSNB flux, following the techniques in K. Nakazato et al., ApJ 804, 75 (2015).

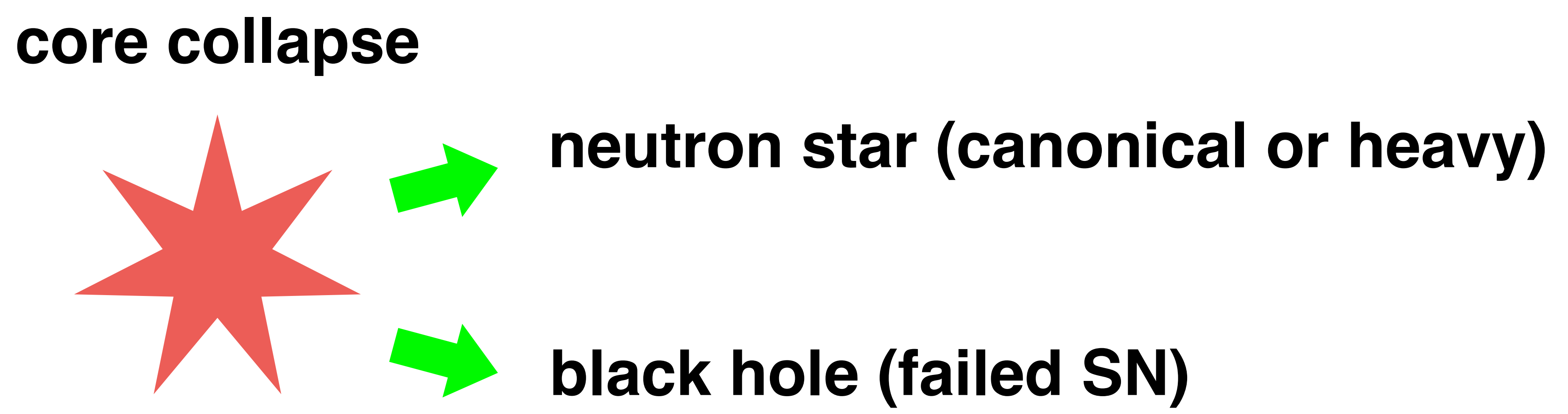

Modeling

- Emitted neutrino spectrum is expected to depend on the remnant after core collapse ("*fate*").
- Consider three major cases as a fate.
  - Canonical mass neutron stars (1.47M_{Sun})
  - High mass neutron stars (1.86M_{Sun})
  - Black holes (failed SNe)
- Use numerical simulations results for neutrino spectru
  205, 2 (2013) & K. Nakazato et al., ApJ 925, 98 (2022
- Calculate DSNB flux, following the techniques in K. Na

core collapse

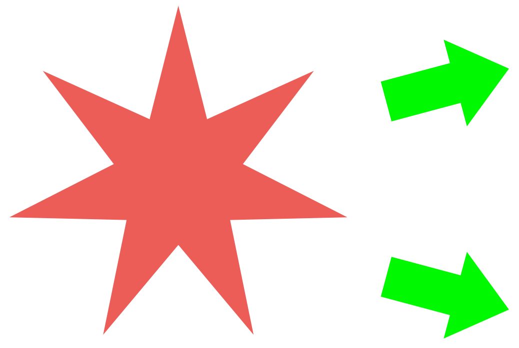

neutron star (canonical or heavy)

black hole (failed SN)

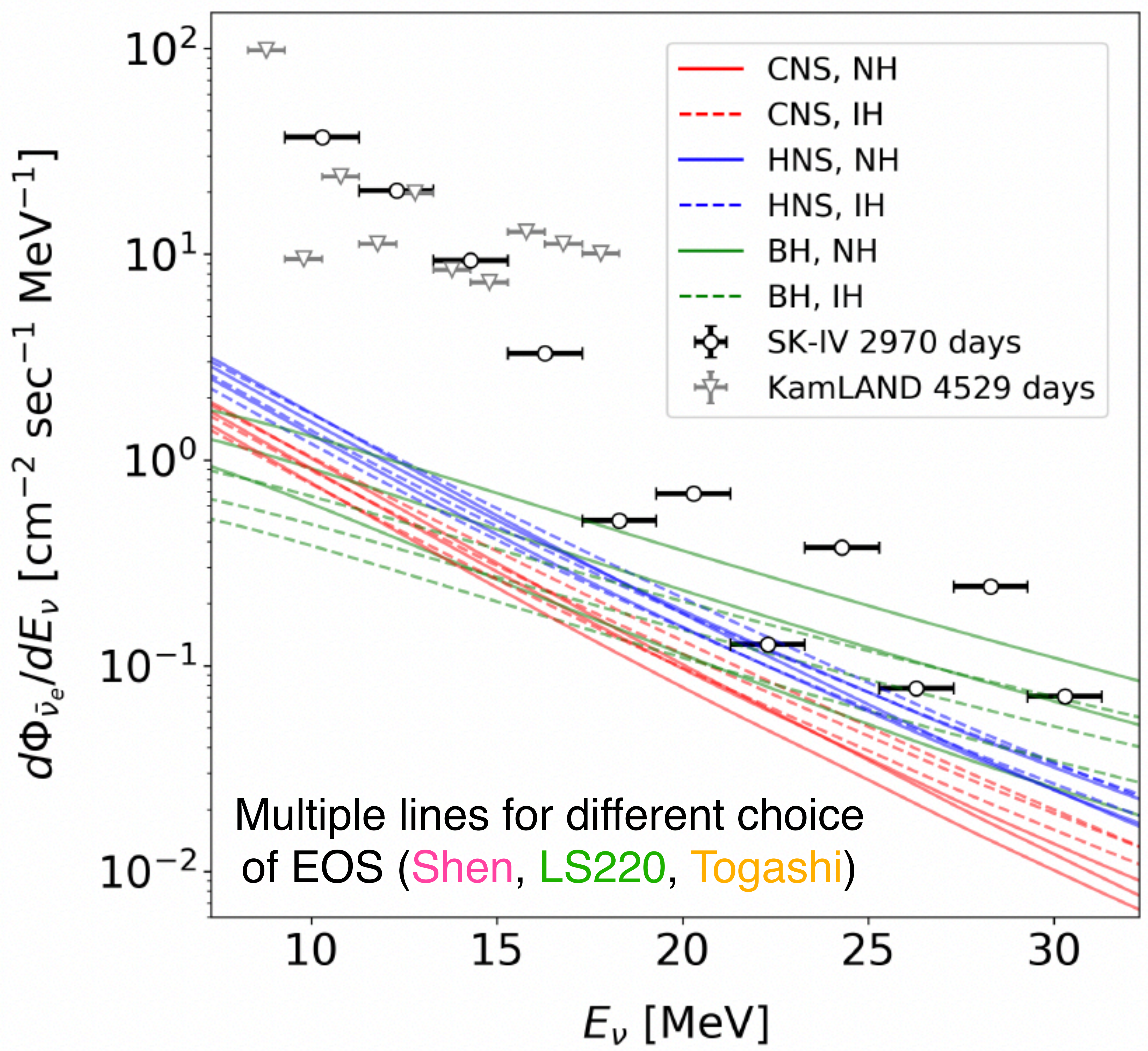

Event Rate

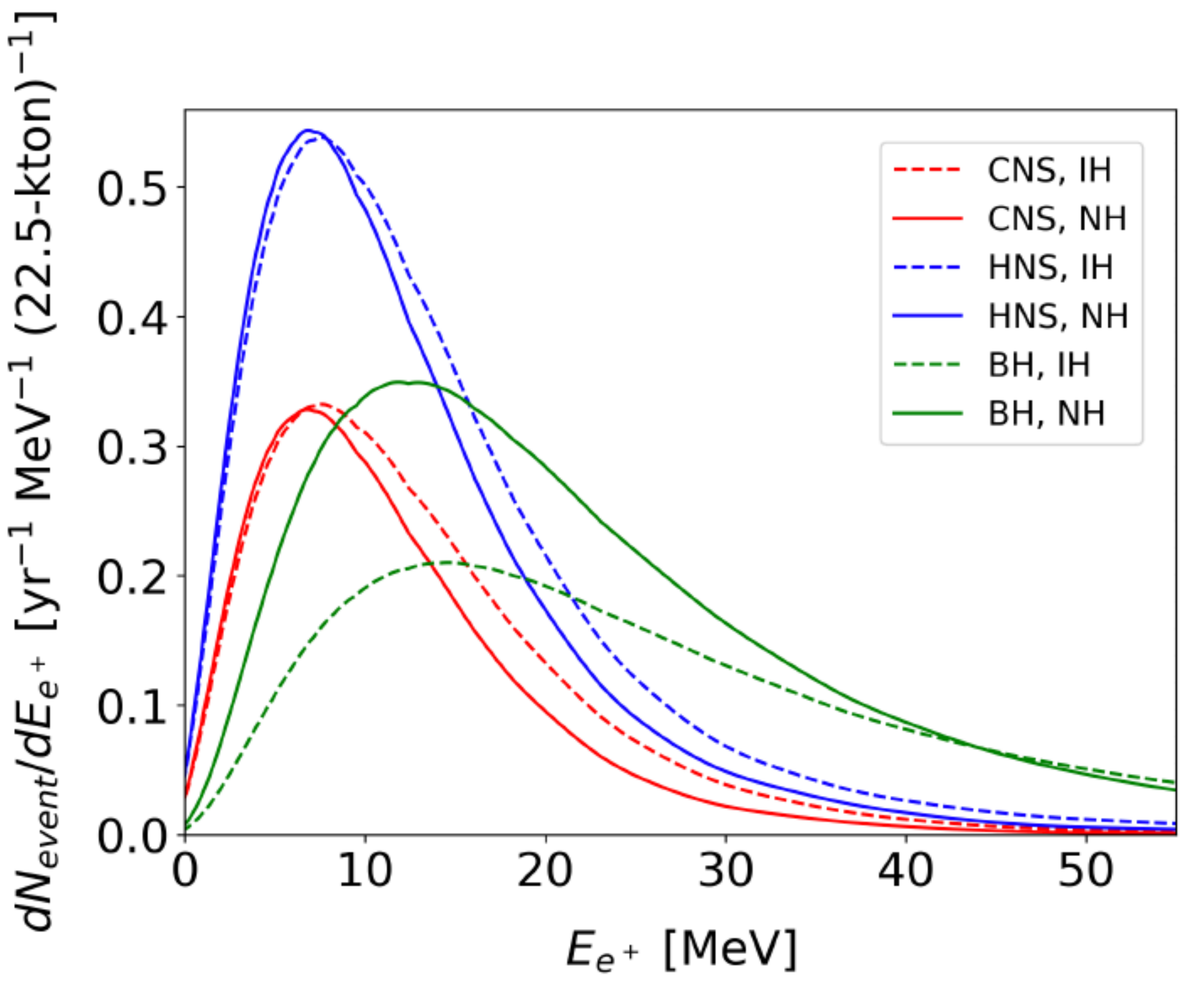

(a) Togashi EOS

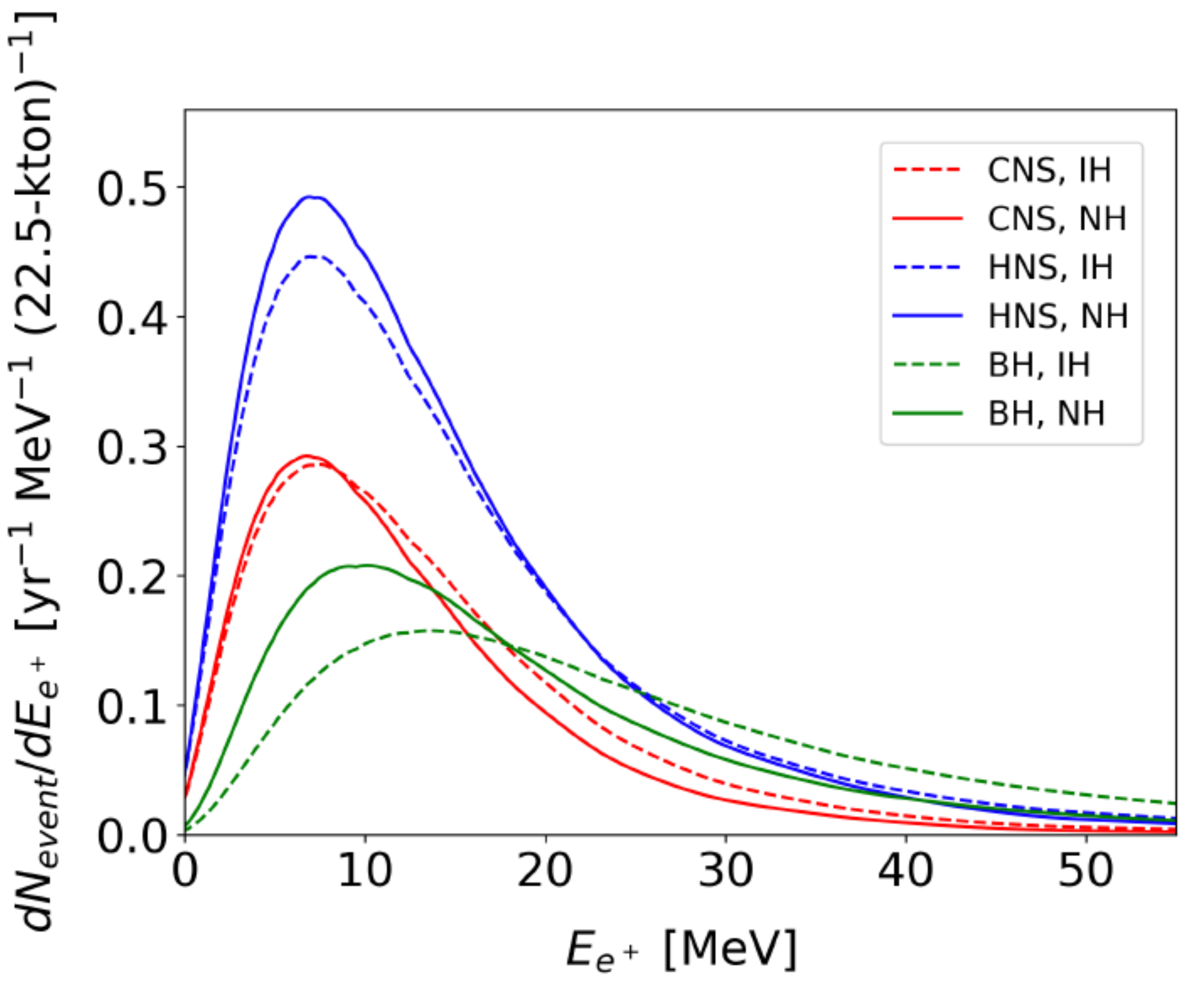

(b) LS220 EOS

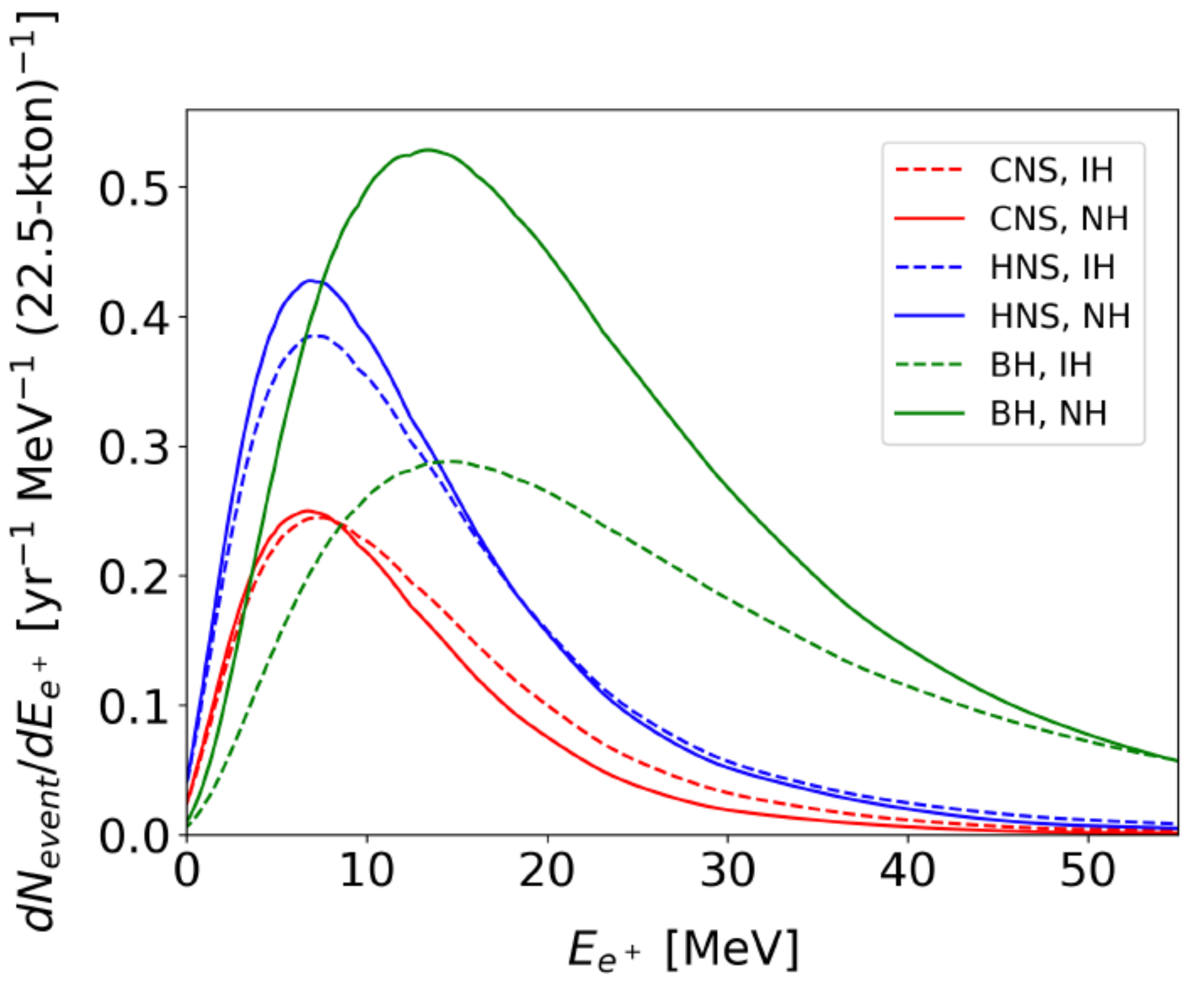

(c) Shen EOS

canonical mass NS, high mass NS, BH

- HNS is generally scale up of CNS. BH serves higher energies than NS.
- EOS impact is larger for BH.
- Neutrino mass hierarchy affects differently for NS and BH (also depends on EOS type).

Integrated Flux (>17.3 MeV)

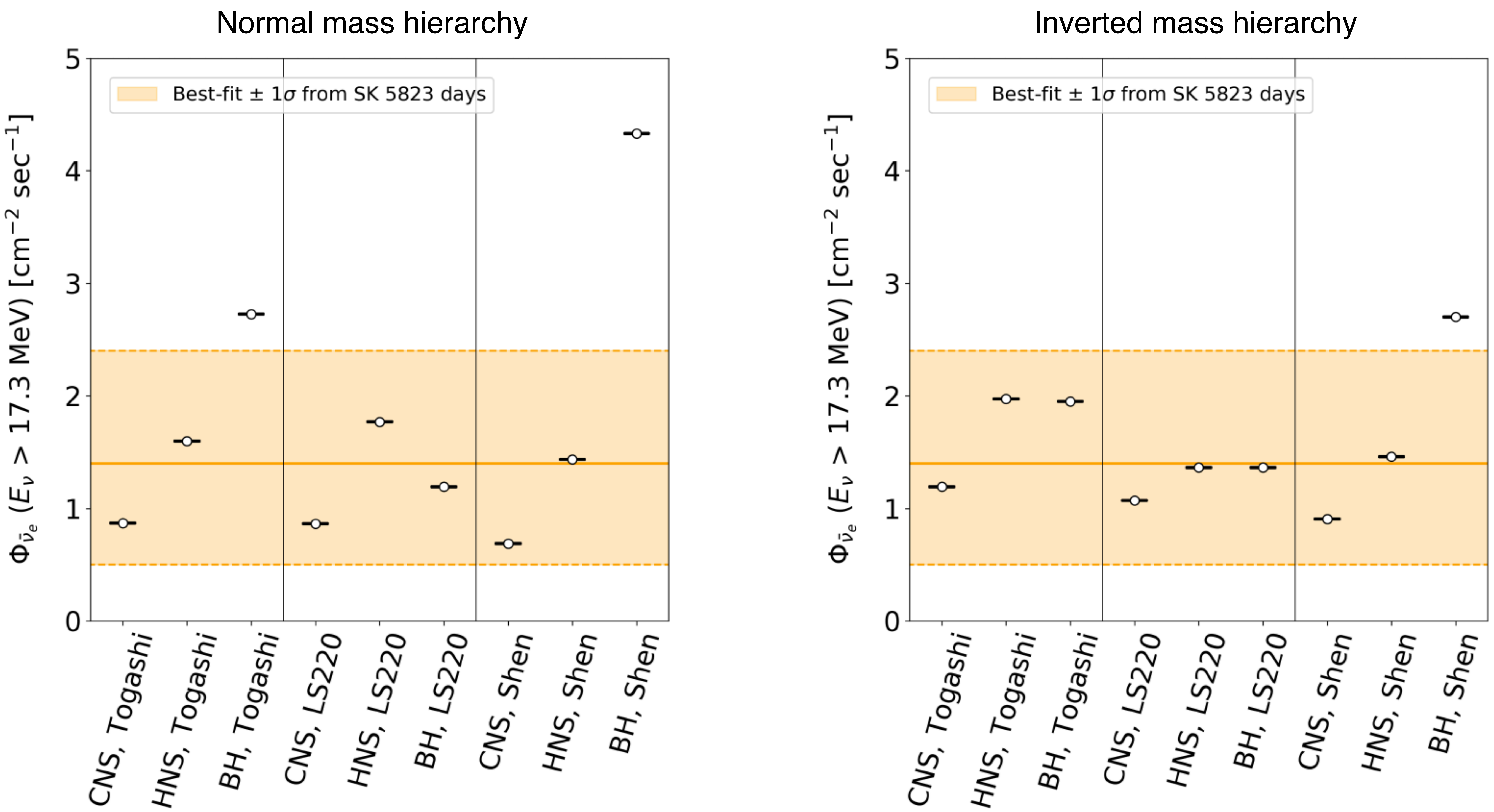

Mixture of Three Fluxes

(*Example*) Integrated DSNB flux for a certain energy range for different {f_{HNS}, f_{BH}} combinations

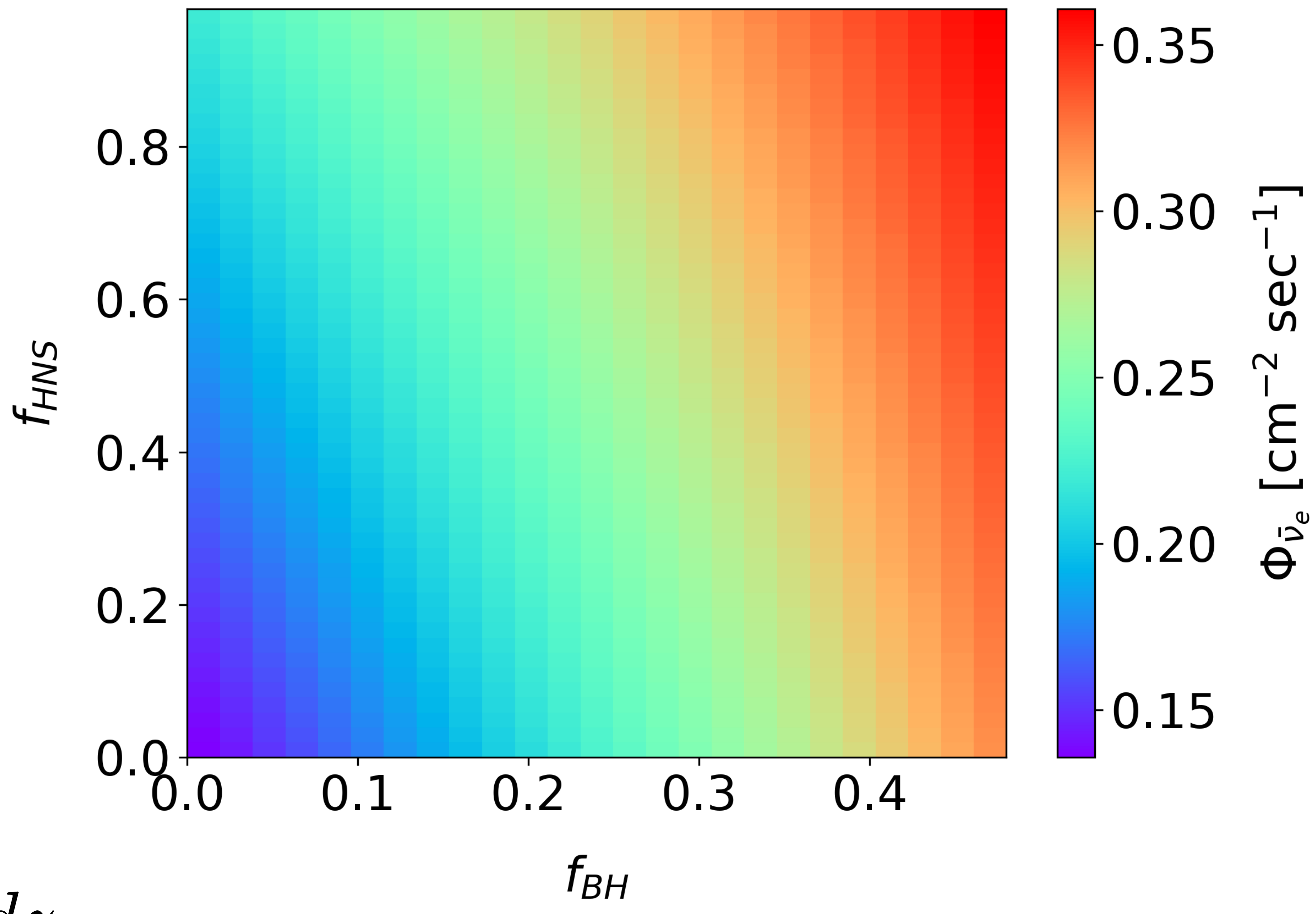

- Mix three cases by fractional parameters, f_{HNS} and f_{BH}, to form a DSNB flux.
  - f_{BH}: fraction of BH to total core-collapse
  - f_{HNS}: fraction of high mass NS to total NS
- Integrated DSNB flux differs for {f_{HNS}, f_{BH}} combinations.

DSNB flux at Earth

Neutrino spectrum from a core-collapse

$$\frac{d\Phi(E_\nu)}{dE_\nu} = c\int_0^{z_{\max}} R_{\rm CC}(z)\left\langle \frac{dN(E'_\nu)}{dE'_\nu}\right\rangle \times \frac{dz}{H_0\sqrt{\Omega_{\rm m}(1+z)^3+\Omega_\Lambda}}$$

$$\left\langle \frac{dN(E'_\nu)}{dE'_\nu}\right\rangle = f_{\rm BH}\frac{dN_{\rm BH}(E'_\nu)}{dE'_\nu} + (1-f_{\rm BH})\times\left[f_{\rm HNS}\frac{dN_{\rm HNS}(E'_\nu)}{dE'_\nu} + (1-f_{\rm HNS})\frac{dN_{\rm CNS}(E'_\nu)}{dE'_\nu}\right]$$

Sensitivity on Fractional Parameters

(*Example*) Integrated DSNB flux for a certain energy range for different {f_{HNS}, f_{BH}} combinations

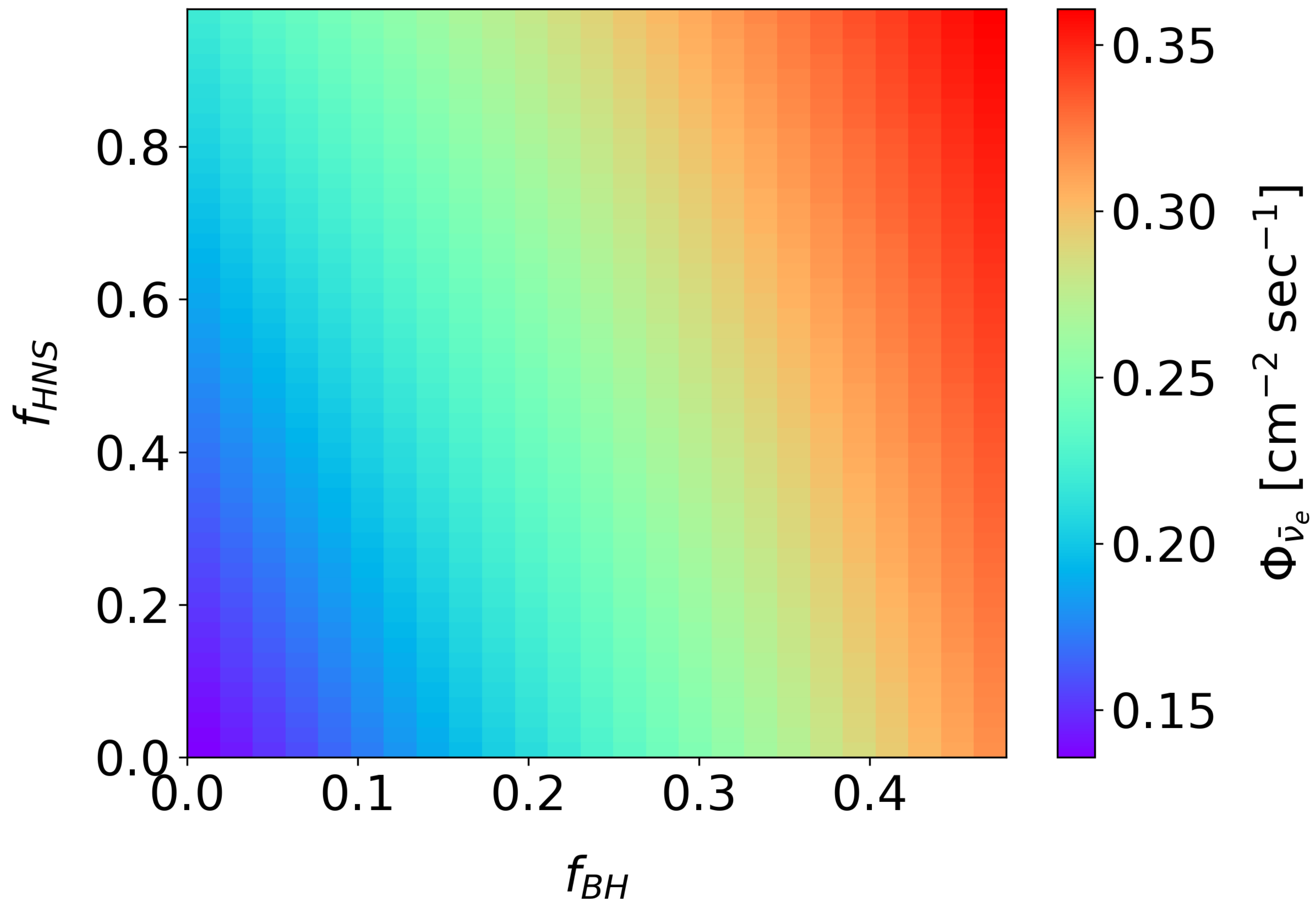

- Mix three cases by fractional parameters, f_{HNS} and f_{BH}, to form a DSNB flux.
  - f_{BH}: fraction of BH to total core-collapse
  - f_{HNS}: fraction of high mass NS to total NS
- Perform experimental sensitivity study as extrapolated from the SK-IV analysis about bkg, drawing contours in {f_{HNS}, f_{BH}} parameter range, based on integrated flux.
- Consider two next-generation detectors.
  - **SK-Gd**: ×1/10 accidental bkg, 70% ntag efficiency
  - **Hyper-Kamiokande**: ×8.4 detector mass, same ntag efficiency

Experimental Sensitivity (2σ C.L.)

Detectable above lines

Normal mass ordering

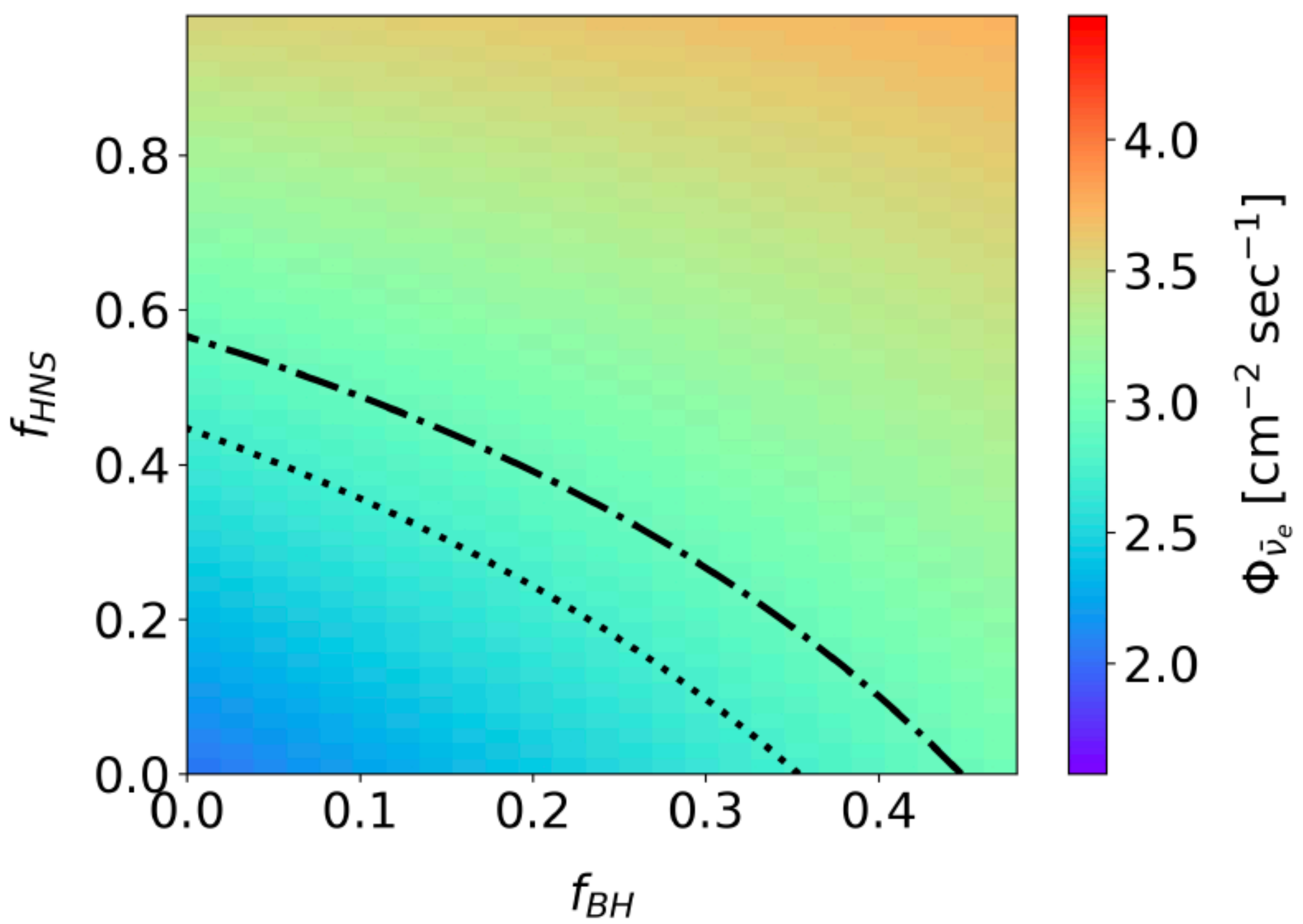

(1a) Togashi EOS,
$13.3 < E_\nu < 31.3\,\mathrm{MeV}$

Togashi

Integrated flux for 13.3 < E_ν < 31.3 MeV

— · — · — SK-Gd 10yr

·············· Hyper-K 3yr

- - - - - - - Hyper-K 5yr

Experimental Sensitivity (2σ C.L.)

Detectable above lines

Normal mass ordering

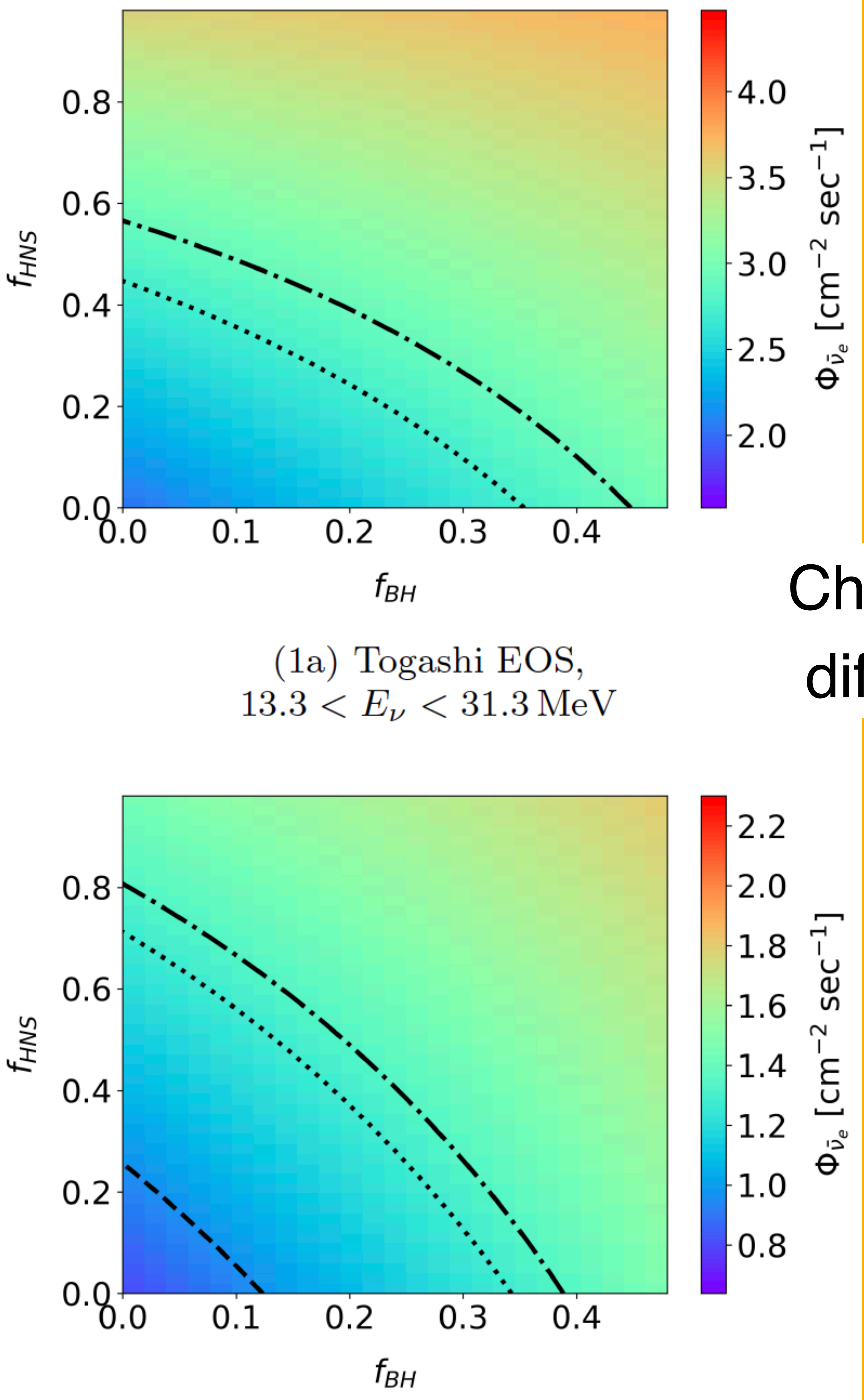

(1a) Togashi EOS, $13.3 < E_\nu < 31.3\,\mathrm{MeV}$

(2a) Togashi EOS, $17.3 < E_\nu < 31.3\,\mathrm{MeV}$

Togashi

Integrated flux for 13.3 < E_ν < 31.3 MeV

Choice of integration range serves different contours in some cases.

Integrated flux for 17.3 < E_ν < 31.3 MeV

- **SK-Gd 10yr** (dash-dotted line)
- **Hyper-K 3yr** (dotted line)
- **Hyper-K 5yr** (dashed line)

Experimental Sensitivity (2σ C.L.)

Detectable above lines

Normal mass ordering

Contours change for different EOSs.

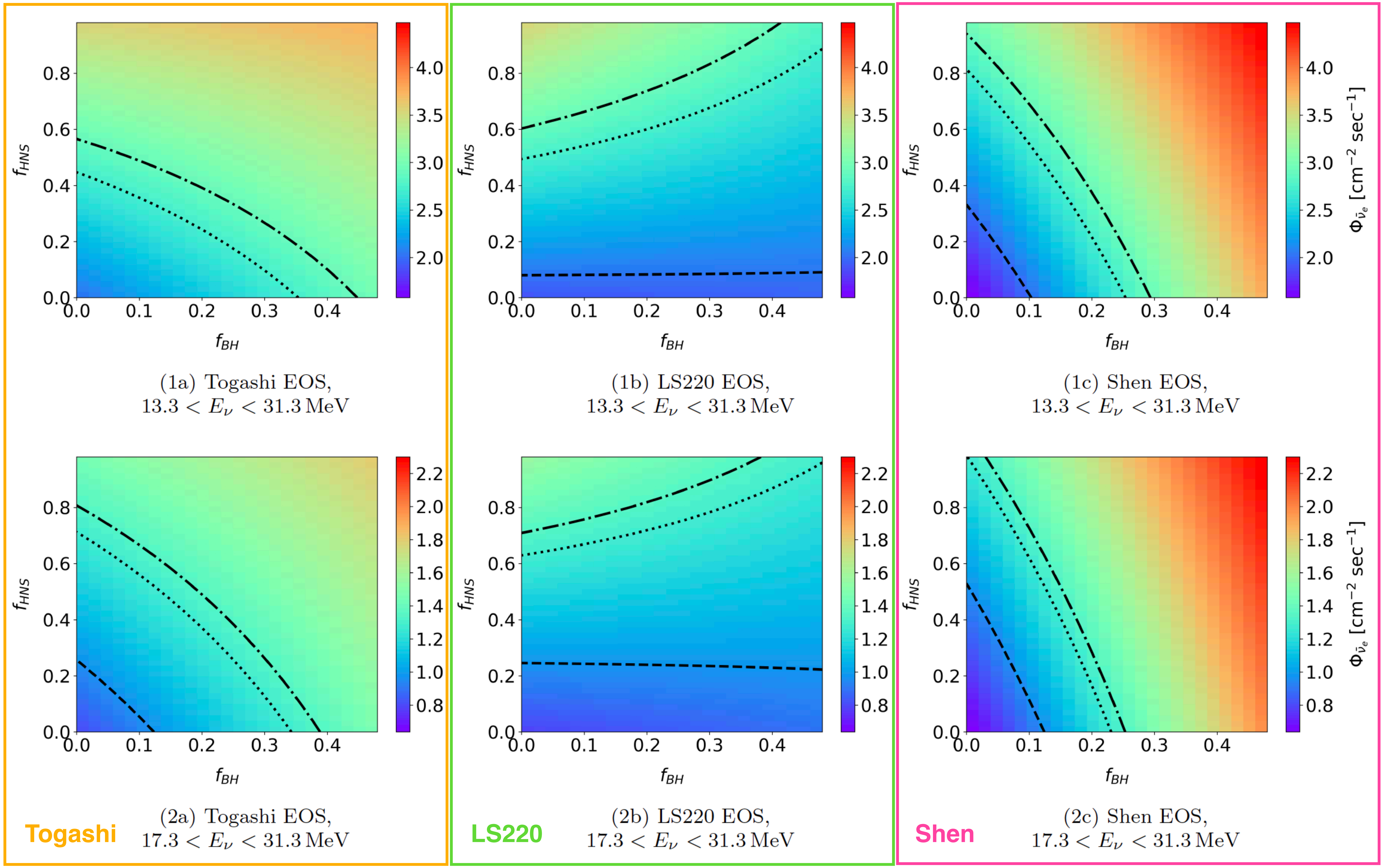

—·—·— **SK-Gd 10yr**

·············· **Hyper-K 3yr**

- - - - - - - **Hyper-K 5yr**

Nuclear EOS Dependence

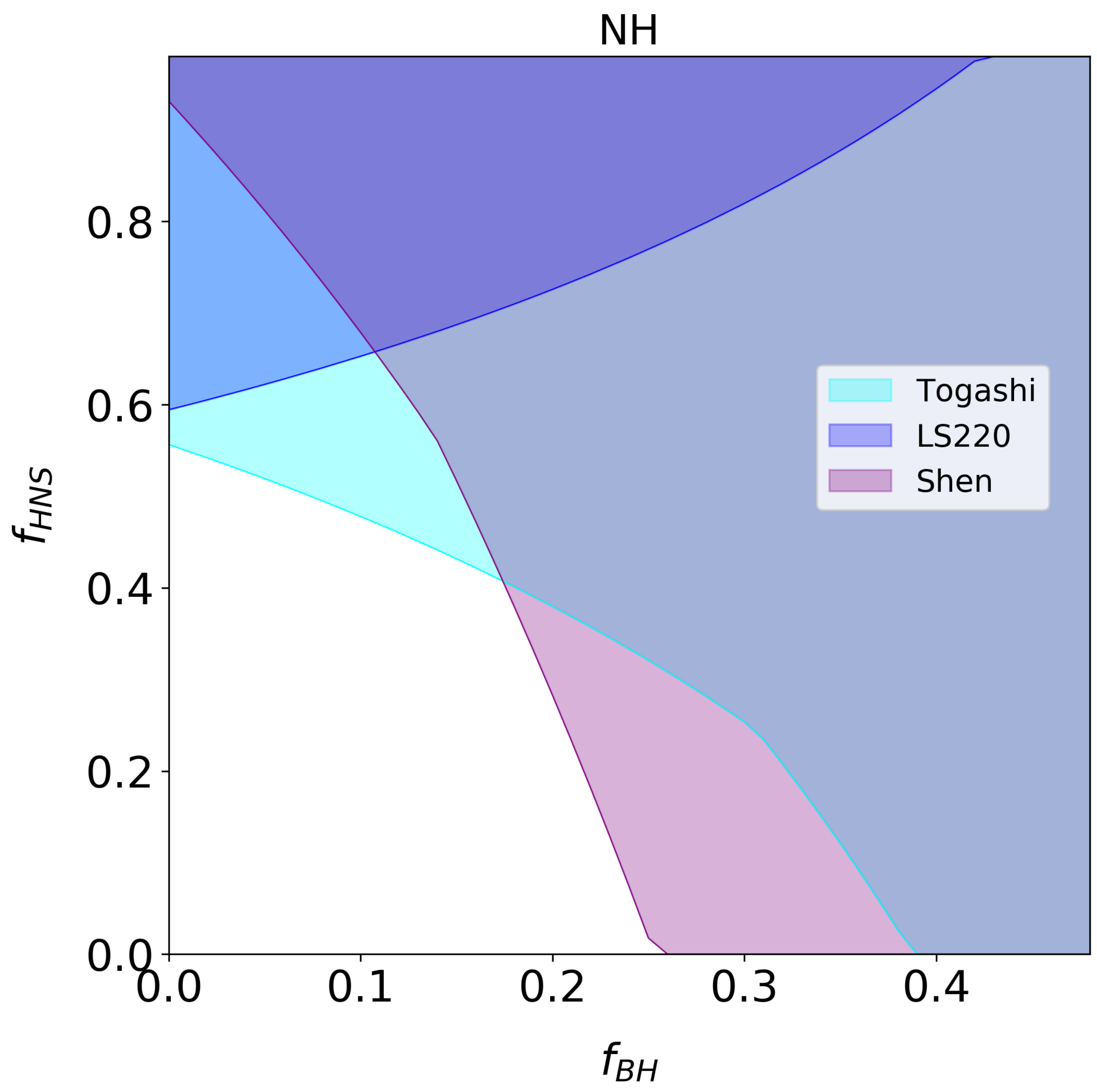

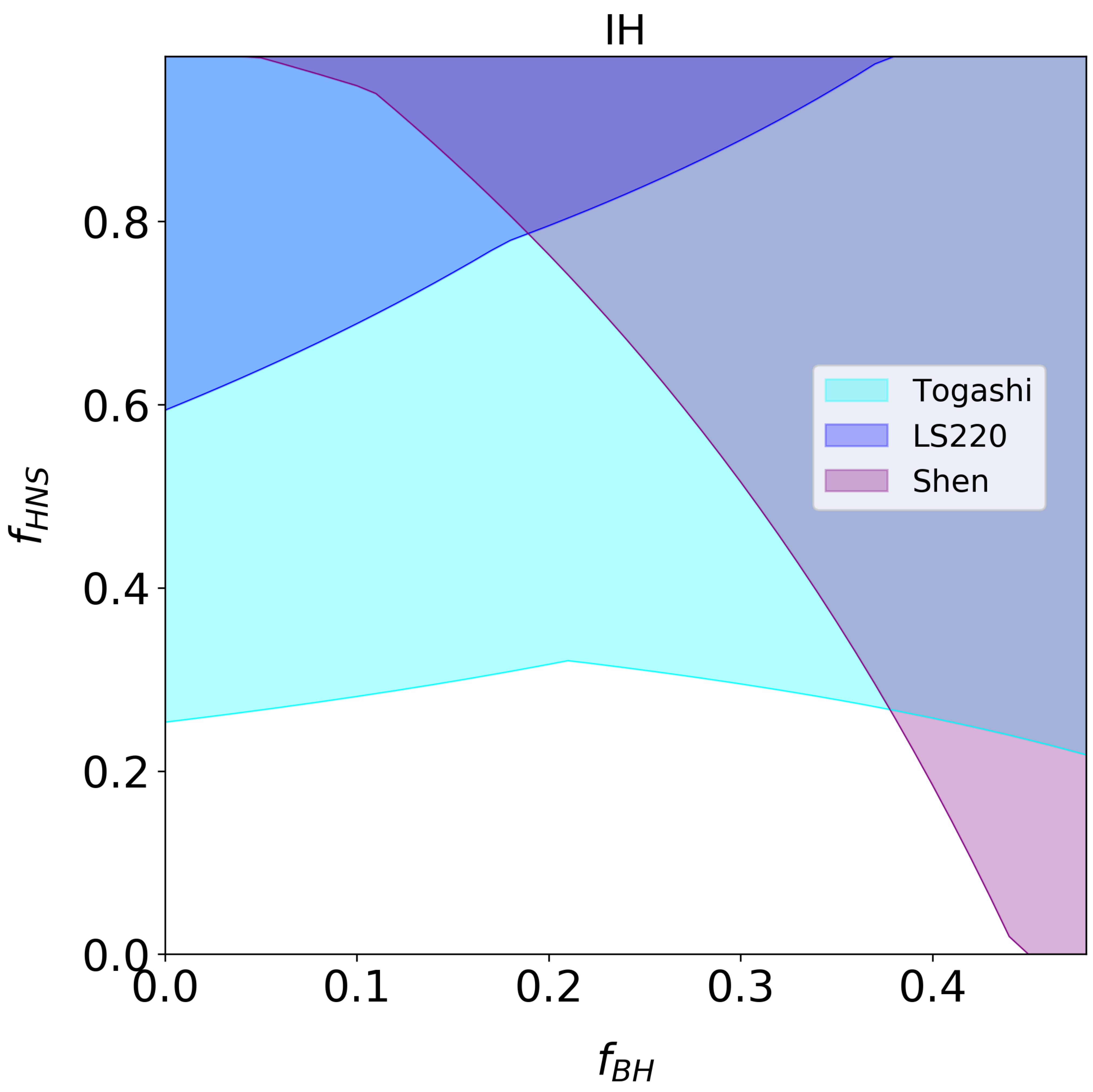

Hyper-K Sensitivity

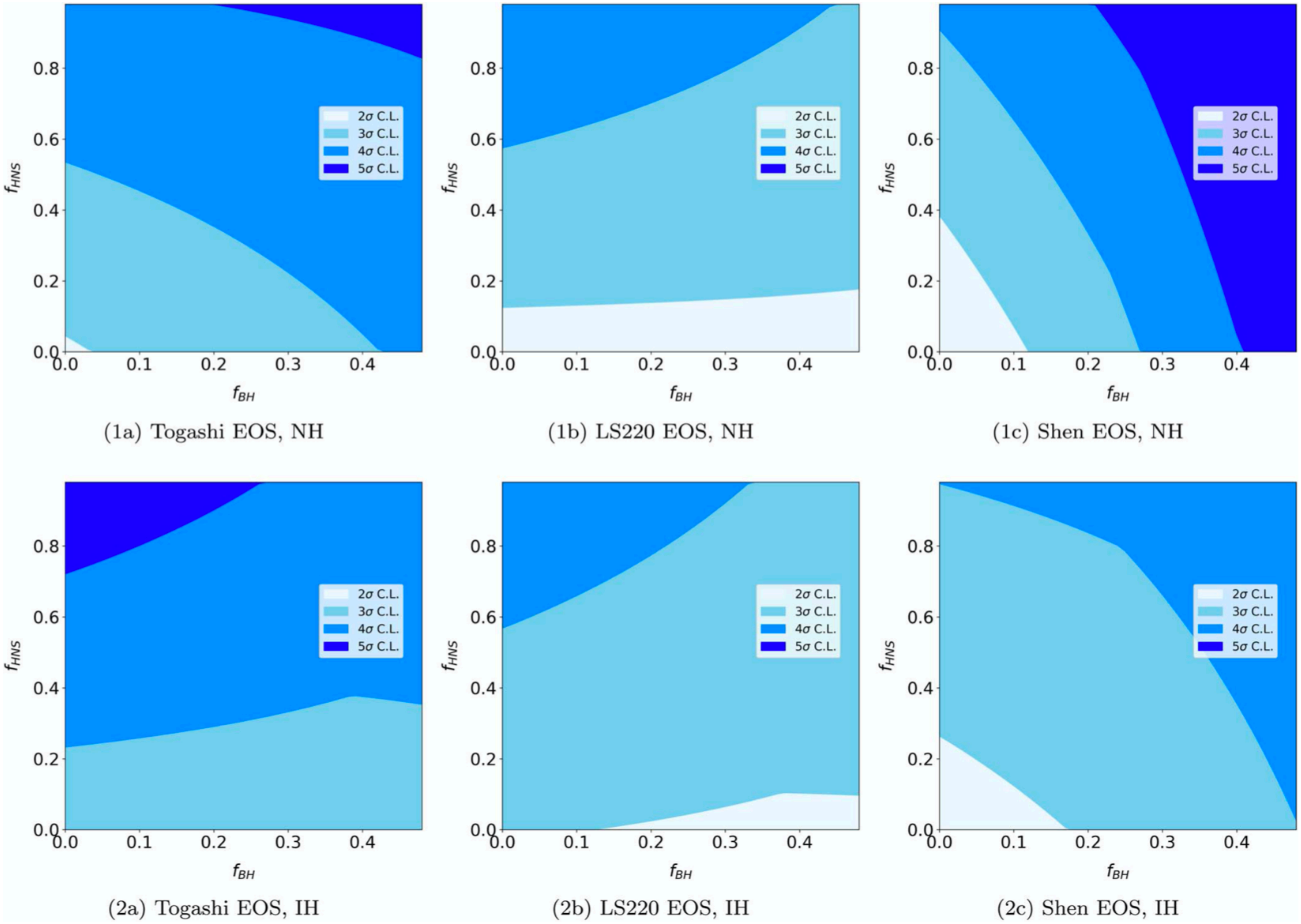

Late Time BH Formation

- Some models predict BH formation with a significant delay (>>1 sec), predicting up to ×~2 larger released neutrino energy because of more mass accretion.
- This leads to stricter constraints on f_{BH} (most obvious in Shen EOS case).

Hyper-K 10yr (Togashi EOS)

D. Kresse et al., ApJ 909, 169 (2021)

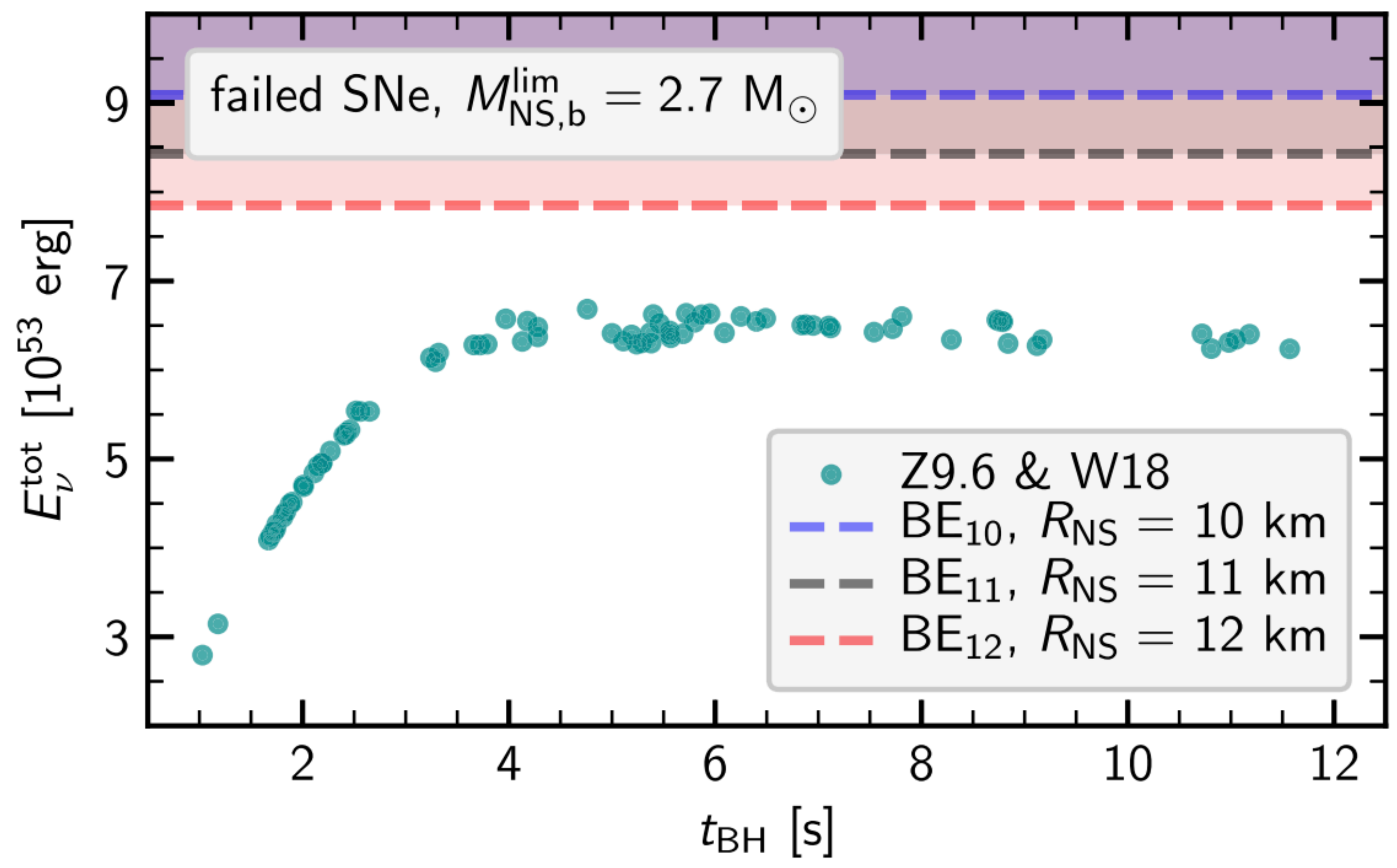

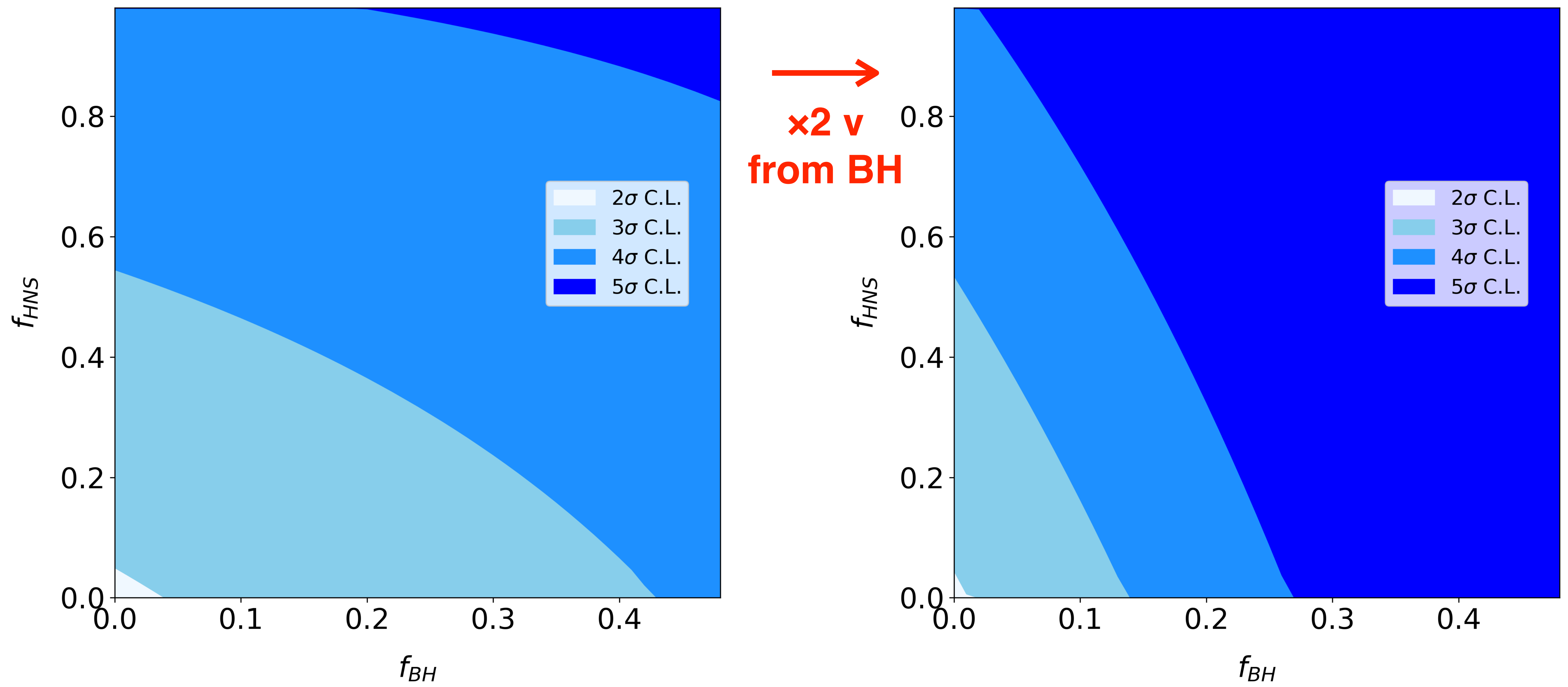

The Astrophysical Journal, 953:151 (9pp), 2023 August 20 https://doi.org/10.3847/1538-4357/ace3ba

Diffuse Neutrino Flux Based on the Rates of Core-collapse Supernovae and Black Hole Formation Deduced from a Novel Galactic Chemical Evolution Model

Yosuke Ashida[1,2], Ken'ichiro Nakazato[3], and Takuji Tsujimoto[4]
[1] Department of Physics and Astronomy, University of Utah, Salt Lake City, UT 84112, USA
[2] Department of Physics and Wisconsin IceCube Particle Astrophysics Center, University of Wisconsin-Madison, Madison, WI 53706, USA
[3] Faculty of Arts and Science, Kyushu University, Fukuoka 819-0395, Japan
[4] National Astronomical Observatory of Japan, Mitaka, Tokyo 181-8588, Japan
Received 2023 May 22; revised 2023 July 1; accepted 2023 July 2; published 2023 August 14

Abstract

Fluxes of the diffuse supernova neutrino background (DSNB) are calculated based on a new modeling of galactic chemical evolution, where a variable stellar initial mass function (IMF), depending on the galaxy type, is introduced and black hole (BH) formation from the failed supernova is considered for progenitors heavier than $18M_{\odot}$. The flux calculations are performed for different combinations of the star formation rate, nuclear equation of state, and neutrino mass hierarchy, to examine the systematic effects from these factors. In any case, our new model predicts the enhanced DSNB $\bar{\nu}_e$ flux at $E_\nu \gtrsim 30$ MeV and $E_\nu \lesssim 10$ MeV, due to more frequent BH formation and a larger core-collapse rate at high redshifts in early-type galaxies, respectively. Event rate spectra of the DSNB $\bar{\nu}_e$ at a detector from the new model are shown, and the detectability at water-based Cherenkov detectors, Super-Kamiokande with a gadolinium dissolution and Hyper-Kamiokande, is discussed. In order to investigate the impacts of the assumptions in the new model, we prepare alternative models, based on different IMF forms and treatments of BH formation, and estimate the discrimination capabilities between the new and alternative models at these detectors.

Unified Astronomy Thesaurus concepts: Neutrino astronomy (1100); Supernova neutrinos (1666); Core-collapse supernovae (304); Massive stars (732); Neutron stars (1108); Black holes (162); Galaxy chemical evolution (580); Star formation (1569); Initial mass function (796)

Constructing New Framework: CCSN Mass Limit

- We set the maximum mass of progenitors for successful explosions to **18M$_{Sun}$**.
  - Observationally, m_{min} ~ 8M$_{Sun}$ and m_{max} ~ 18M$_{Sun}$ are supported.
  - There is a theoretical work that implies failed SNe above ~20M$_{Sun}$.
- Many galactic chemical evolution schemes adopt a high m_{max} (50~100M$_{Sun}$).
  - Our m_{max} =18M$_{Sun}$ assumption reduces the number of CCSNe to **~70%**.
  - Accordingly, the total amount of heavy elements is reduced to **~50%**.

S. J. Smartt, PASA 32 (2015)

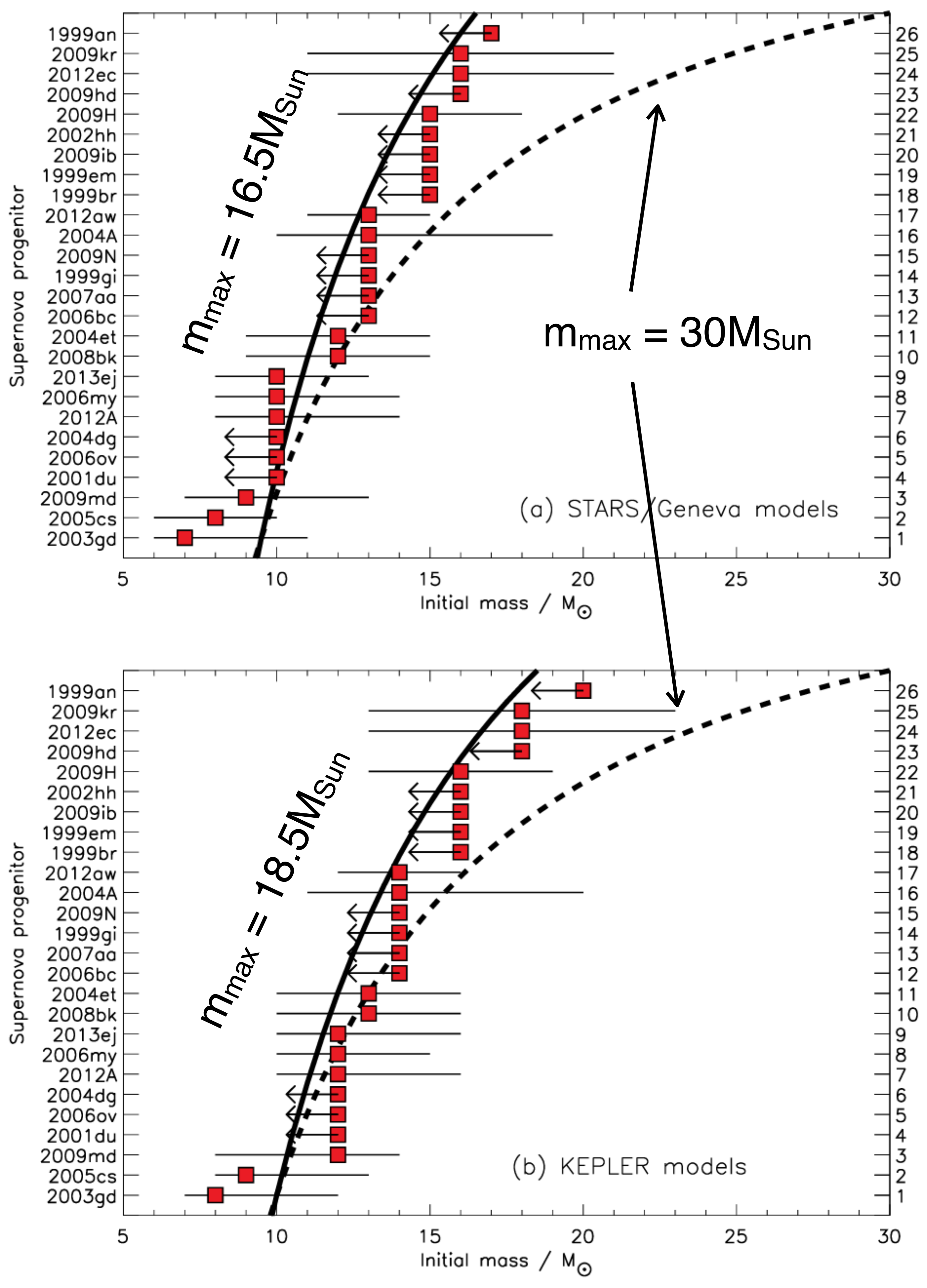

T. Sukhbold et al., ApJ 821, 38 (2016)

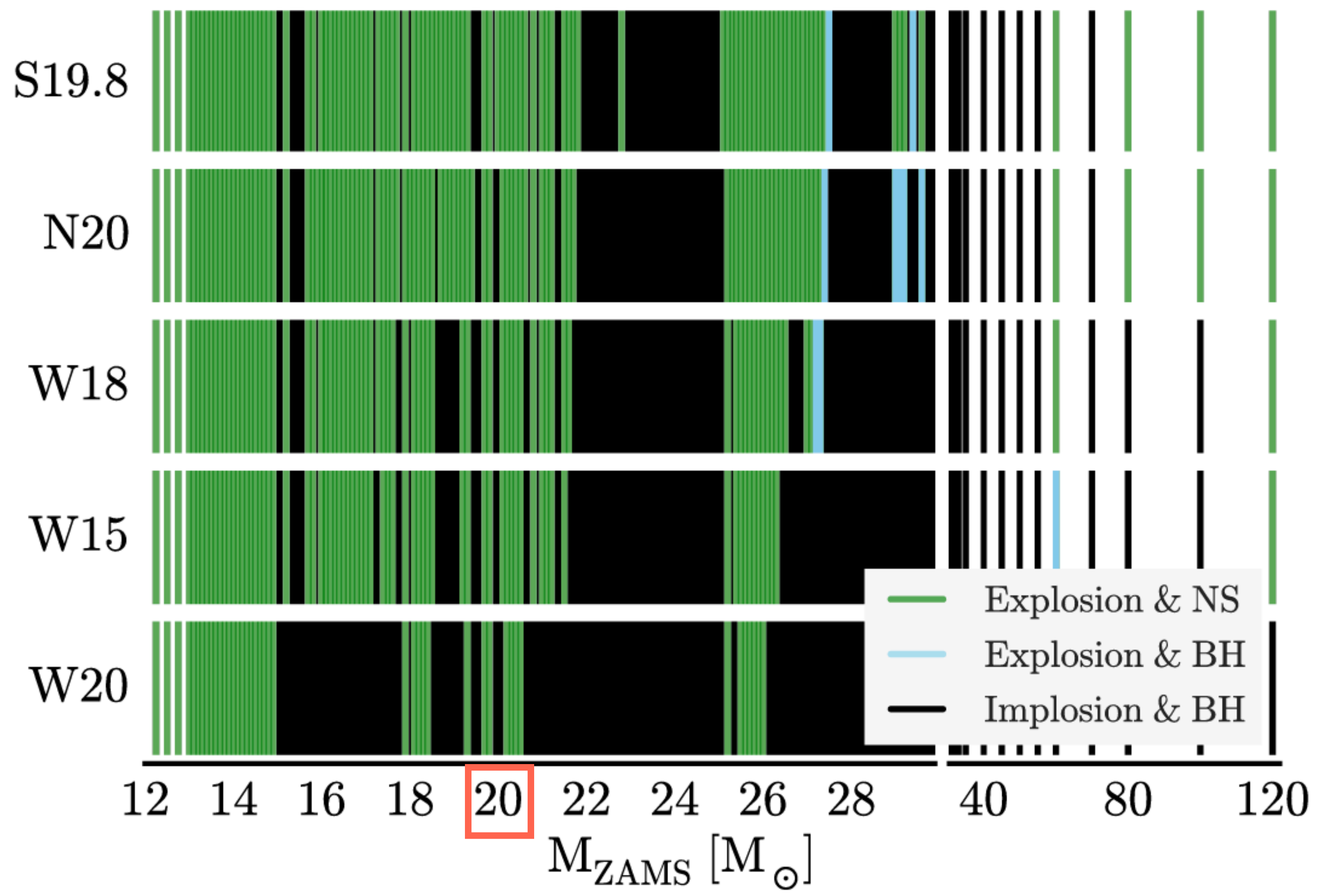

Constructing New Framework: Variable IMF

T. Tsujimoto, MNRAS 518, 3475 (2023)

- In order to achieve consistency with observed chemical abundance, we propose a new evolution model.
- We categorize galaxies into five and assume different initial mass functions (IMF) depending types.
- The fraction for BH formation from this model is **33~42%** (higher rate than many other DSNB models).

How star formation proceeds?

moderate mode

late-type galaxies (Sbc, Scd, Sdm)

Salpeter IMF

(x = –1.35)

bursting mode

early-type galaxies (E/S0, Sab)

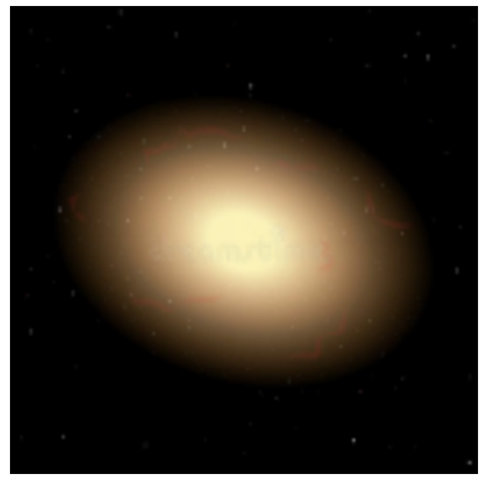

Flat IMF

(x = –0.9)

f_{BH} = 4~39% from failed SN monitoring (C. M. Basinger et al., arXiv:2007.15658)

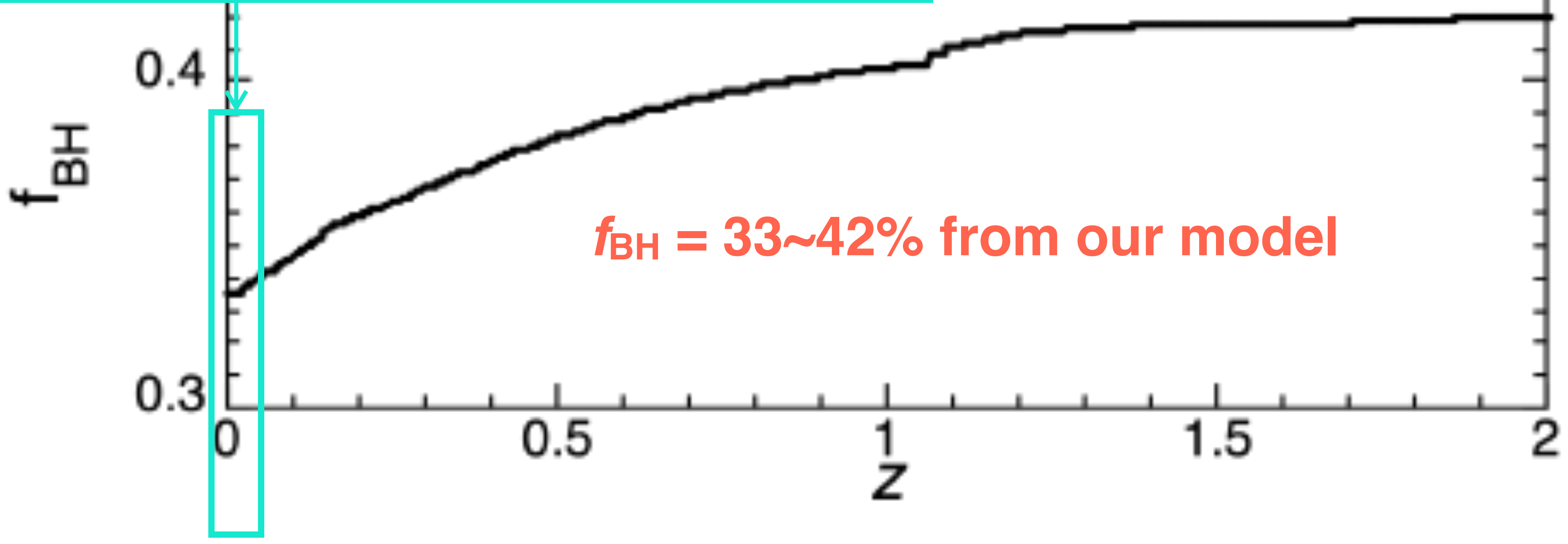

Our model nomenclature

Name	IMF form	BH treatment
GDIMF-wBH (ref.)	Variable	BHs for 18–100$M_\odot$
GDIMF-noBH	Variable	No BH
SalIMF-wBH	Salpeter	BHs for 18–100$M_\odot$
SalIMF-noBH	Salpeter	No BH

Calculated DSNB Flux

- Our model shows DSNB flux enhancements at high and low energies.
- High energy (>30 MeV): Large contribution from BH formation.
- Low energy (<10 MeV): Redshifted neutrinos from early-type galaxies with large CCSN rates.

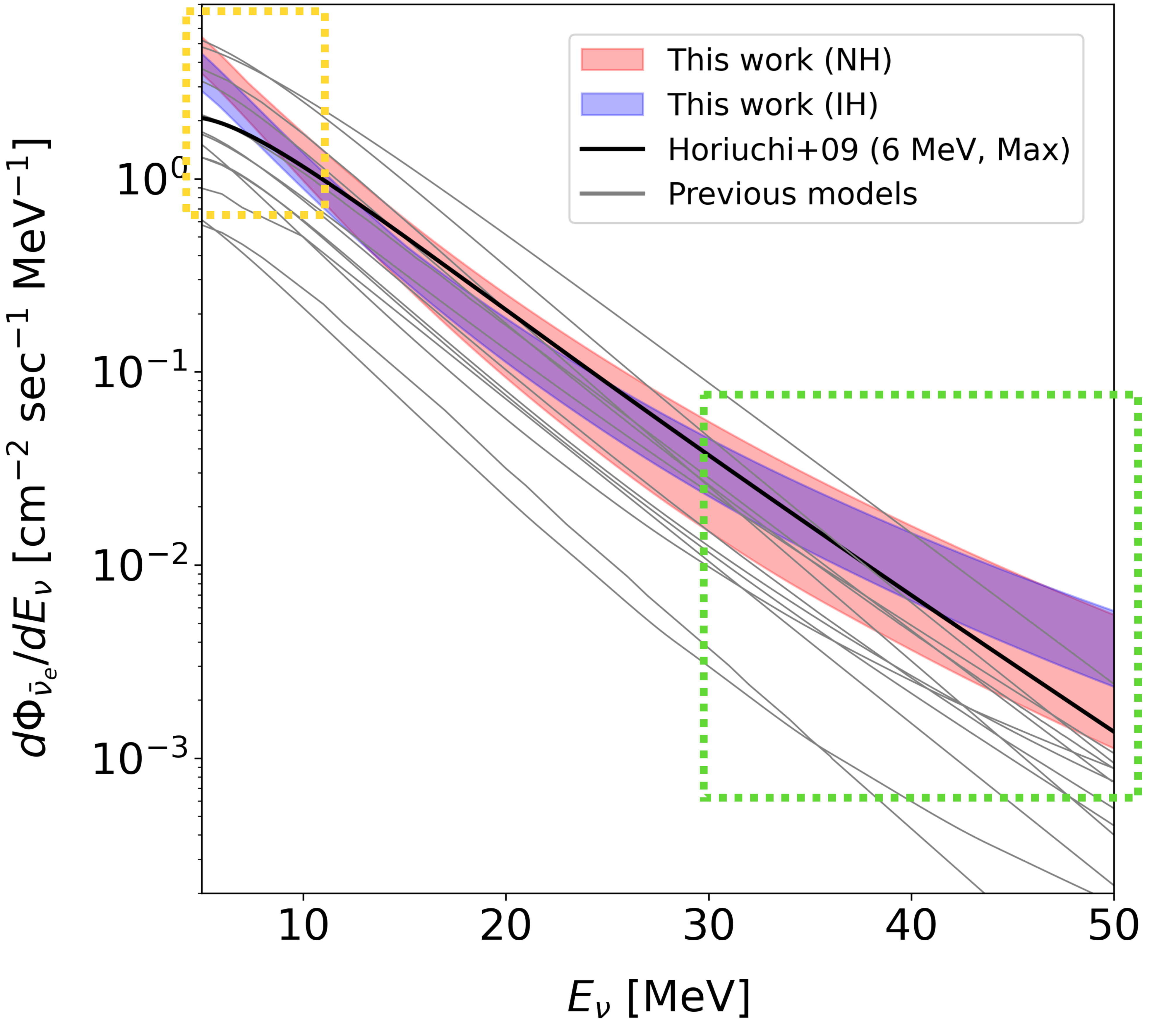

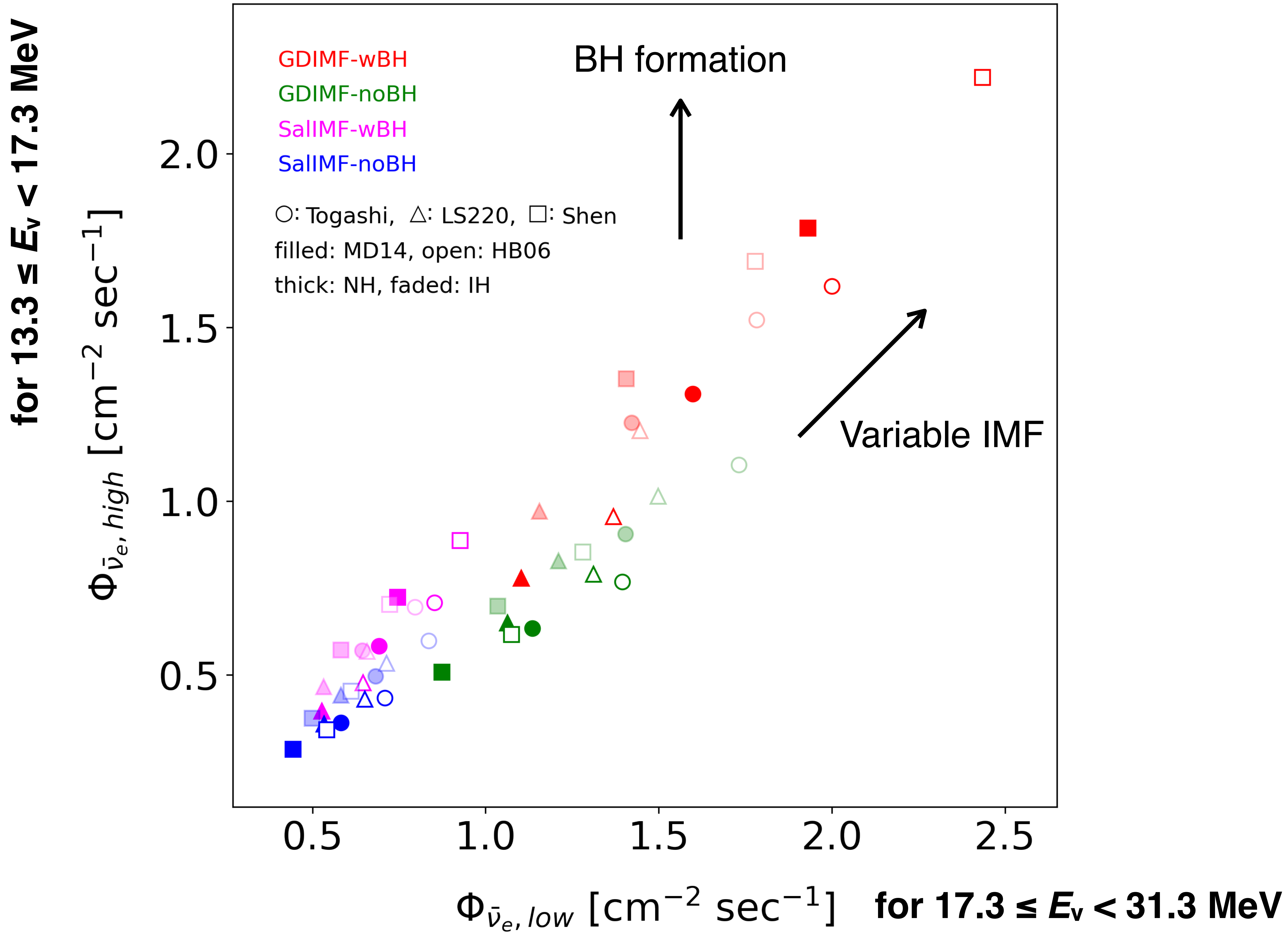

Event Rate

- Event rate spectrum at a water volume is calculated with IBD cross section.
- SK-Gd w/ 70% ntag efficiency over 10yr = 15~18 signals
- Hyper-K w/ Super-K ntag efficiency over 10yr = 50~60 signals

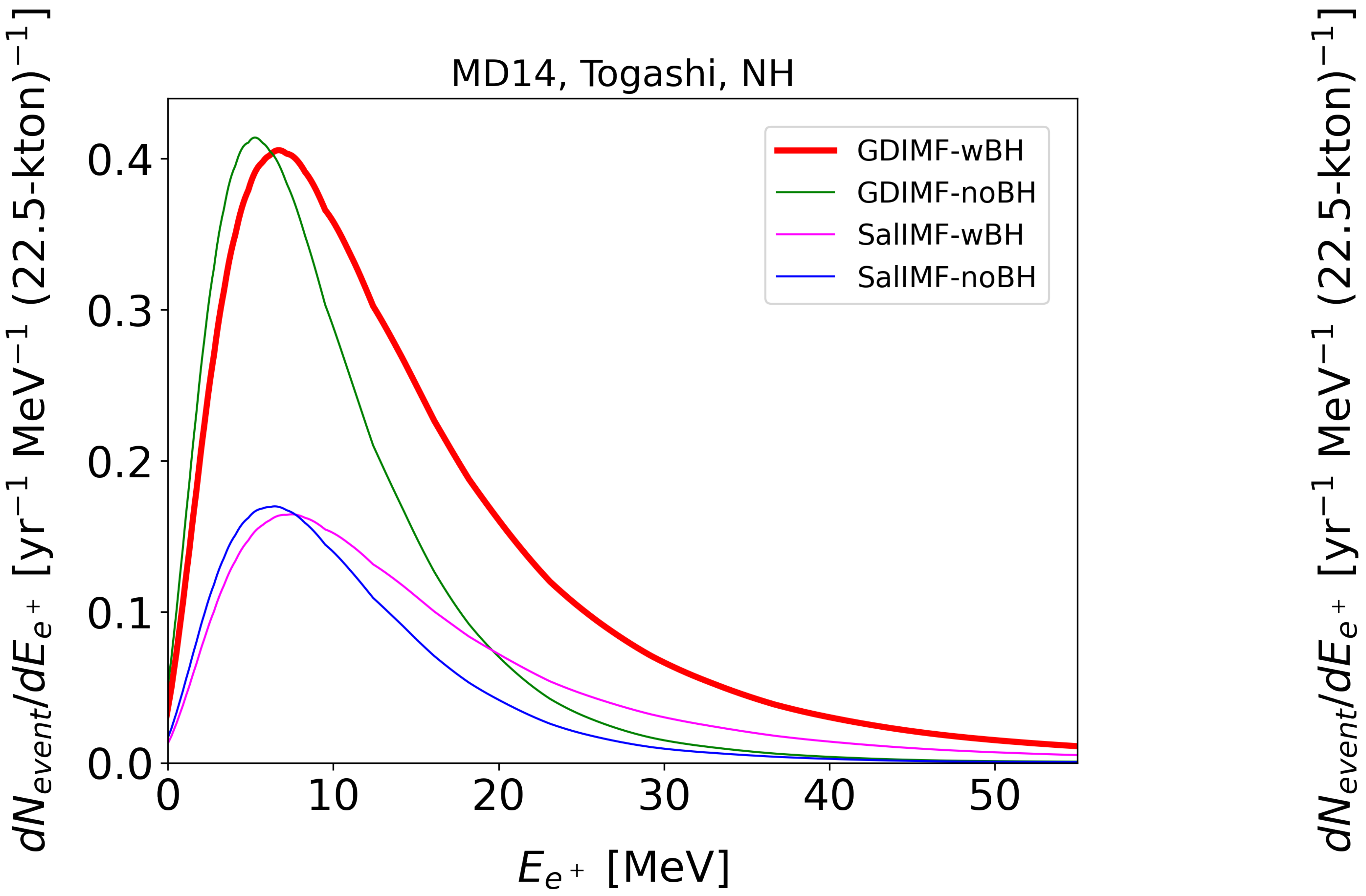

Sensitivity Estimation

Bayes' theorem:

$$\underbrace{P(\text{model}|\text{data})}_{\text{Posterior}} = \frac{\overbrace{P(\text{data}|\text{model})}^{\text{Likelihood (frequentist)}} \times \overbrace{P(\text{model})}^{\text{Prior}}}{\underbrace{\sum_{\text{model}} P(\text{data}|\text{model}) \times P(\text{model})}_{\text{Normalization}}}$$

- Prior: P(model) = 1/N for testing N models.
- Likelihood: prepared based on signal+background expectations for each model.
- Utilize two energy ranges (13.3–17.3 MeV & 17.3–31.3 MeV).
- Use real data for SK-IV, and nominal expectations for SK-Gd and Hyper-K.

Likelihood

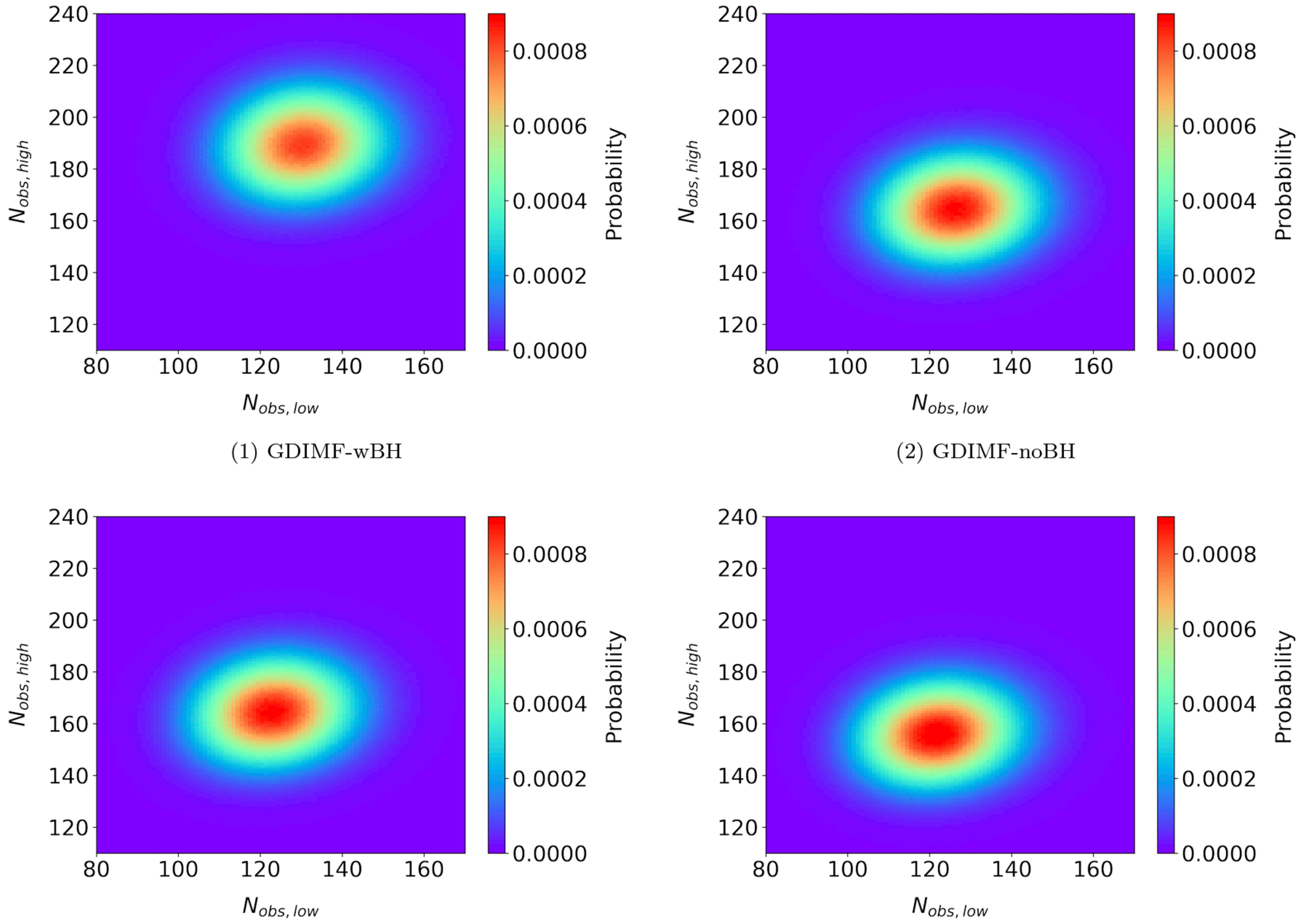

(1) GDIMF-wBH

(2) GDIMF-noBH

(3) SalIMF-wBH

(4) SalIMF-noBH

Signal Significance

- Our reference model is tested against background only at different detectors based on Bayes' theorem.
- Background model used for likelihood is based on extrapolation from Super-K analysis.
- In most cases, our signal models can be detected well over background.

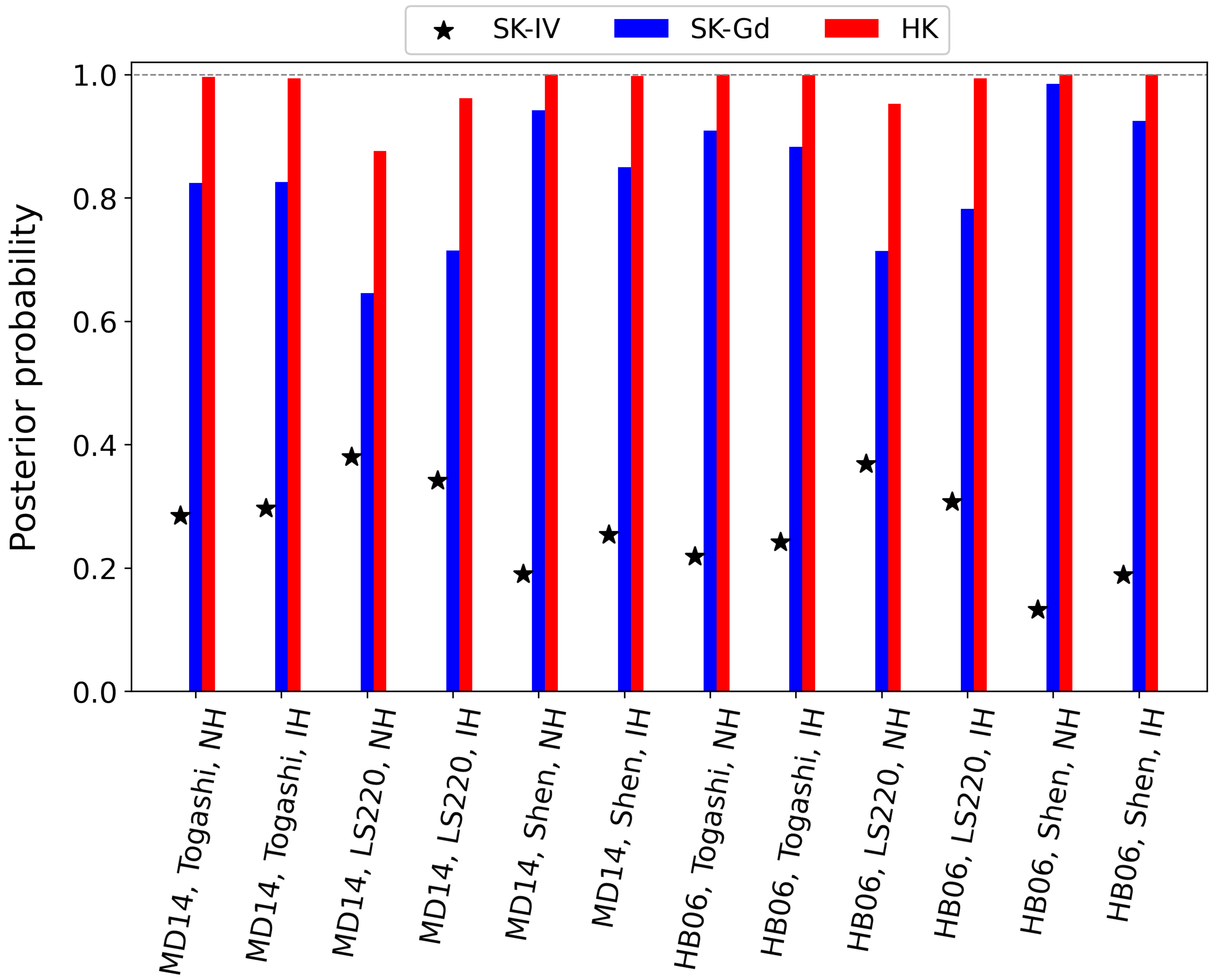

Model Discrimination

- Our reference model is tested against alternative models with different assumptions on IMF and BH.
- In NH case, the reference model is well discriminated from others.
- In IH case, only IMF assumption can be tested well.
- The results differ for other choices of SFR and nuclear EOS (all results are discussed in the paper).

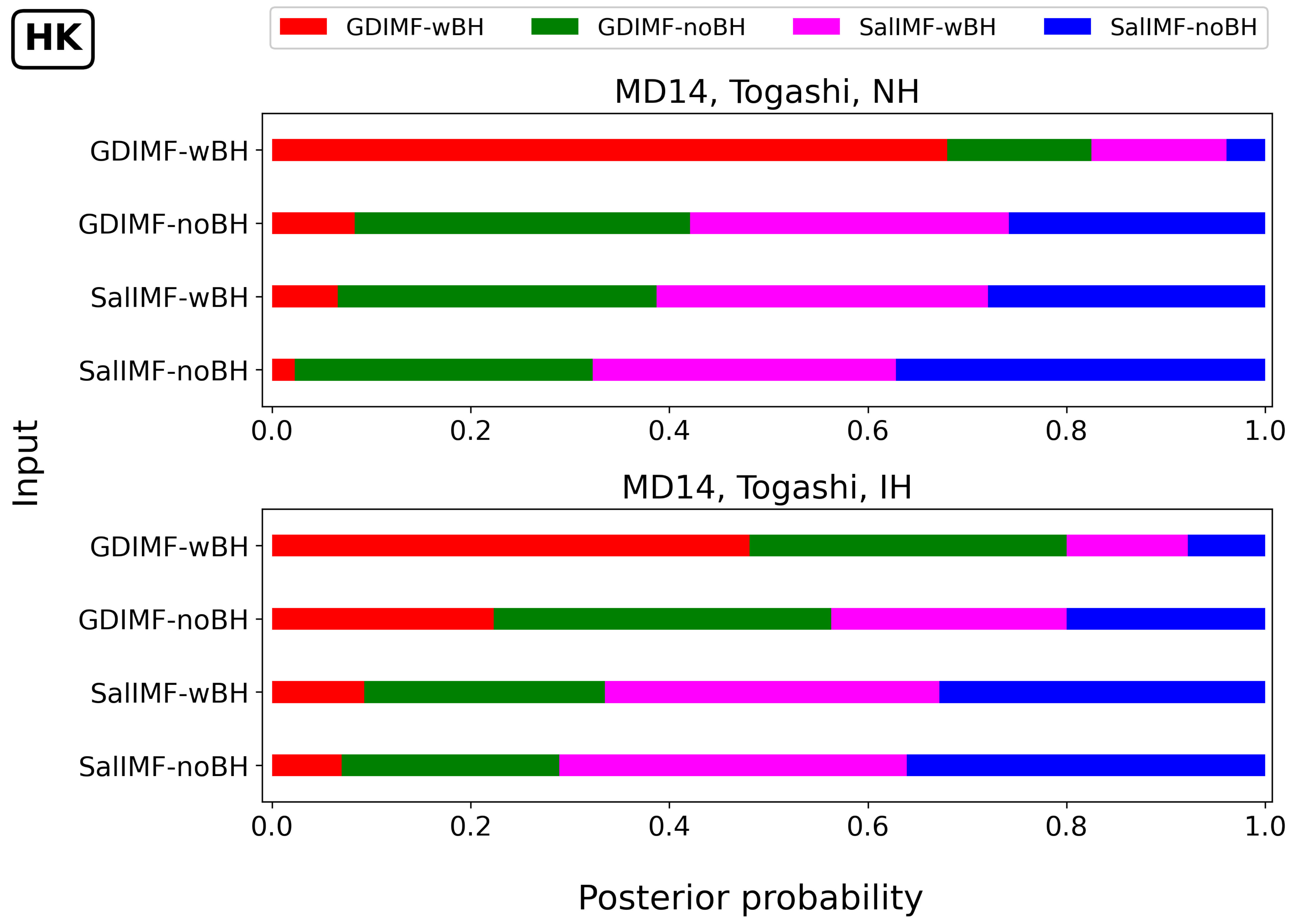

EOS & SFR Dependences

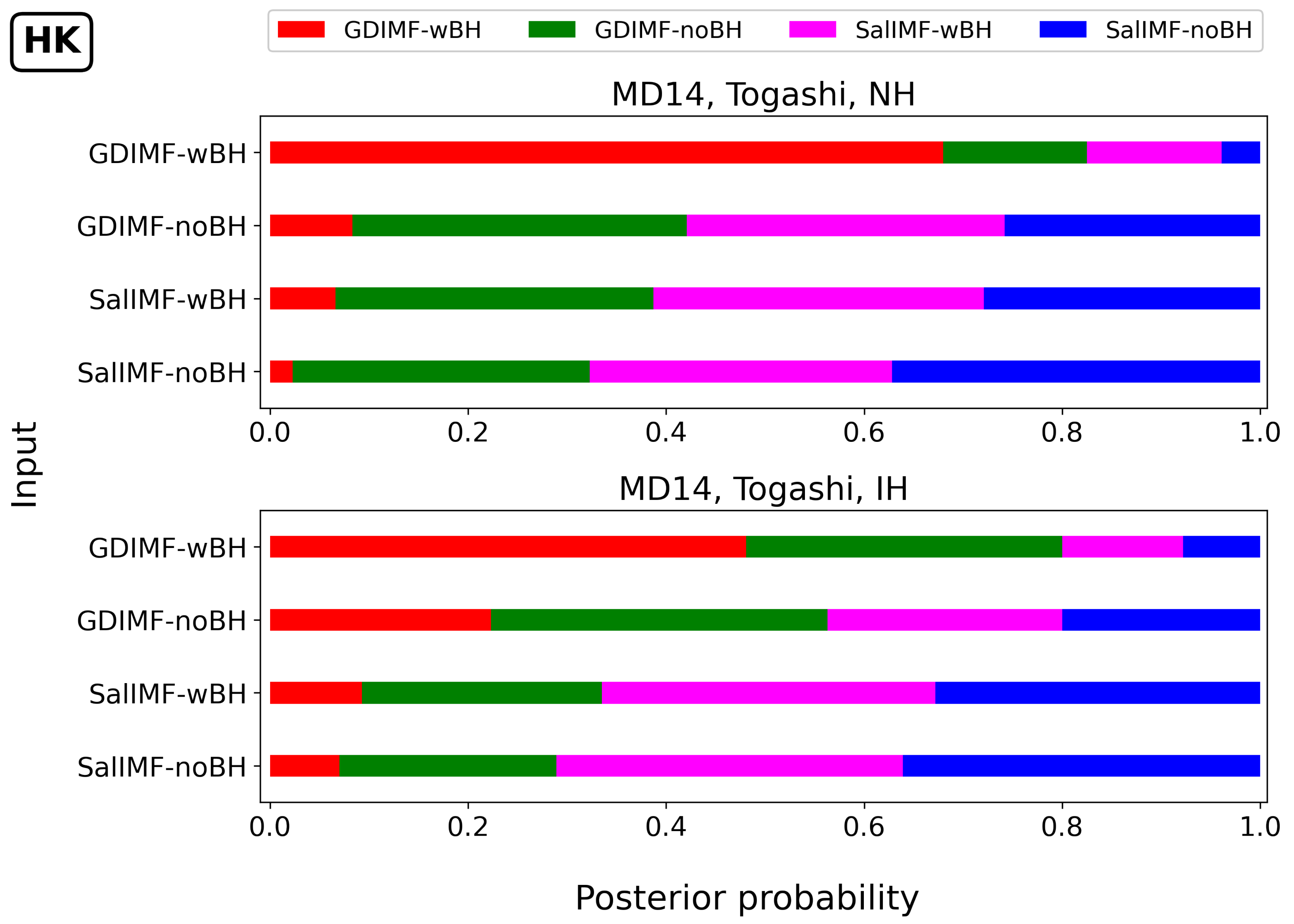

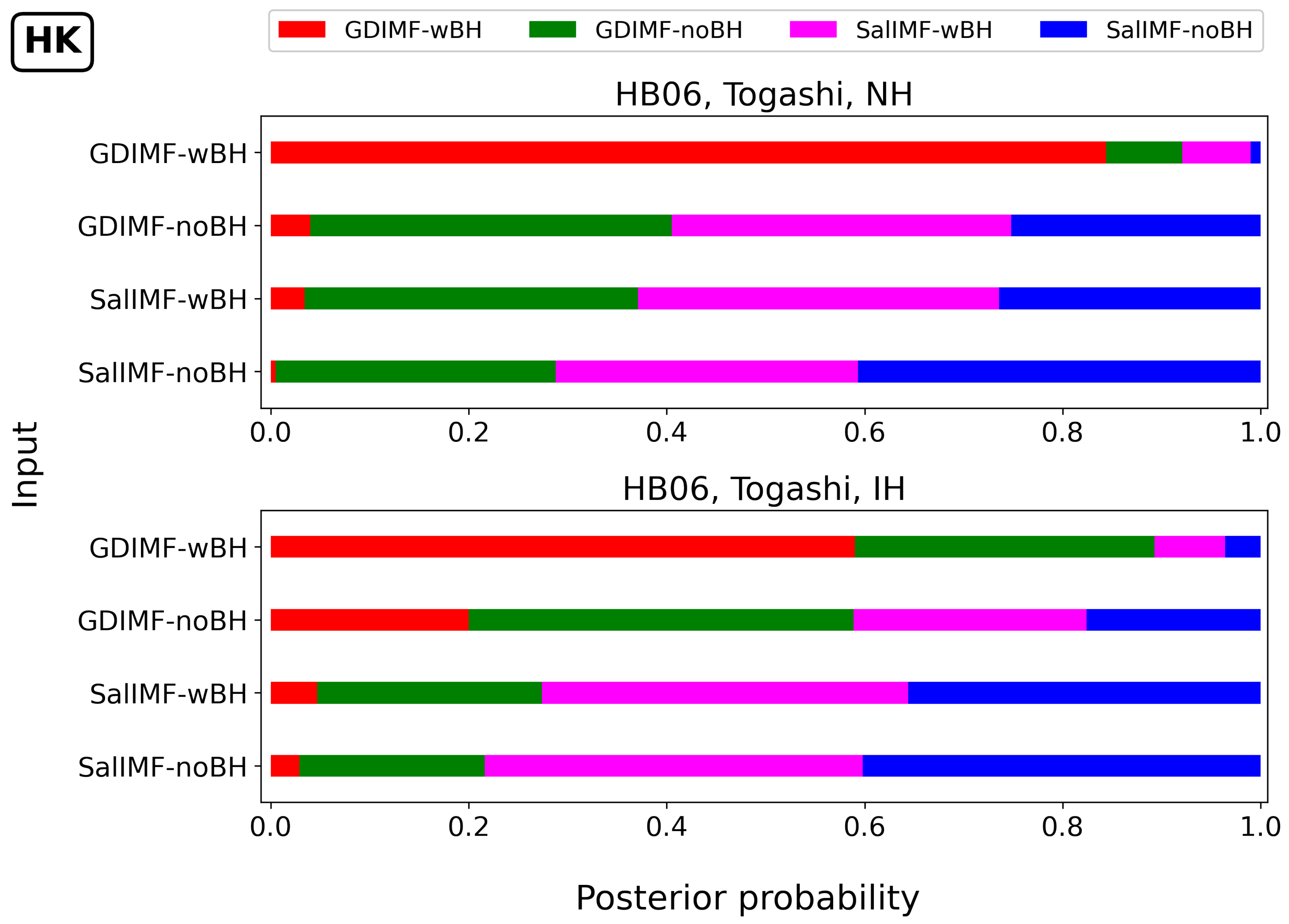

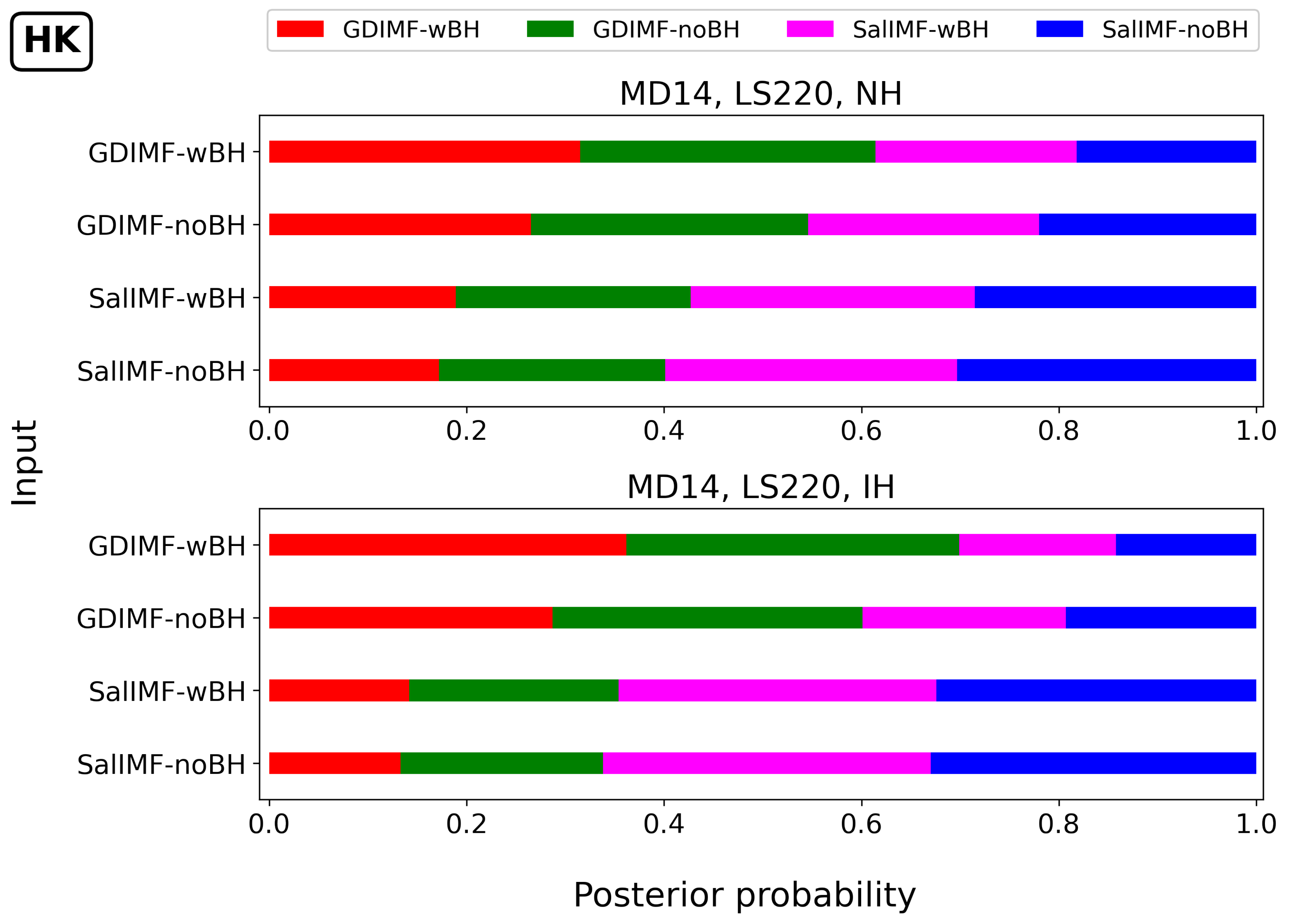

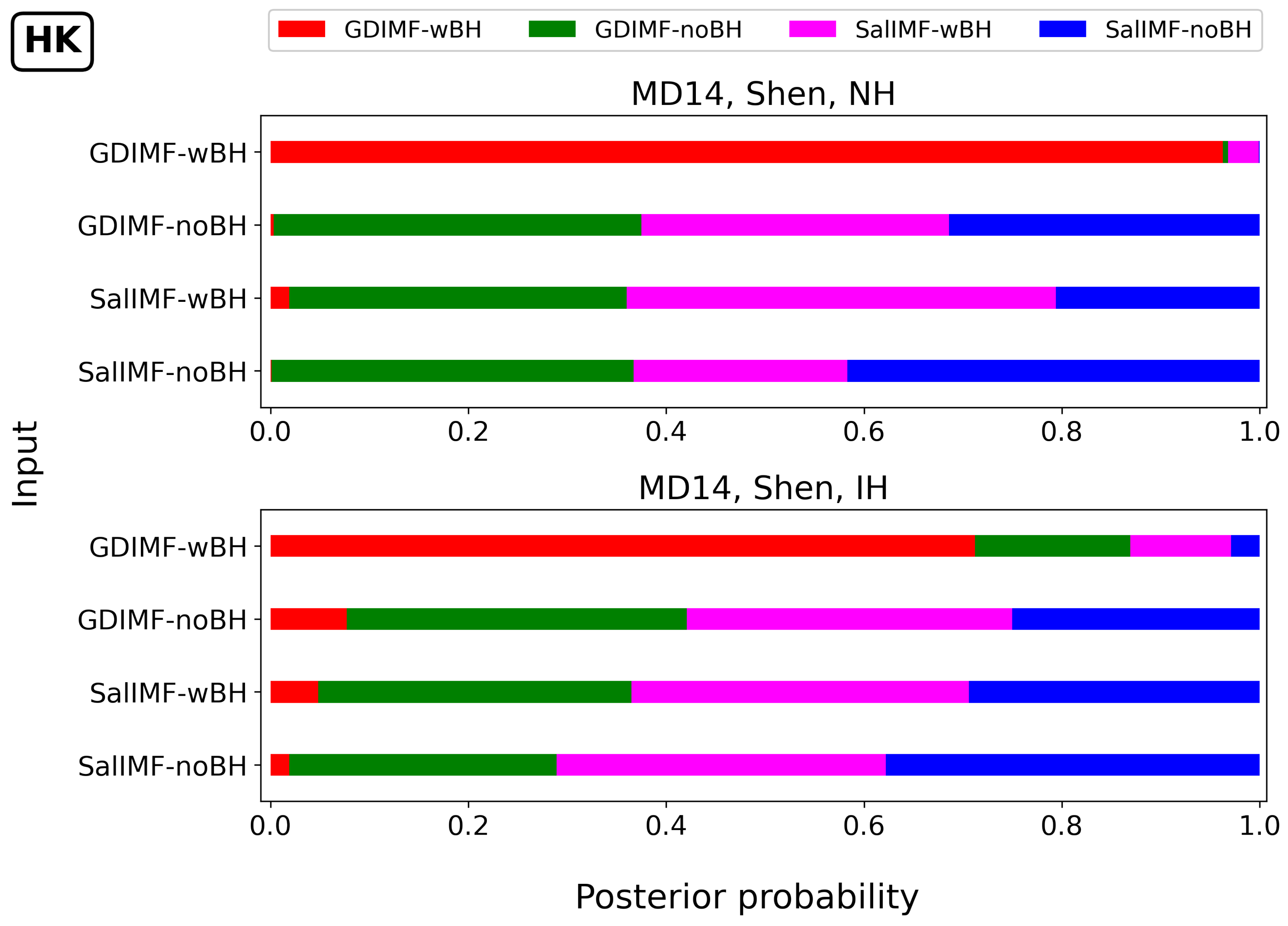

Summary

- **ApJ 937, 30 (2022): New proposal to constrain stellar collapse fate with DSNB**
  - Model implemented based on numerical calculations performed separately for the canonical mass neutron star, the high mass neutron star, and the black hole.
  - Sensitivity to the fractions of each remnant estimated for different nuclear EOS and mass hierarchy.

- **ApJ 953, 151 (2023): DSNB flux based on a novel galactic chemical evolution model**
  - New evolution model proposed based on the assumptions of BH formation for progenitors with $>18M_{Sun}$ and galaxy-dependent IMF.
  - The resulting DSNB flux showing a unique feature of enhancements at high and low energies.
  - Signal detectability and model discrimination possibility discussed.

Thanks for your attention!

Supplements

"Neutrino Heating" Scenario

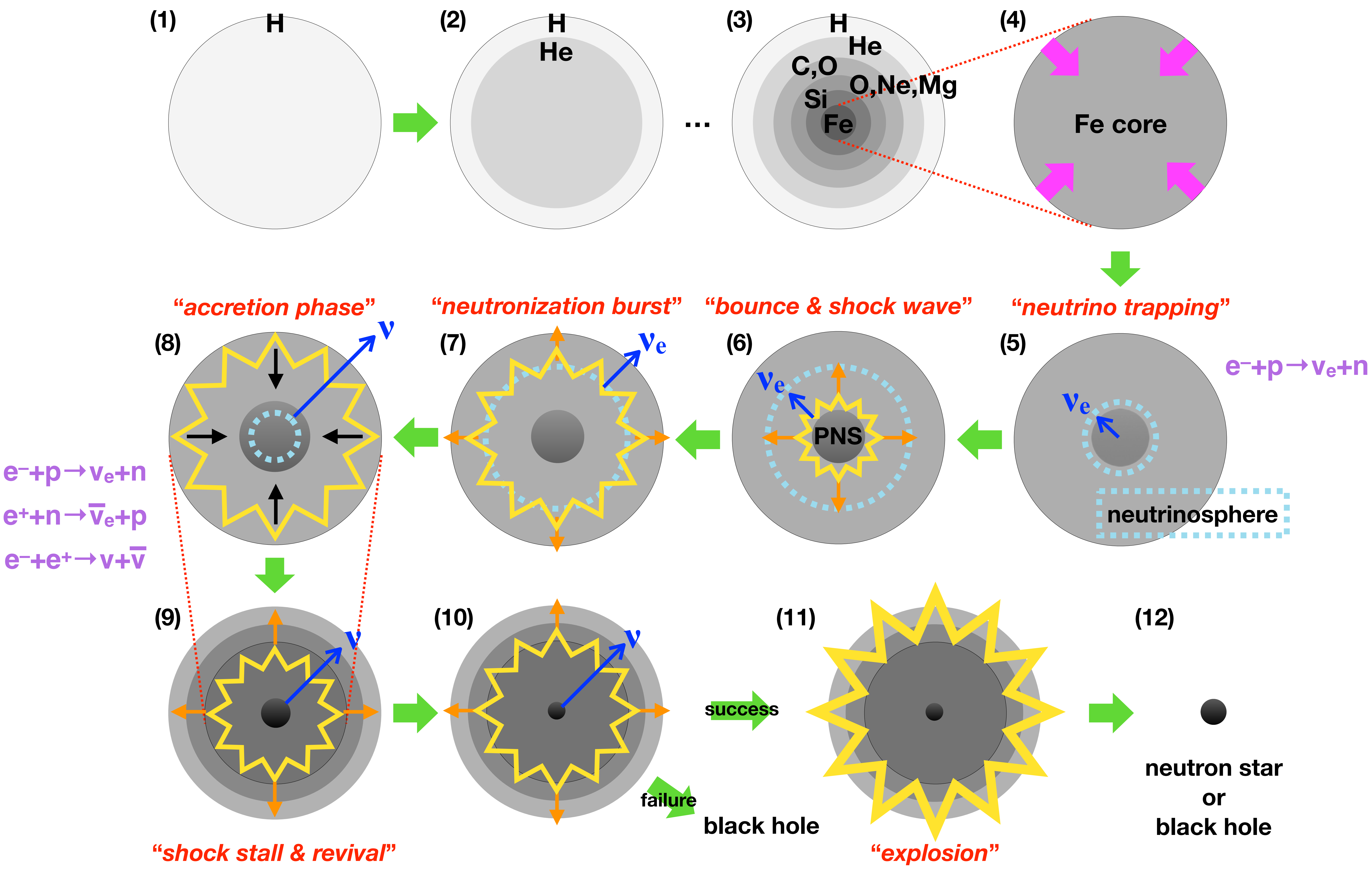

Mass Hierarchy Impact

$$\begin{aligned}\frac{dN_{\bar{\nu}_e}}{dE_\nu} &= |U_{e1}|^2\frac{dN_{\bar{\nu}_1}}{dE_\nu} + |U_{e2}|^2\frac{dN_{\bar{\nu}_2}}{dE_\nu} + |U_{e3}|^2\frac{dN_{\bar{\nu}_3}}{dE_\nu} \\ &= \cos^2\theta_{12}\cos^2\theta_{13}\frac{dN_{\bar{\nu}_1}}{dE_\nu} + \sin^2\theta_{12}\cos^2\theta_{13}\frac{dN_{\bar{\nu}_2}}{dE_\nu} + \sin^2\theta_{13}\frac{dN_{\bar{\nu}_3}}{dE_\nu} \\ &\sim 0.68\cdot\frac{dN_{\bar{\nu}_1}}{dE_\nu} + 0.30\cdot\frac{dN_{\bar{\nu}_2}}{dE_\nu} + 0.02\cdot\frac{dN_{\bar{\nu}_3}}{dE_\nu},\end{aligned}$$

$$\Rightarrow \quad \frac{dN_{\bar{\nu}_e}}{dE_\nu} \sim 0.68\cdot\frac{dN^0_{\bar{\nu}_e}}{dE_\nu} + 0.32\cdot\frac{dN^0_{\bar{\nu}_x}}{dE_\nu}.$$

Normal: All flavors

$$\Rightarrow \quad \frac{dN_{\bar{\nu}_e}}{dE_\nu} \sim \frac{dN^0_{\bar{\nu}_x}}{dE_\nu}.$$

Inverted: NuMu+NuTau

Contributions from Different Redshifts

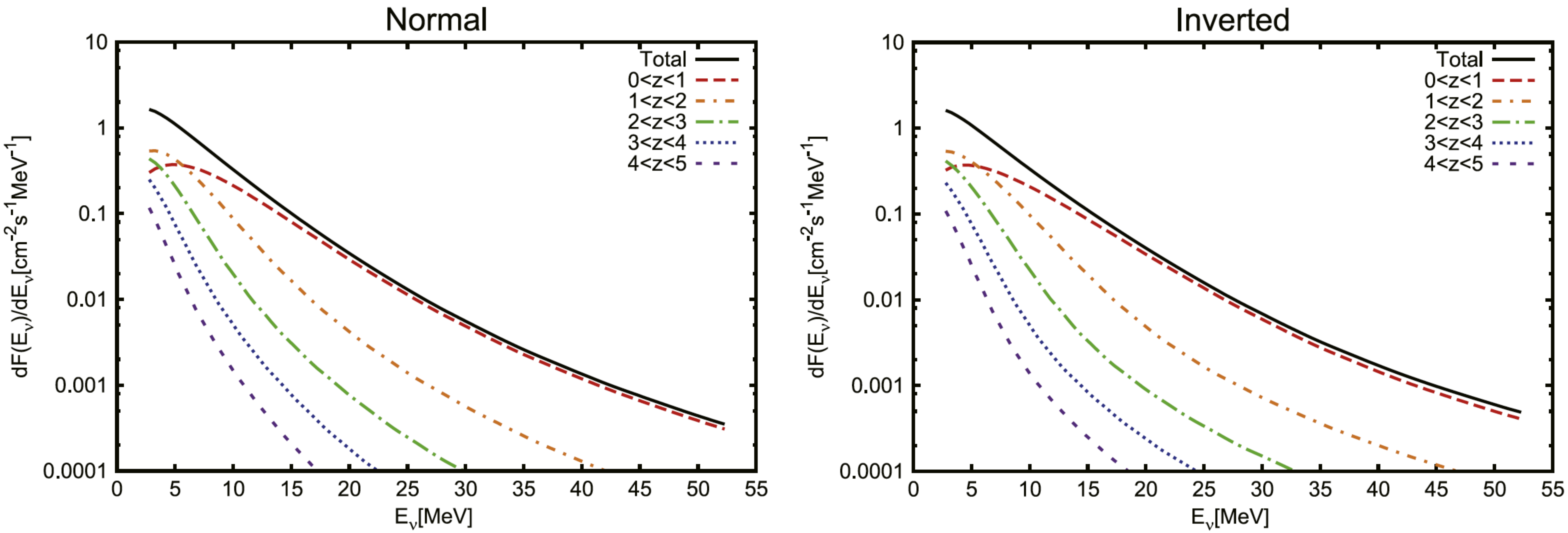

Figure 10. Total fluxes of SRNs (solid) and contributions from various redshift ranges for the reference model. The lines except for the solid line correspond, from top to bottom, to the redshift ranges $0 < z < 1, 1 < z < 2, 2 < z < 3, 3 < z < 4$, and $4 < z < 5$, for $E_\nu > 10$ MeV. The left and right panels show the cases for normal and inverted mass hierarchies, respectively.

K. Nakazato et al., ApJ 804, 75 (2015)

Nuclear EOS Impact (BH Formation Case)

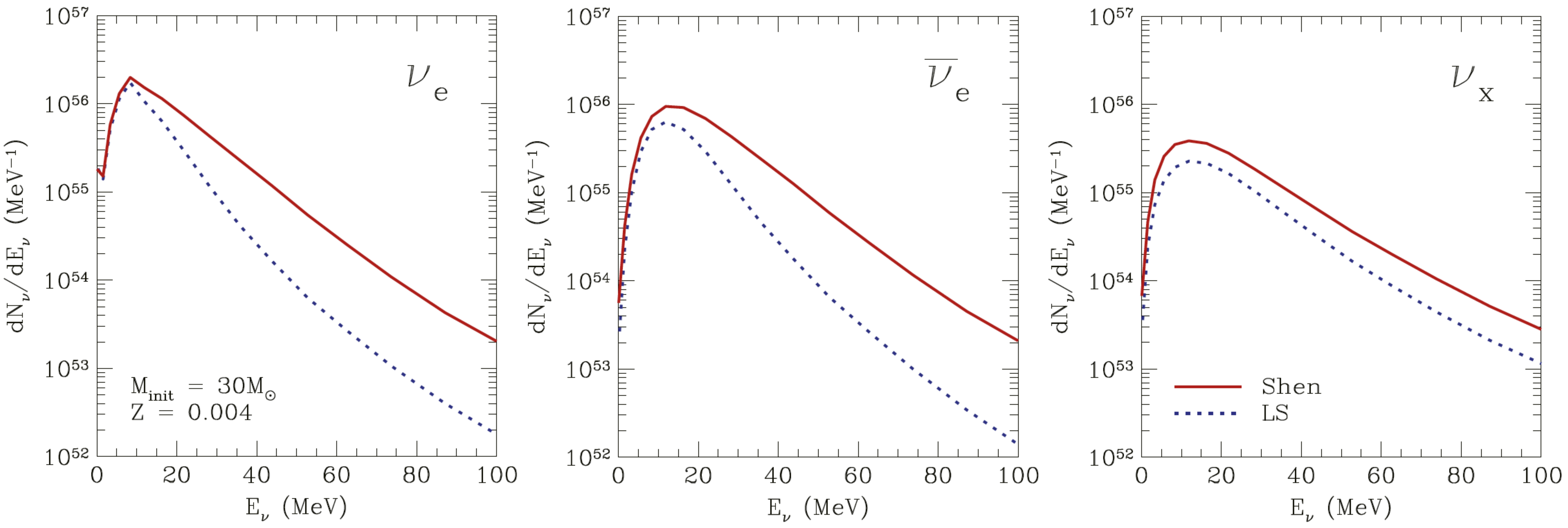

Figure 6. Neutrino number spectra for black hole formation with $30M_\odot$, $Z = 0.004$ and Shen EOS (solid) and LS EOS (dotted). The left, central, and right panels correspond to ν_e, $\bar{\nu}_e$, and ν_x $(=\nu_\mu = \bar{\nu}_\mu = \nu_\tau = \bar{\nu}_\tau)$, respectively.

Shen is stiffer than LS (maximum mass of neutron stars is higher).

K. Nakazato et al., ApJ 804, 75 (2015)

Failed SN & Electron-Capture SN Contributions

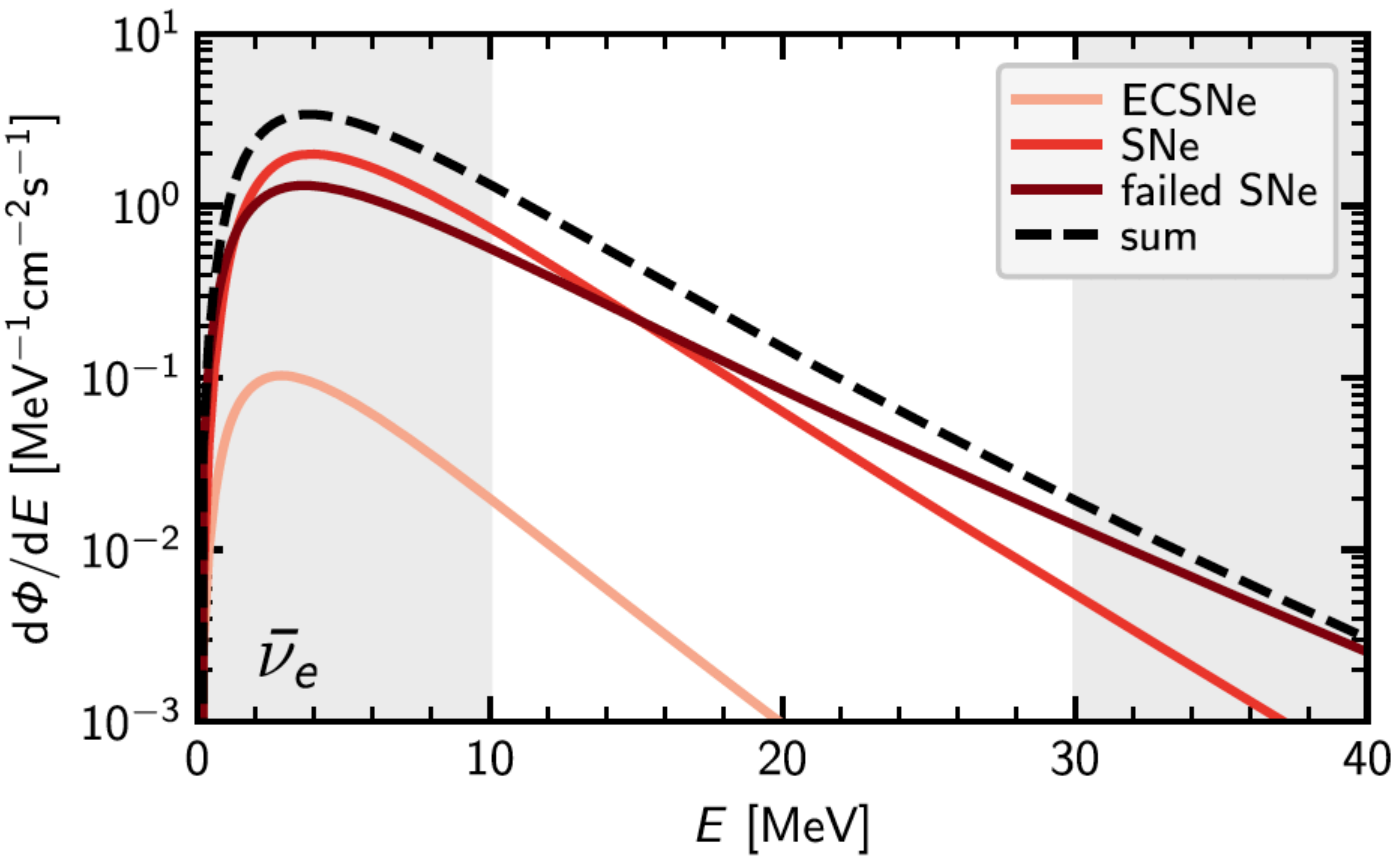

ECSNe = electron-capture supernovae
(marginal one around mass threshold, w/ ONeMg core)

D. Kresse et al., ApJ 909, 169 (2021)

Model Setup Details

Table 1. Properties of the compact remnant and time-integrated neutrino signal for each fate component.

EOS	remnant	$M_{\rm NS,g}$ $[M_\odot]$	$R_{\rm NS}$ [km]	$t_{\rm BH}$ [sec]	$\langle E_{\nu_e} \rangle$ [MeV]	$\langle E_{\bar{\nu}_e} \rangle$ [MeV]	$\langle E_{\nu_x} \rangle$ [MeV]	$E_{\nu_e,{\rm tot}}$ $[10^{52}$ erg]	$E_{\bar{\nu}_e,{\rm tot}}$ $[10^{52}$ erg]	$E_{\nu_x,{\rm tot}}$ $[10^{52}$ erg]
Togashi	canonical mass NS	1.32	11.5	—	9.2	10.9	11.8	4.47	4.07	4.37
	high mass NS	1.63	11.5	—	9.5	11.2	11.9	7.26	6.93	7.17
	BH (Failed SN)	—	—	0.533	16.1	20.4	23.4	6.85	5.33	2.89
LS220	canonical mass NS	1.34	12.7	—	9.1	10.7	11.3	4.25	3.84	3.94
	high mass NS	1.65	12.4	—	9.8	11.2	11.2	7.29	6.88	6.36
	BH (Failed SN)	—	—	0.342	12.5	16.4	22.3	4.03	2.87	2.11
Shen	canonical mass NS	1.35	14.3	—	9.0	10.6	11.3	3.65	3.22	3.35
	high mass NS	1.67	14.1	—	9.6	11.2	11.2	6.22	5.88	5.40
	BH (Failed SN)	—	—	0.842	17.5	21.7	23.4	9.49	8.10	4.00

NOTE—For the successful SN models, $M_{\rm NS,g}$ and $R_{\rm NS}$ are the gravitational mass and radius of NSs, respectively. For the failed SN models, $t_{\rm BH}$ is the time to a BH formation measured from the core bounce. $\langle E_{\nu_i} \rangle$ and $E_{\nu_i,{\rm tot}}$ are the average and total energies of the time-integrated neutrino signal for ν_i, where ν_x represents the average of ν_μ, $\bar{\nu}_\mu$, ν_τ, and $\bar{\nu}_\tau$.

Super-Kamiokande Experiment

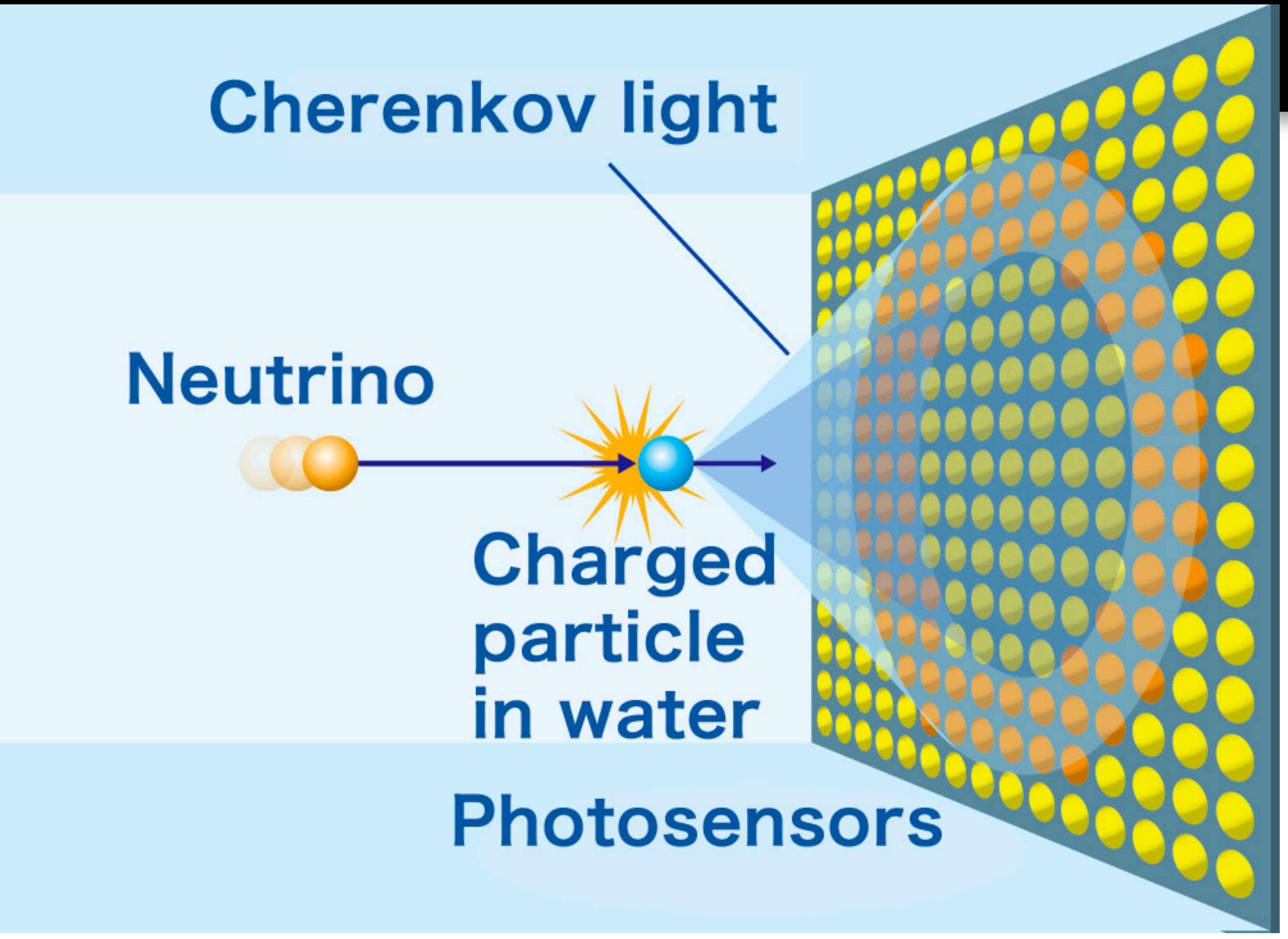

- A **water Cherenkov** detector located 1,000 m under mountain in Japan.
  - Detecting Cherenkov light emitted from relativistic changed particles in water.
- Composed of two layers;
  - ***Inner***: 11,129 20-inch PMTs, detection volume ~22.5 kton
  - ***Outer***: 1,885 8-inch PMTs, veto for atmospheric μ
- Operated since 1996, separated into *six* phases depending on detector configuration (SK-I to VI).
  - Results from SK-I to IV (5,823 days in total) will be shown.

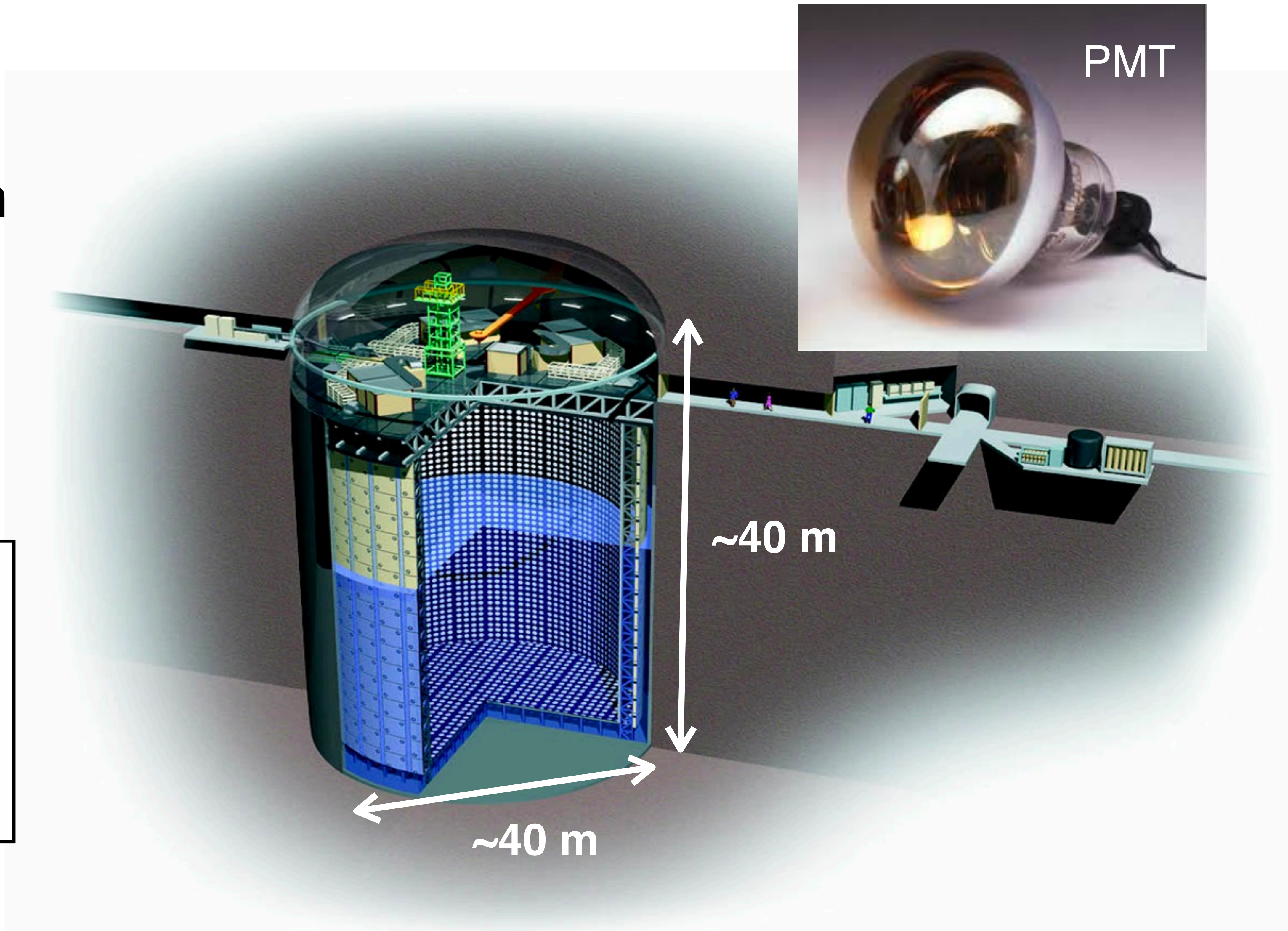

PHYSICAL REVIEW D **104,** 122002 (2021)

Diffuse supernova neutrino background search at Super-Kamiokande

K. Abe,[1,43] C. Bronner,[1] Y. Hayato,[1,43] K. Hiraide,[1] M. Ikeda,[1] S. Imaizumi,[1] J. Kameda,[1,43] Y. Kanemura,[1] Y. Kataoka,[1]

Previous Super-K Searches

1. **SK-I/II/III 2,853 days** [Phys. Rev. D 85, 052007 (2012)]
   - *No* ntag (only e^+ prompt signal)
   - Higher energy threshold ($E_\nu > 17.3$ MeV)
   - Atmospheric ν bkg estimated with old models
   - Unbinned likelihood spectral fitting

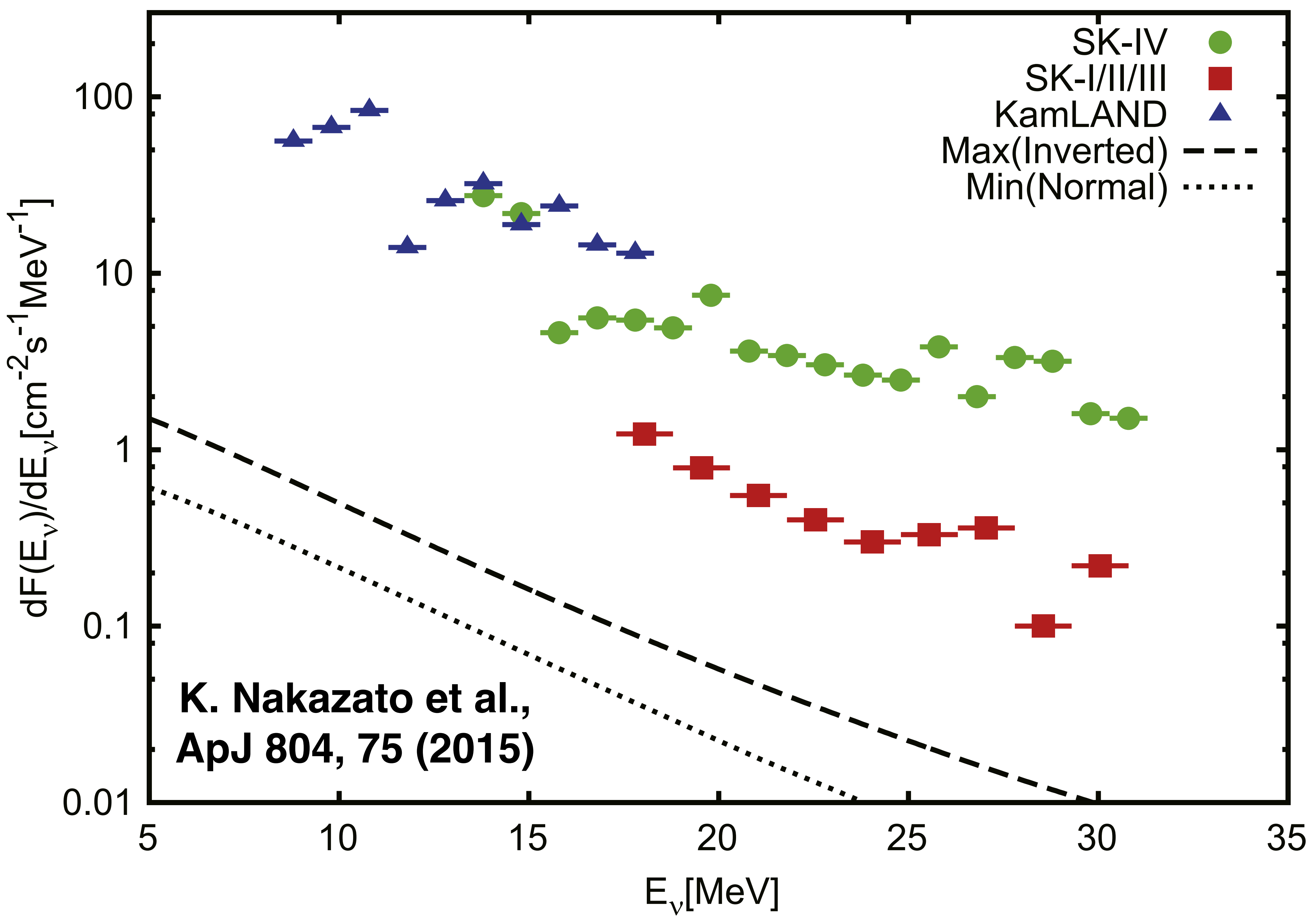

2. **SK-IV 960 days** [Astropart. Phys. 60, 41 (2015)]
   - Ntag applied for the first time (electronics upgrade in SK-IV)
   - Poor performance of spallation cut & ntag
   - Only accidental bkg estimated (underestimate of bkg)
     - *No* framework for ntag on atmospheric ν simulations
     - *No* reliable method for estimation of ^{9}Li
   - Bin-by-bin differential upper limits; no spectral fitting result

New analysis improves *pros* and solves *cons* in old analyses!

Improvements in SK-IV Analysis

- ★ Larger statistics: SK-IV 2,970 days + SK-I/II/III 2,853 days (5,823 days in total)
- ★ Better ntag performance
- ★ Improved spallation cut

→ Search energy threshold lowered

- ★ Novel method of estimating spallation ^{9}Li bkg developed
- ★ More reliable and precise estimation of atmospheric ν bkg
- ★ Bin-by-bin upper limits & unbinned likelihood fitting performed w/ better systematic uncertainty treatment

Most sensitive search achieved!

★ My work
★ My colleagues' work

DSNB Signal at Super-K

- Signal = **inverse beta decay (IBD)**, $\bar{\nu}_e$ **+ p → e⁺ + n** (largest xsec)
  - **e^+** = "*prompt*" signal (main signal range: **10~30 MeV**)
  - **n** = "*delayed*" signal via **a 2.2 MeV γ-ray** from thermal capture on hydrogen (**$\tau \sim$ 200 μs**)

- Many types of backgrounds mimicking this signature.
  - Need to *reduce* them to as much as DSNB signal.
  - Need to *precisely model/estimate* them.

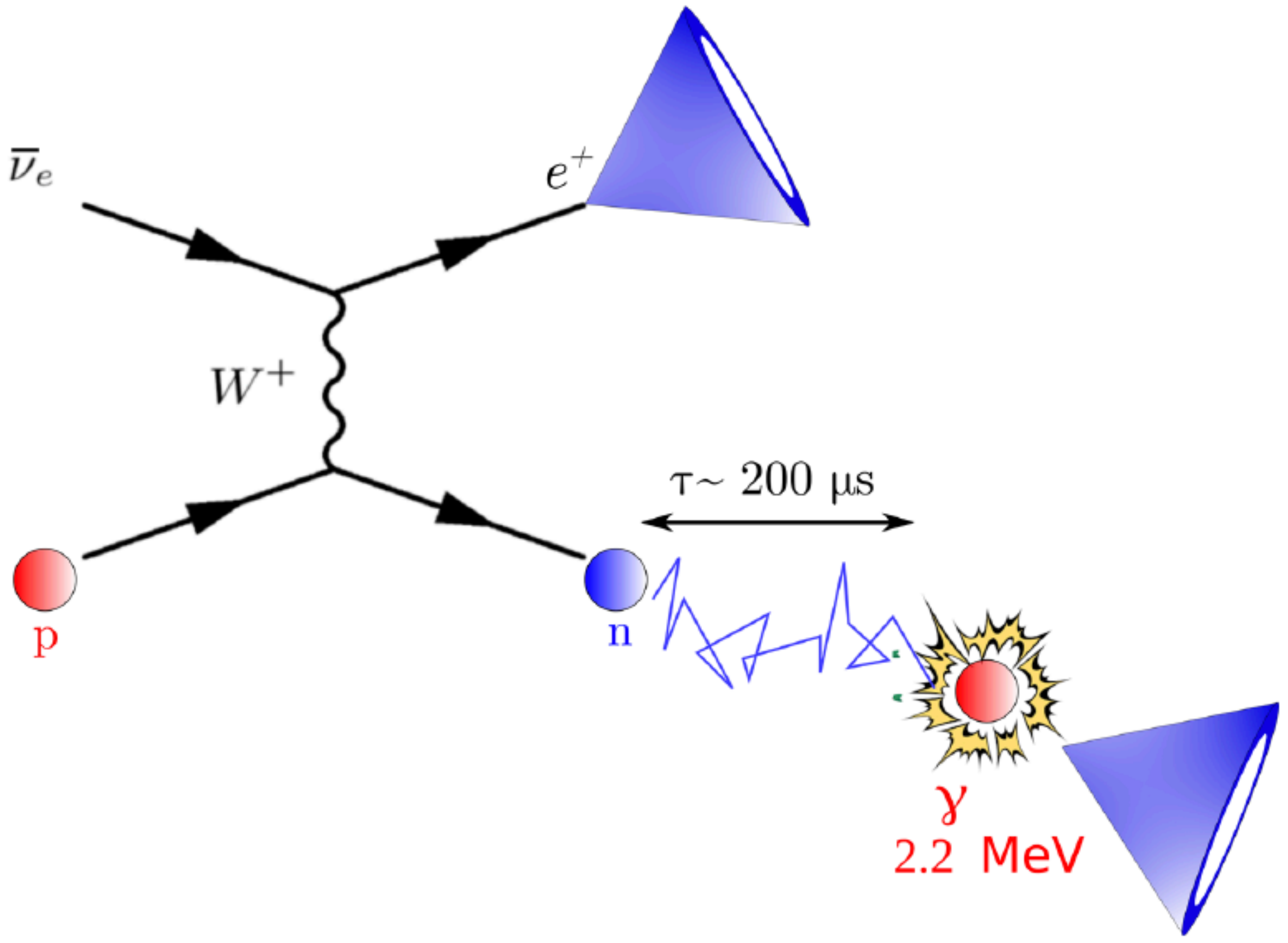

Background

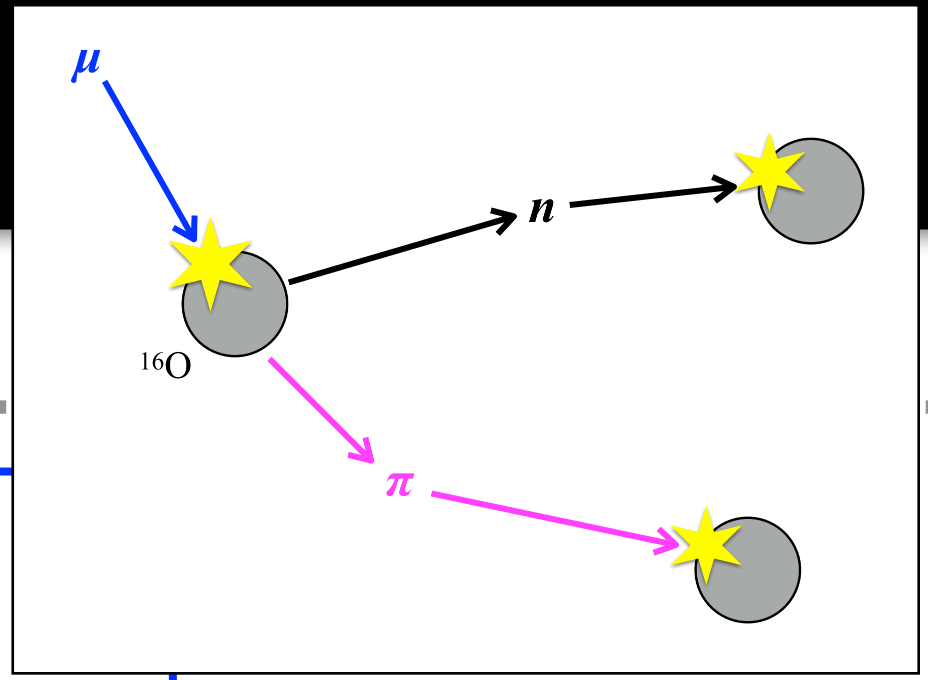

Muon spallation

- Decay without neutron
- Decay with neutron (^{9}Li, etc)

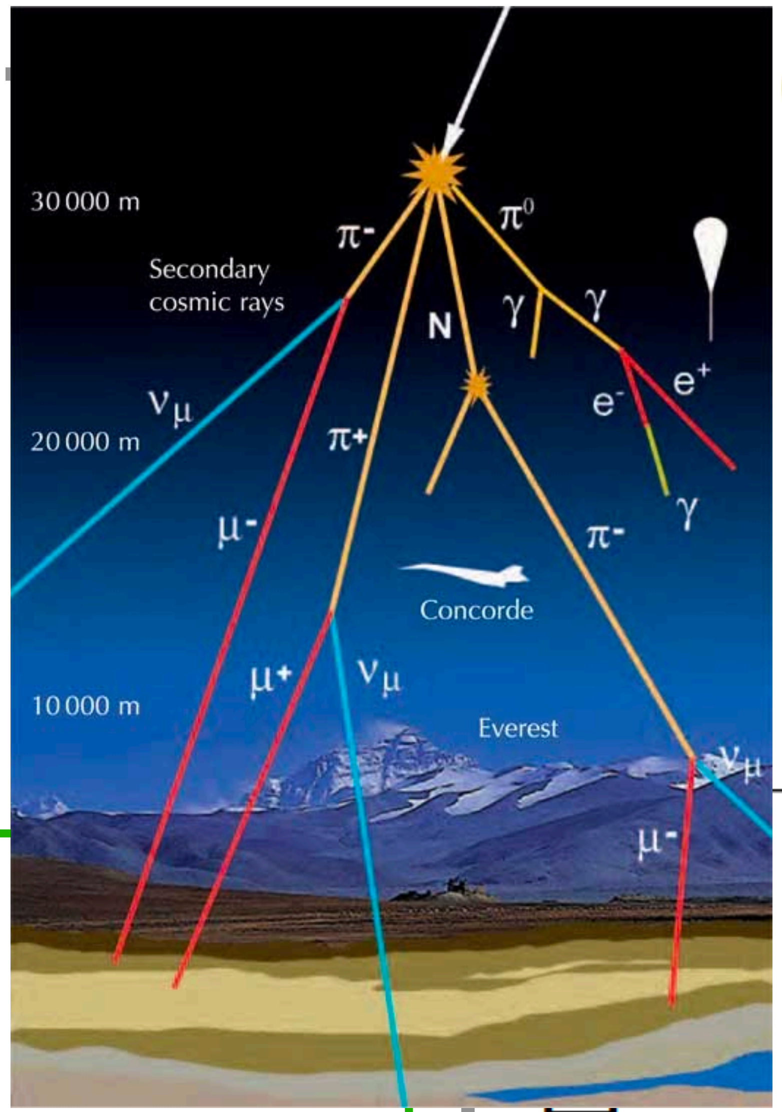

Atmospheric neutrinos

- Neutral-current quasielastic interactions (NCQE)
- $\nu_e/\overline{\nu}_e$ charged-current (CC) interactions
- Muon/pion-producing interactions (CCQE, CC1π, NC1π, etc)

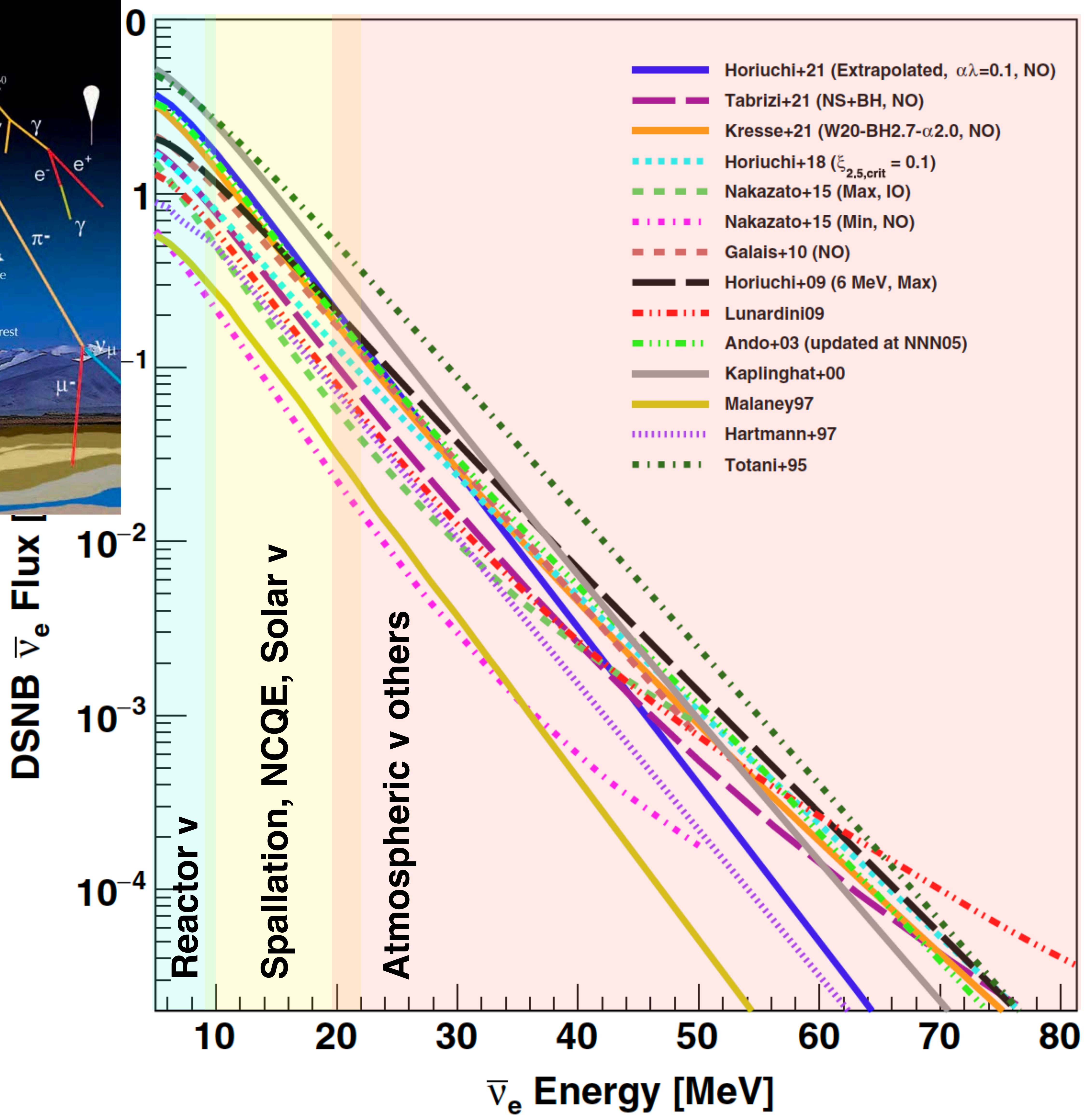

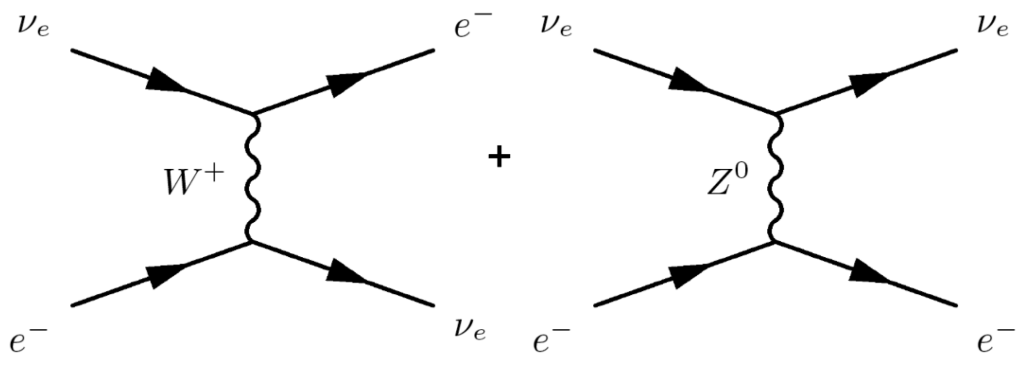

Solar neutrinos (electron scattering)

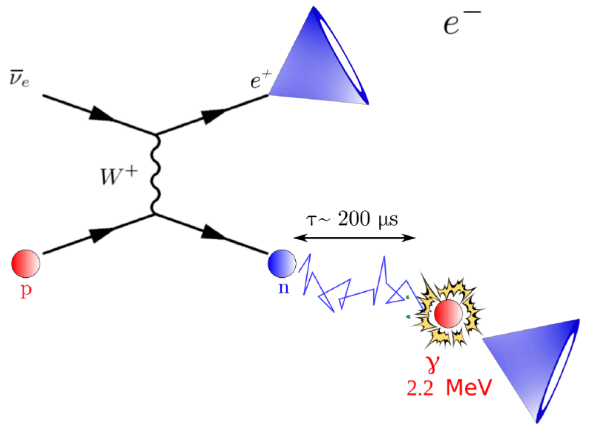

Reactor neutrinos (IBD)

Muon Spallation

Muon spallation
- Decay without neutron
- Decay with neutron (^{9}Li, etc)

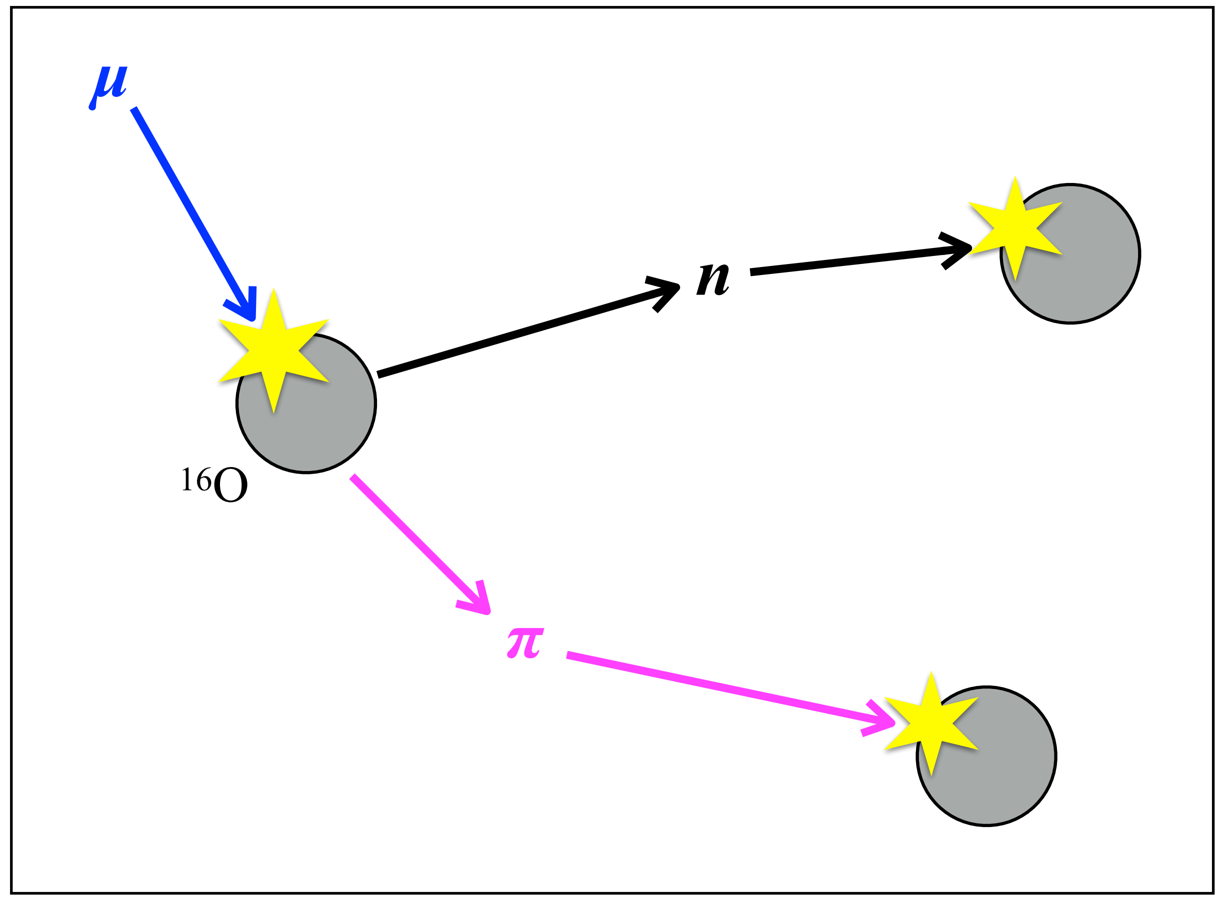

Energetic atmospheric μ on oxygen in Super-K

↓

Hadronic particles

↓

Radioactive isotopes

↓

β/γ decay (delayed by msec~10 sec)

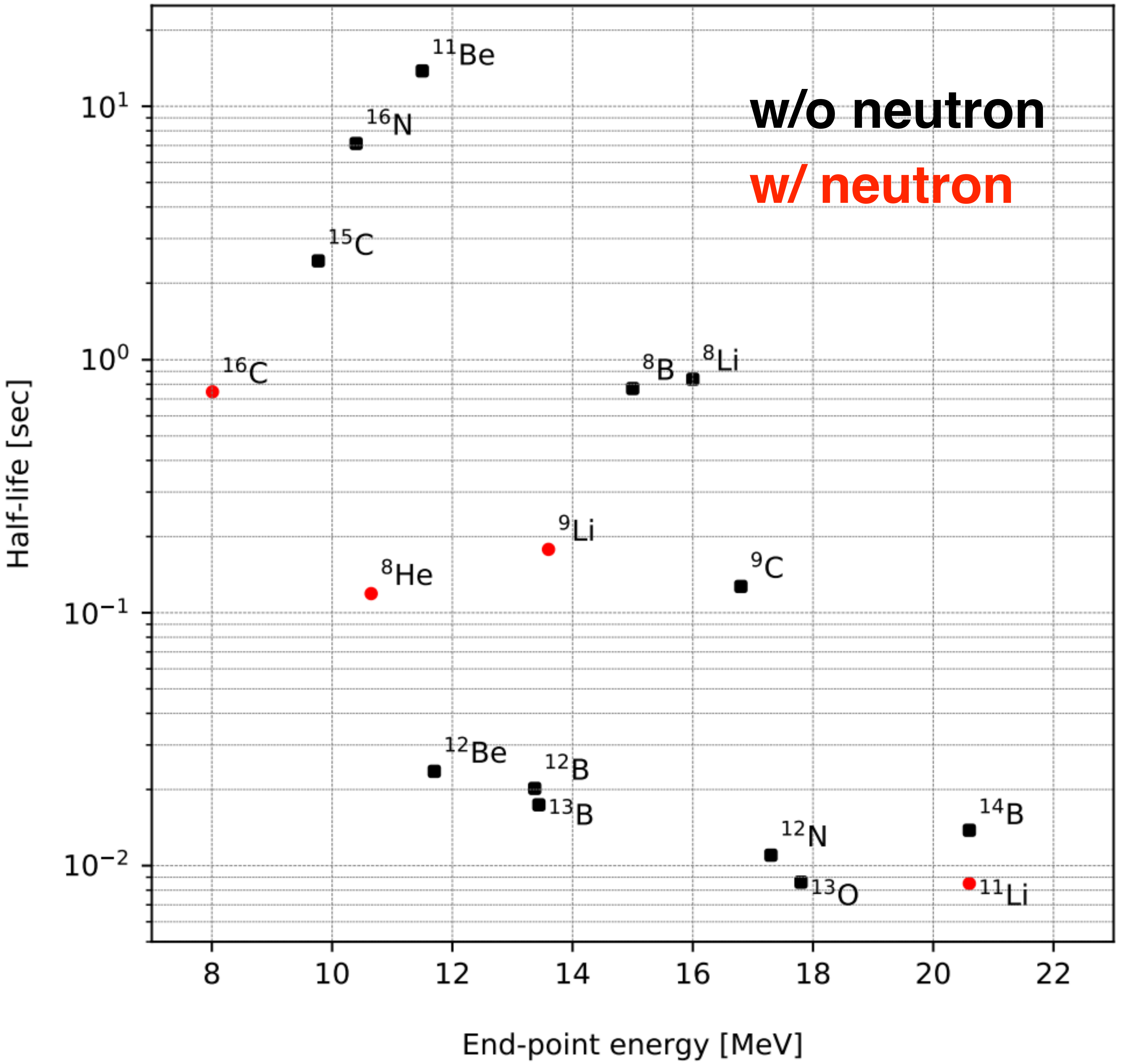

Muons for Spallation

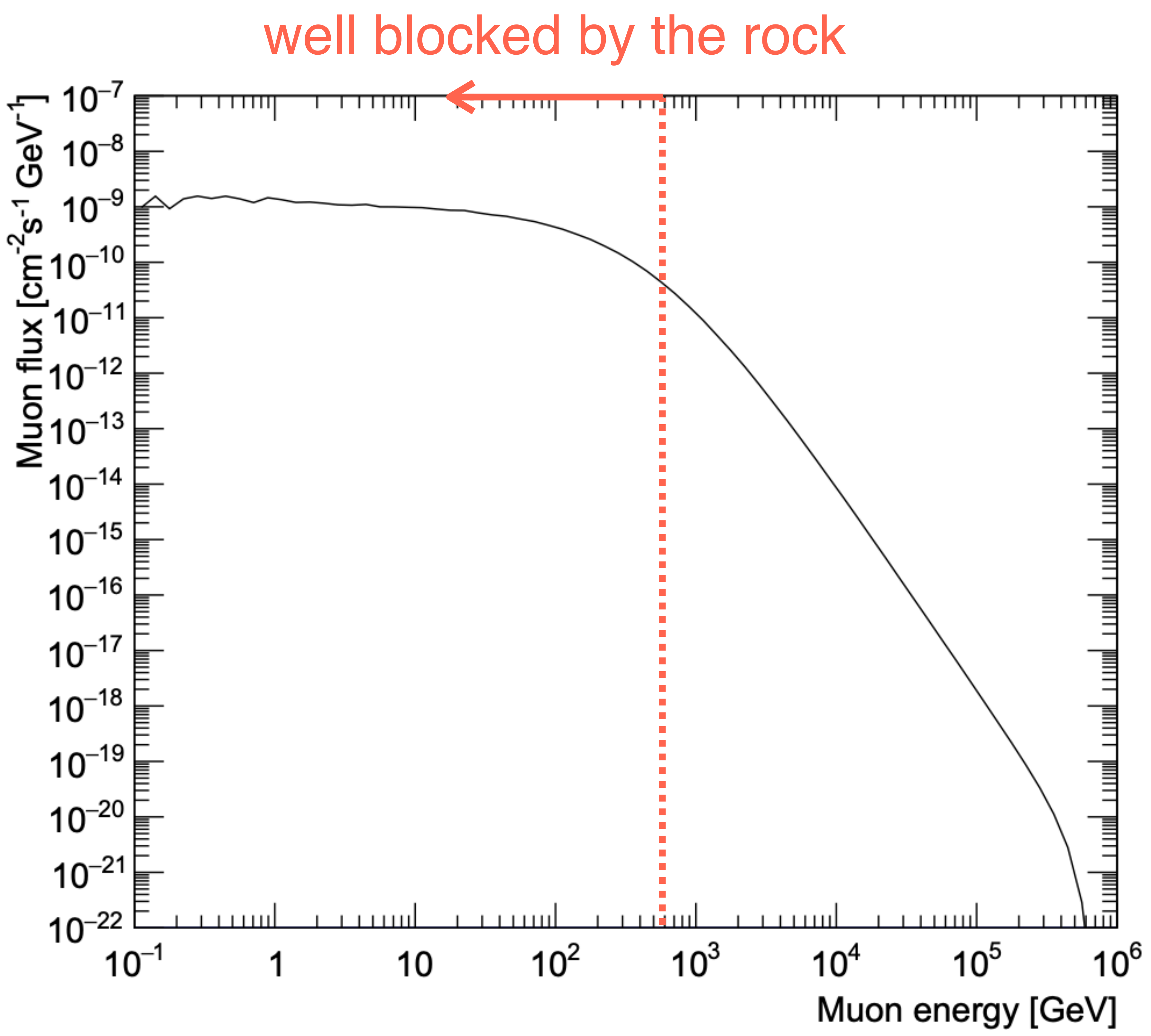

FIG. 2. Muon energy spectrum at the location of SK detector in the mine inside Mt. Ikenoyama.

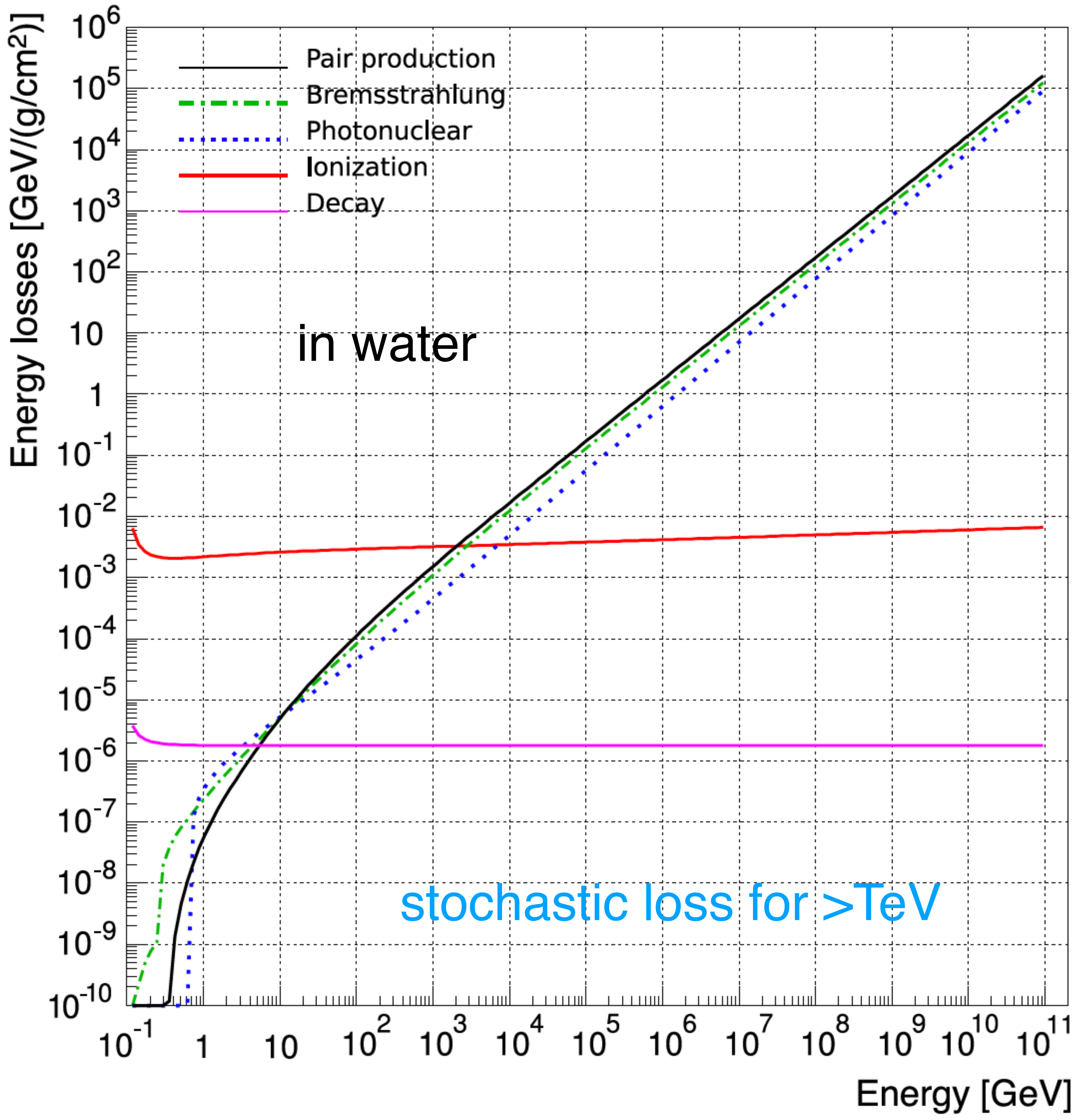

Spallation by FLUKA

S. W. Li and J. F. Beacom, Phys. Rev. C 89, 045801 (2014)
S. W. Li and J. F. Beacom, Phys. Rev. D 91, 105005 (2015)

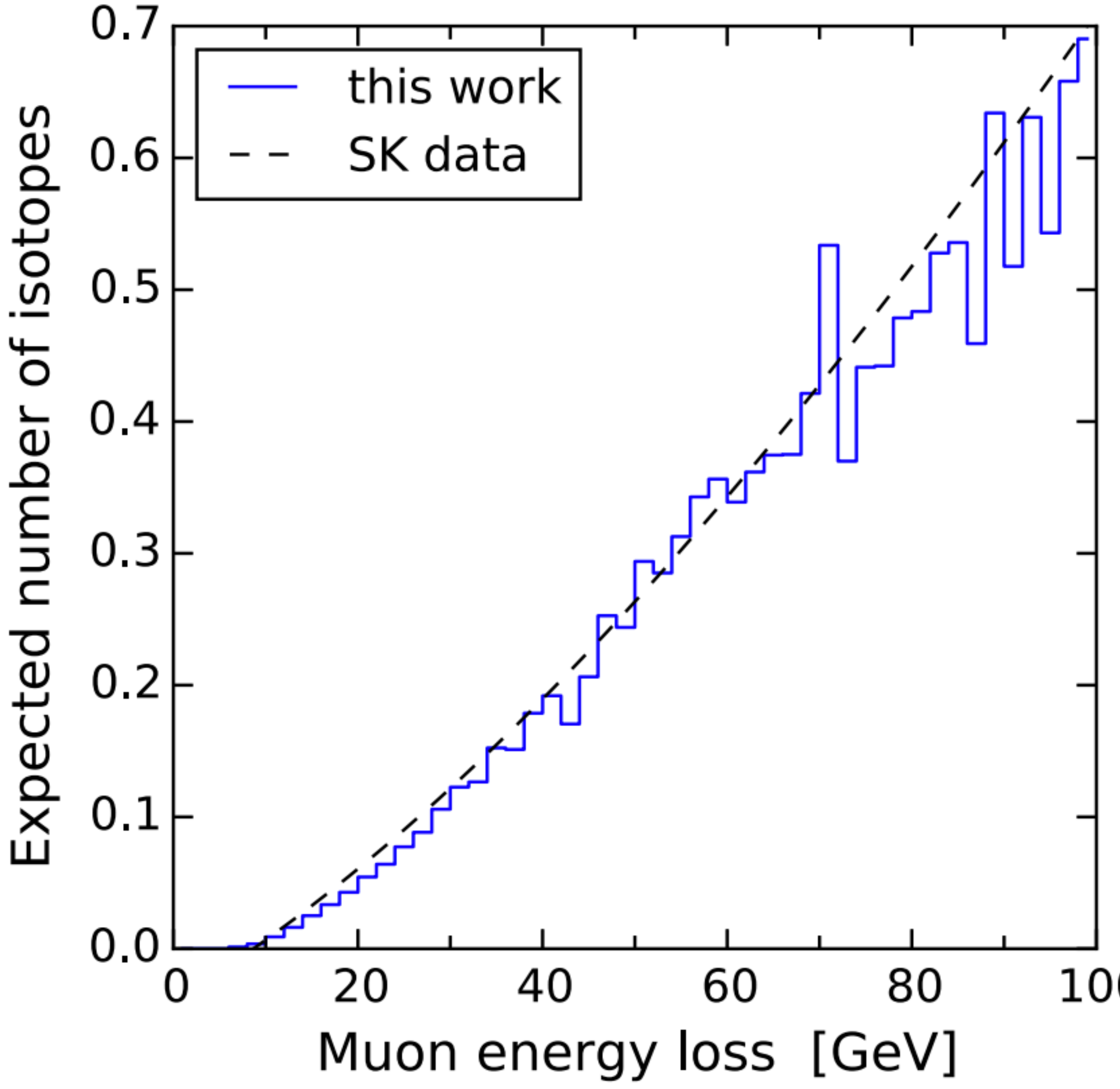

FIG. 8 (color online). The expected number of background isotopes as a function of the total muon energy loss. The solid line is our calculation assuming vertical through going muons that travel 32.2 m in the FV, and the dashed line is the (corrected to match assumptions) Super-K measurement.

Isotope	Half-life (s)	Decay mode	Yield (total) ($\times 10^{-7} \mu^{-1} g^{-1} cm^2$)	Yield ($E > 3.5$ MeV) ($\times 10^{-7} \mu^{-1} g^{-1} cm^2$)	Primary process
n			2030		
^{18}N	0.624	β^-	0.02	0.01	^{18}O(n,p)
^{17}N	4.173	$\beta^- n$	0.59	0.02	^{18}O($n,n+p$)
^{16}N	7.13	$\beta^-\gamma$ (66%), β^- (28%)	18	18	(n,p)
^{16}C	0.747	$\beta^- n$	0.02	0.003	($\pi^-,n+p$)
^{15}C	2.449	$\beta^-\gamma$ (63%), β^- (37%)	0.82	0.28	($n,2p$)
^{14}B	0.0138	$\beta^-\gamma$	0.02	0.02	($n,3p$)
^{13}O	0.0086	β^+	0.26	0.24	($\mu^-,p+2n+\mu^-+\pi^-$)
^{13}B	0.0174	β^-	1.9	1.6	($\pi^-,2p+n$)
^{12}N	0.0110	β^+	1.3	1.1	($\pi^+,2p+2n$)
^{12}B	0.0202	β^-	12	9.8	($n,\alpha+p$)
^{12}Be	0.0236	β^-	0.10	0.08	($\pi^-,\alpha+p+n$)
^{11}Be	13.8	β^- (55%), $\beta^-\gamma$ (31%)	0.81	0.54	($n,\alpha+2p$)
^{11}Li	0.0085	$\beta^- n$	0.01	0.01	($\pi^+,5p+\pi^++\pi^0$)
^{9}C	0.127	β^+	0.89	0.69	($n,\alpha+4n$)
^{9}Li	0.178	$\beta^- n$ (51%), β^- (49%)	1.9	1.5	($\pi^-,\alpha+2p+n$)
^{8}B	0.77	β^+	5.8	5.0	($\pi^+,\alpha+2p+2n$)
^{8}Li	0.838	β^-	13	11	($\pi^-,\alpha+{}^2$H$+p+n$)
^{8}He	0.119	$\beta^-\gamma$ (84%), $\beta^- n$ (16%)	0.23	0.16	($\pi^-,{}^3$H$+4p+n$)
^{15}O			351		(γ,n)
^{15}N			773		(γ,p)
^{14}O			13		($n,3n$)
^{14}N			295		($\gamma,n+p$)
^{14}C			64		($n,n+2p$)
^{13}N			19		($\gamma,{}^3$H)
^{13}C			225		($n,{}^2$H$+p+n$)
^{12}C			792		(γ,α)
^{11}C			105		($n,\alpha+2n$)
^{11}B			174		($n,\alpha+p+n$)
^{10}C			7.6		($n,\alpha+3n$)
^{10}B			77		($n,\alpha+p+2n$)
^{10}Be			24		($n,\alpha+2p+n$)
^{9}Be			38		($n,2\alpha$)
sum			3015	50	

^{18}O is very little (~0.2%) (^{17}N)

small amount >3.5 MeV (^{16}C)

very short life-time (^{11}Li)

low energy (end point ~8 MeV) (^{8}B, ^{8}Li)

Not direct backgrounds in SK:

- stable
- long half-life
- invisible decay
- low energy

Atmospheric Neutrinos

★ My own analysis in T2K

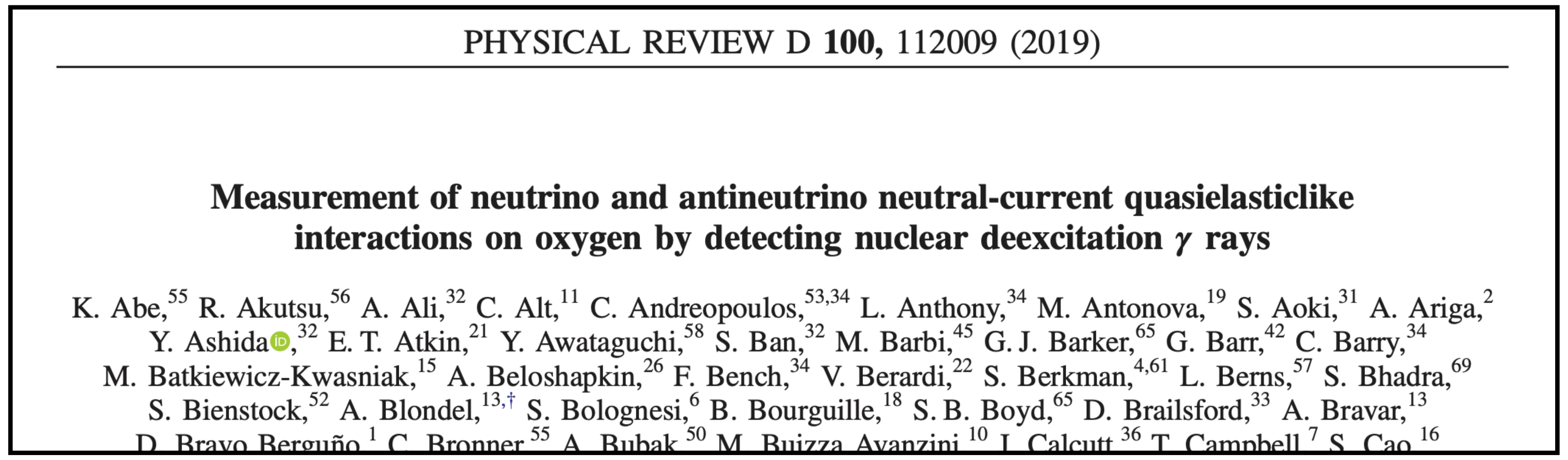
PHYSICAL REVIEW D **100**, 112009 (2019)

Measurement of neutrino and antineutrino neutral-current quasielasticlike interactions on oxygen by detecting nuclear deexcitation γ rays

K. Abe,[55] R. Akutsu,[56] A. Ali,[32] C. Alt,[11] C. Andreopoulos,[53,34] L. Anthony,[34] M. Antonova,[19] S. Aoki,[31] A. Ariga,[2] Y. Ashida,[32] E. T. Atkin,[21] Y. Awataguchi,[58] S. Ban,[32] M. Barbi,[45] G. J. Barker,[65] G. Barr,[42] C. Barry,[34] M. Batkiewicz-Kwasniak,[15] A. Beloshapkin,[26] F. Bench,[34] V. Berardi,[22] S. Berkman,[4,61] L. Berns,[57] S. Bhadra,[69] S. Bienstock,[52] A. Blondel,[13,†] S. Bolognesi,[6] B. Bourguille,[18] S. B. Boyd,[65] D. Brailsford,[33] A. Bravar,[13]

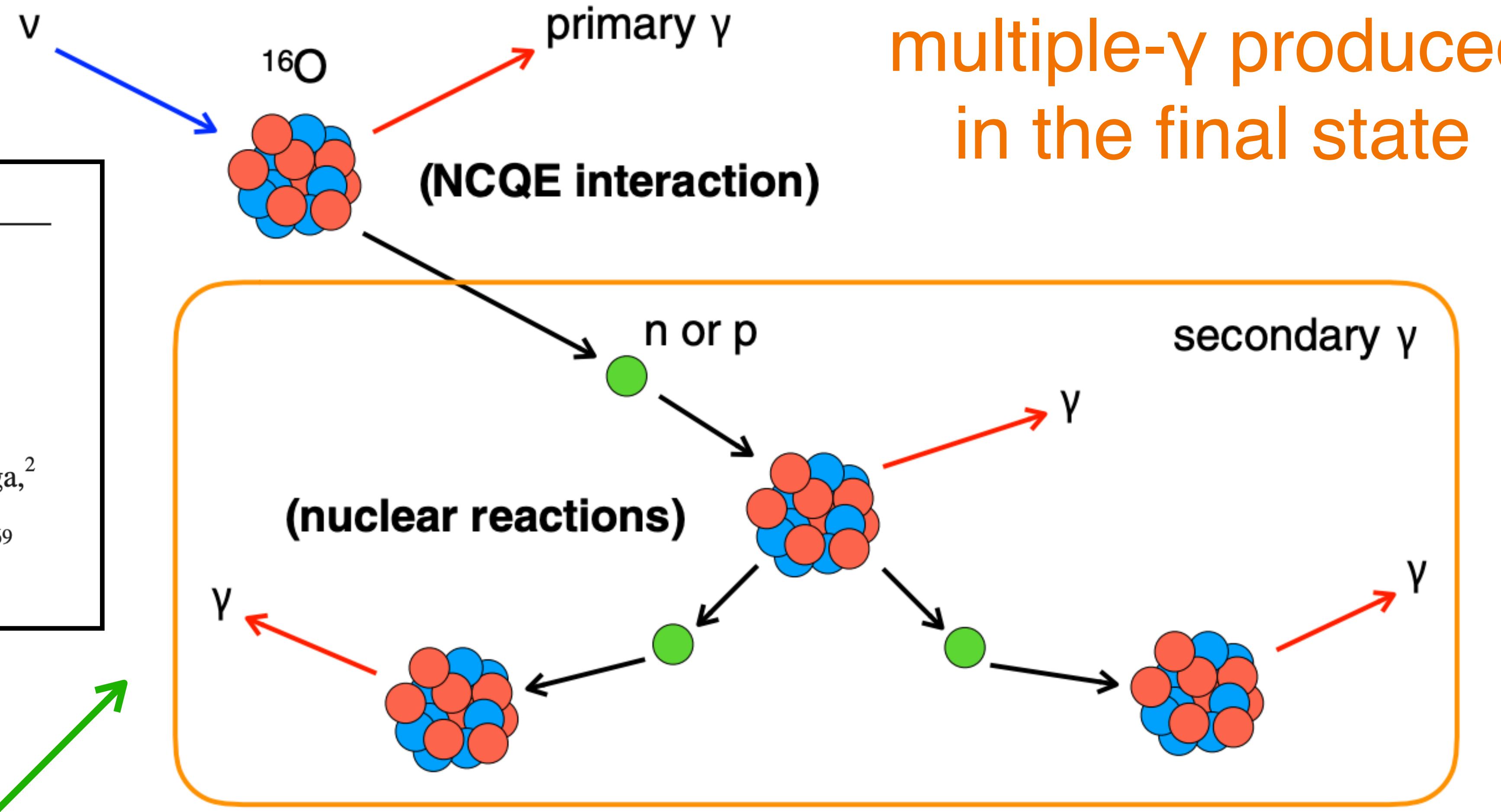

multiple-γ produced in the final state

Atmospheric neutrinos

- Neutral-current quasielastic interactions (NCQE)
- $\nu_e/\bar{\nu}_e$ charged-current (CC) interactions
- Muon/pion-producing interactions (CCQE, CC1π, NC1π, etc)

invisible (<120 MeV/c)

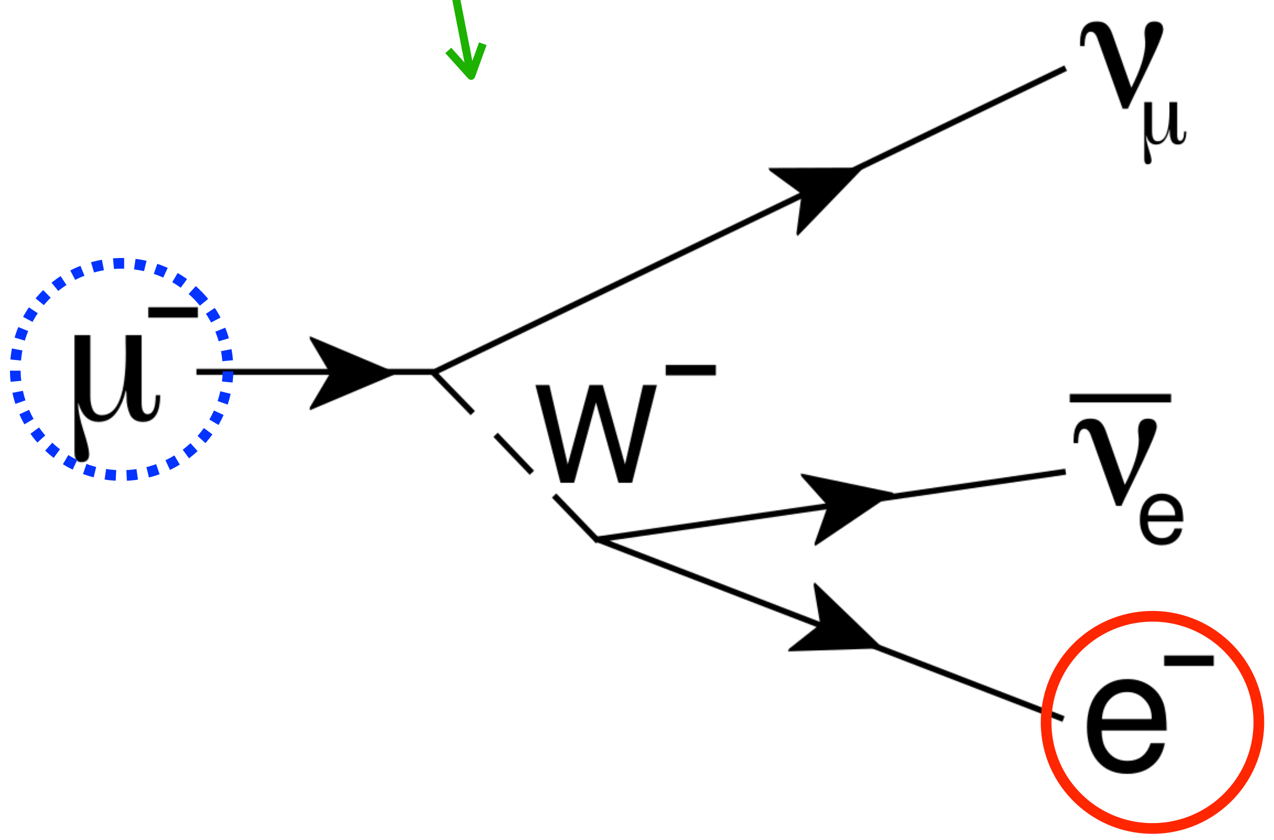

visible (decay-e)

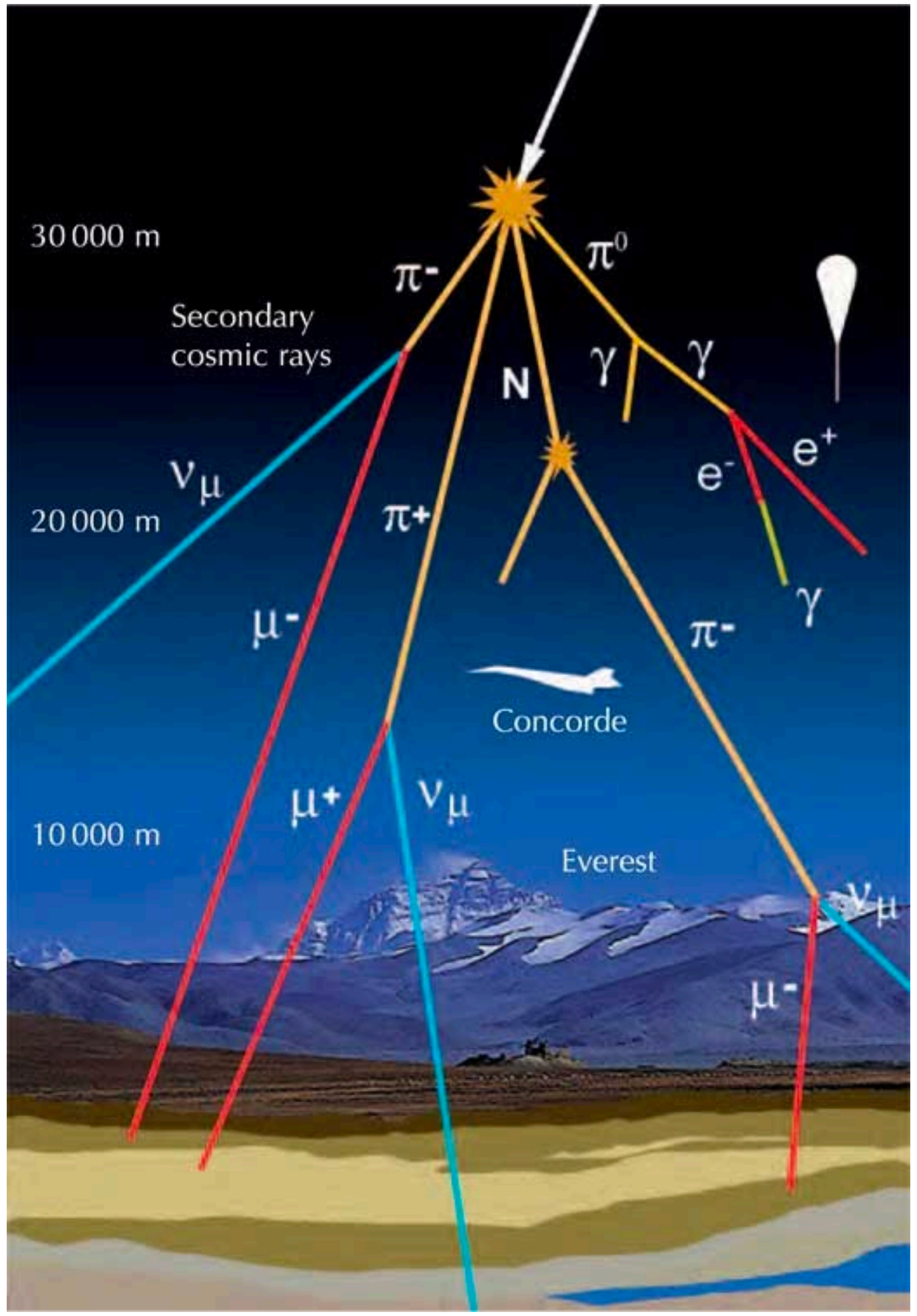

Atmospheric vs. T2K Fluxes

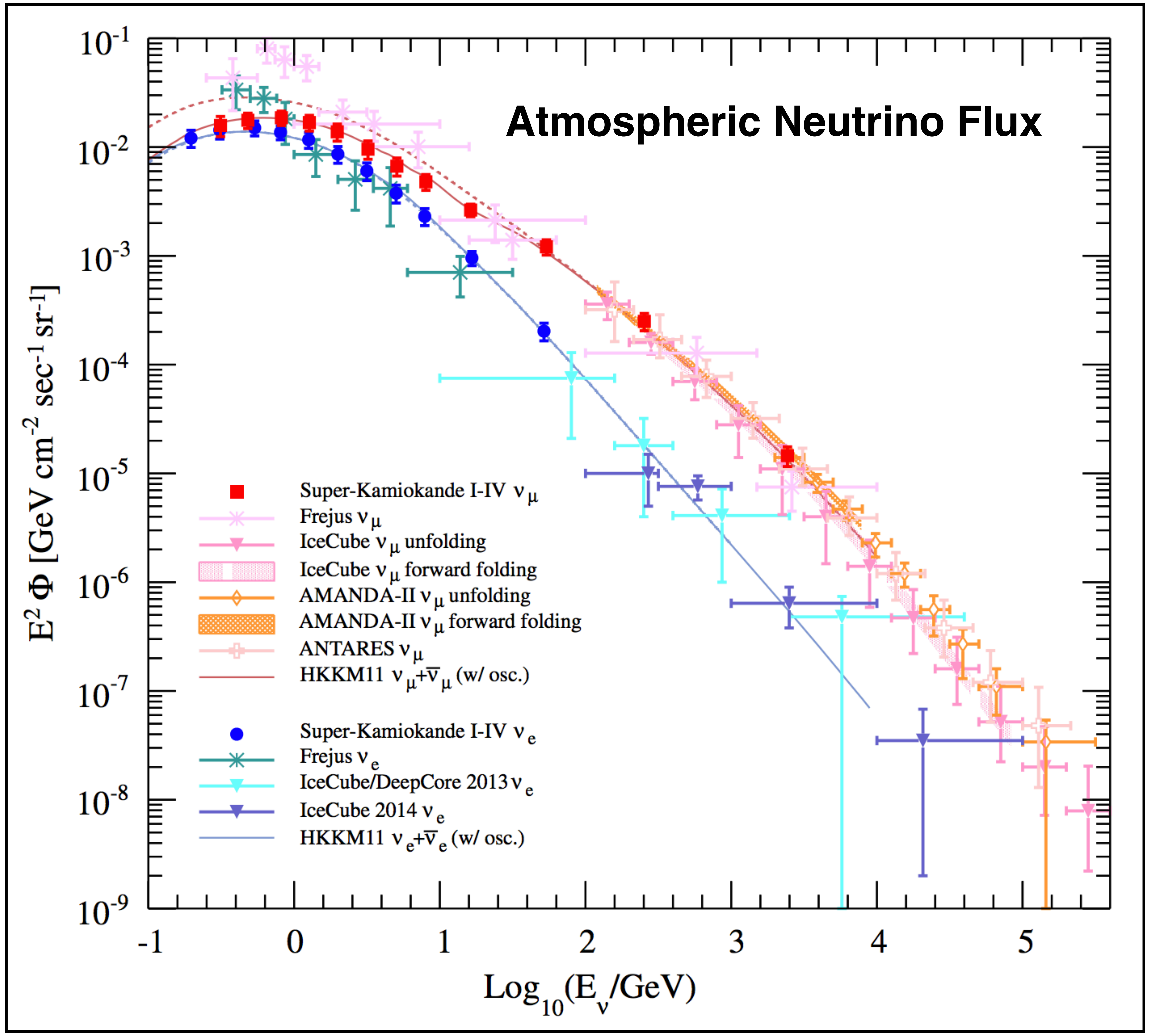

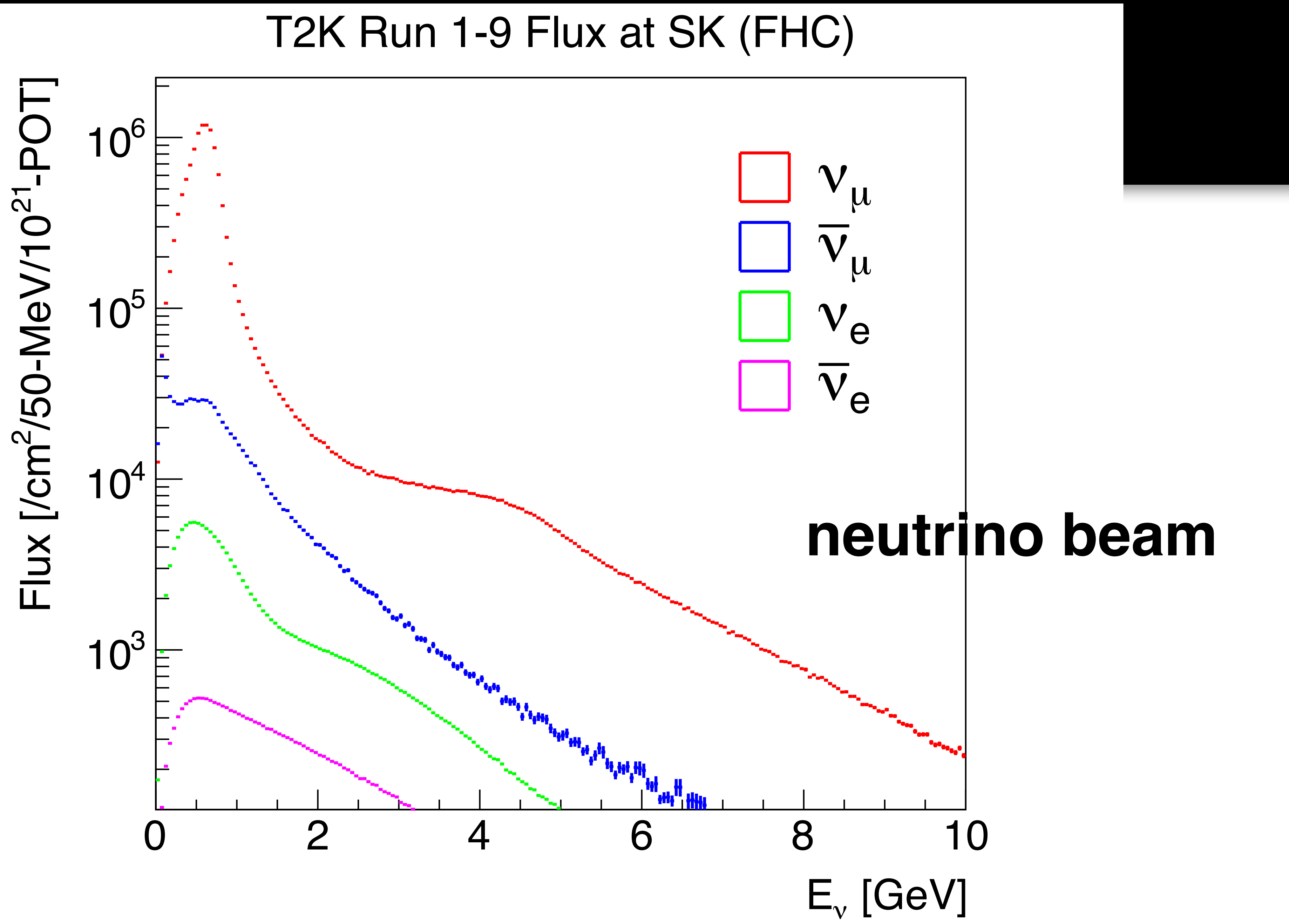

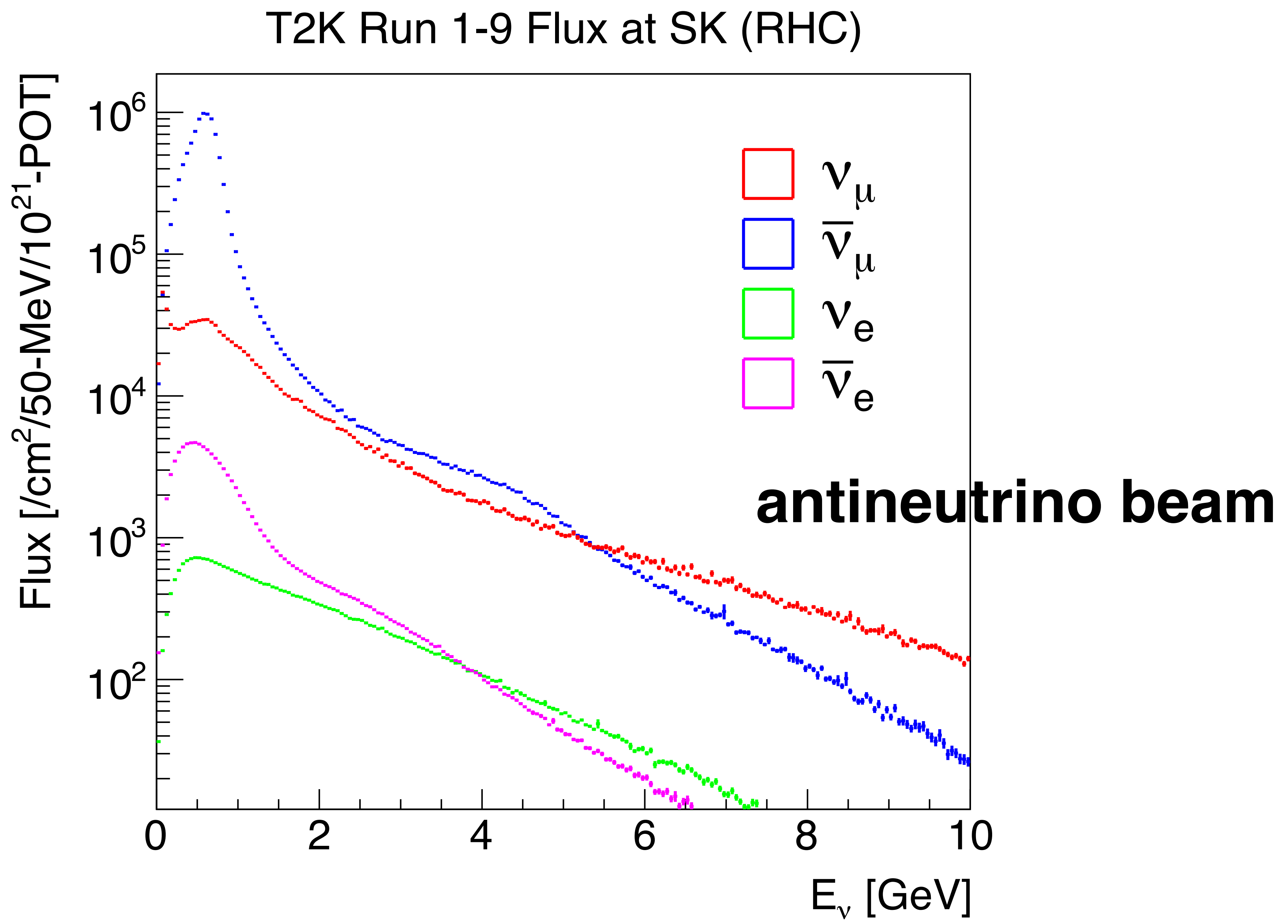

NCQE Constraint by T2K

K. Abe et al. (T2K Collaboration), Phys. Rev. D 100, 112009 (2019)

- **NCQE cross section is measured at Super-K using T2K beams.**
  - Similar flux energy peak between T2K and atmospheric (~600 MeV), same detector
    - → Effective constraint
  - Well-known flux, known beam timing, changeable beam polarity
    - → Final precision of cross section ~30%

★ My own analysis in T2K

PHYSICAL REVIEW D **100,** 112009 (2019)

Measurement of neutrino and antineutrino neutral-current quasielasticlike interactions on oxygen by detecting nuclear deexcitation γ rays

K. Abe,[55] R. Akutsu,[56] A. Ali,[32] C. Alt,[11] C. Andreopoulos,[53,34] L. Anthony,[34] M. Antonova,[19] S. Aoki,[31] A. Ariga,[2] Y. Ashida,[32] E. T. Atkin,[21] Y. Awataguchi,[58] S. Ban,[32] M. Barbi,[45] G. J. Barker,[65] G. Barr,[42] C. Barry,[34] M. Batkiewicz-Kwasniak,[15] A. Beloshapkin,[26] F. Bench,[34] V. Berardi,[22] S. Berkman,[4,61] L. Berns,[57] S. Bhadra,[69] S. Bienstock,[52] A. Blondel,[13,†] S. Bolognesi,[6] B. Bourguille,[18] S. B. Boyd,[65] D. Brailsford,[33] A. Bravar,[13] D. Bravo Berguño,[1] C. Bronner,[55] A. Bubak,[50] M. Buizza Avanzini,[10] J. Calcutt,[36] T. Campbell,[7] S. Cao,[16]

- In this work, NCQE bkg is estimated with a ~60% uncertainty.
  - More reliable data-driven estimate (previously theory-based, 100% uncertainty)
  - DSNB search sensitivity is improved by ~20% for this.

Background: Experimental Classification

Classification by physical source

Muon spallation

- Decay without neutron
- Decay with neutron (^{9}Li, etc)

Atmospheric neutrinos

- Neutral-current quasielastic interactions (NCQE)
- $\nu_e/\bar{\nu}_e$ charged-current (CC) interactions
- Muon/pion-producing interactions (CCQE, CC1π, NC1π, etc)

Solar neutrinos (electron scattering)

Reactor neutrinos (IBD)

Classification by final state

Background w/ true neutron

→ 2.2 MeV γ-ray emitted later

- ^{9}Li ★
- Atmospheric ν ★ (NCQE, $\bar{\nu}$ CC)
- Reactor ν

PMT dark noise, radioactive in the wall, etc

Background w/o true neutron

→ low energy noise accidentally paired

- Spallation ★
- Atmospheric ν
- Solar ν

Spallation Cut

- Much improved performance achieved.
  - Additional variables about muon dE/dx, correlations between variables considered, etc.
  - Helped to lower analysis threshold.
- Reliable estimation of ^{9}Li bkg based on data developed.

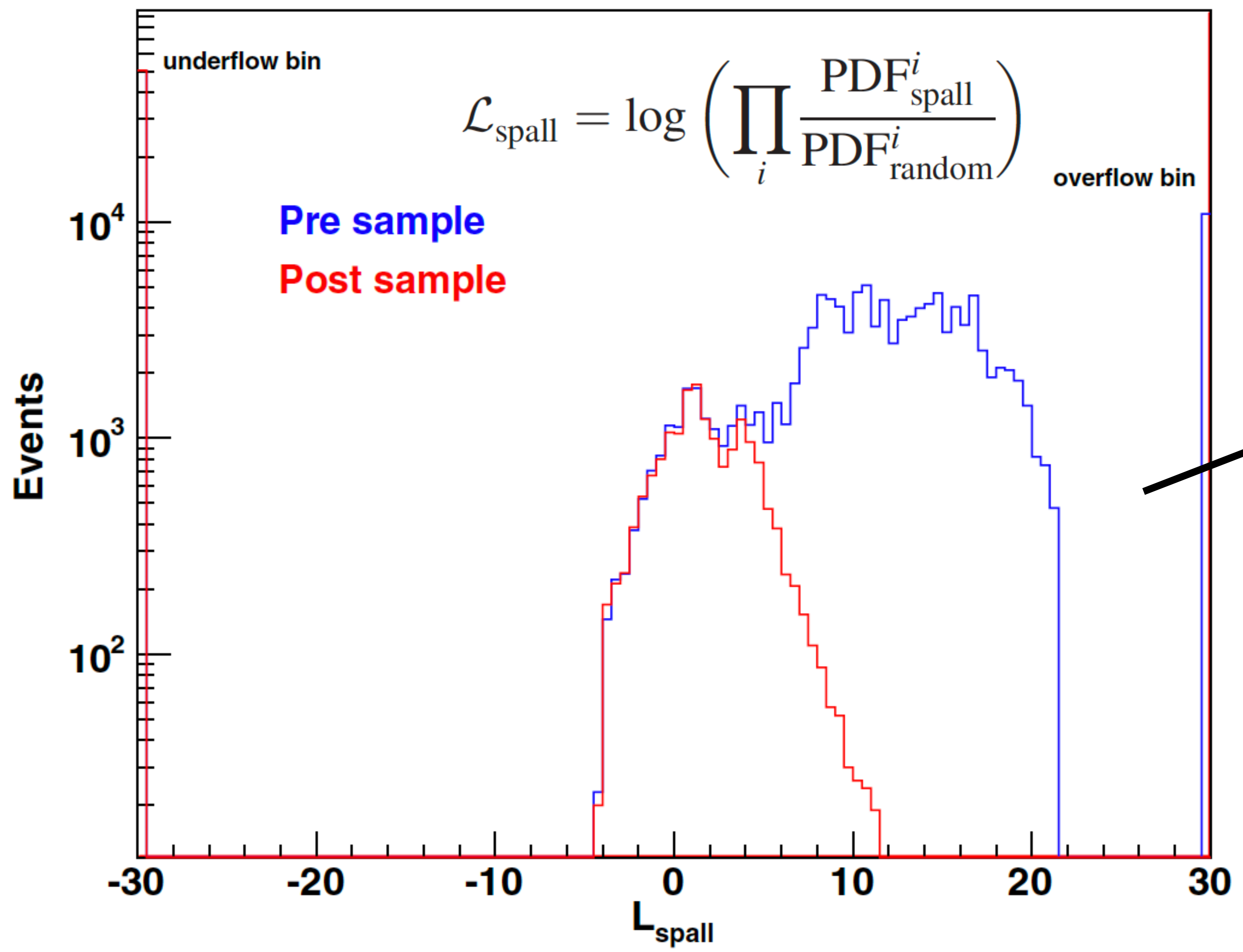

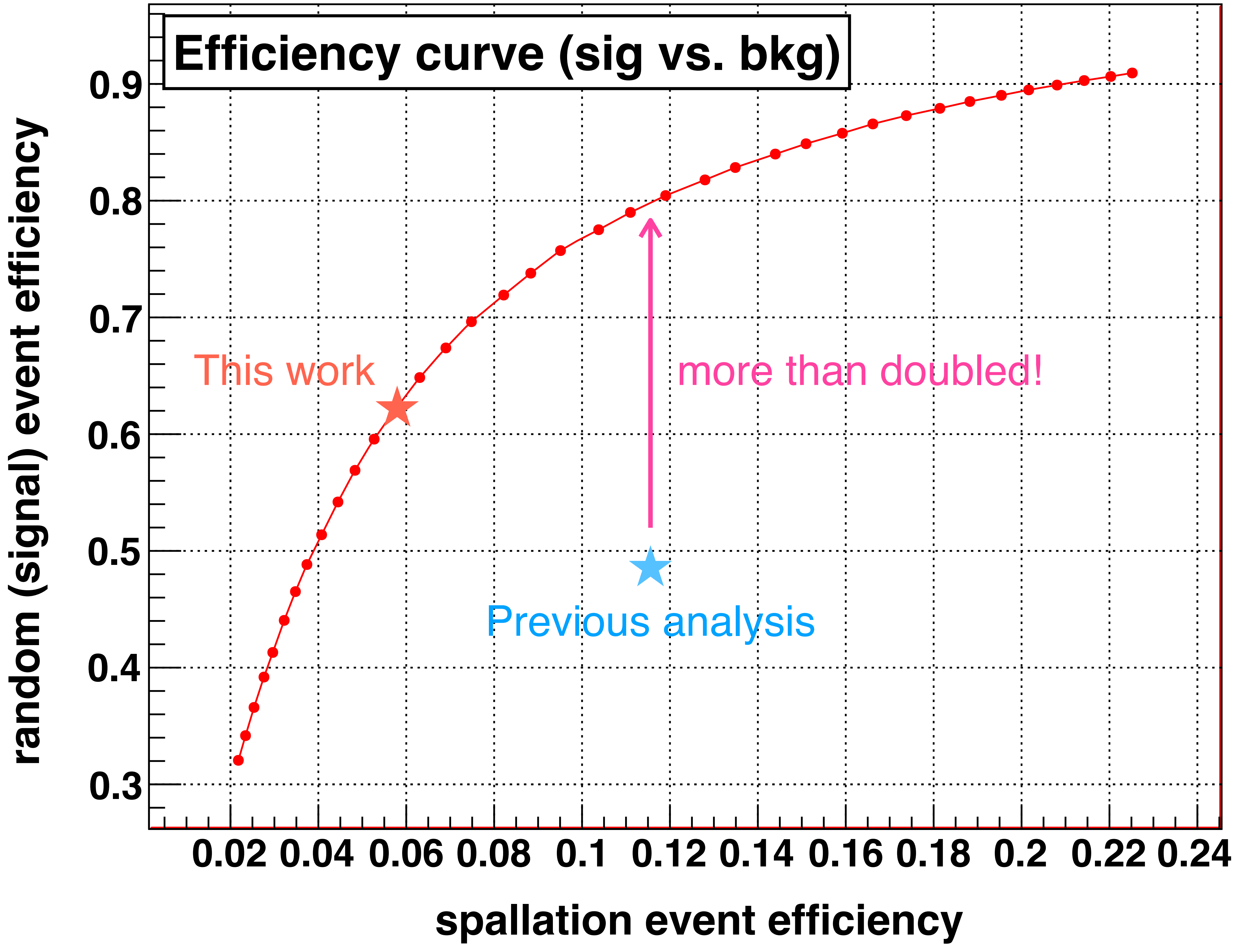

Signal Efficiency and Selected Events

- Signal efficiency is ~10% at low energies and 20~30% at high energies.
- The present work improves much over the previous analysis (better signal efficiency, smaller systematics).
- DSNB signal is comparable to background around 20 MeV.
- No significant excess over expectation is observed in any bin (minimum p-value is 0.05).

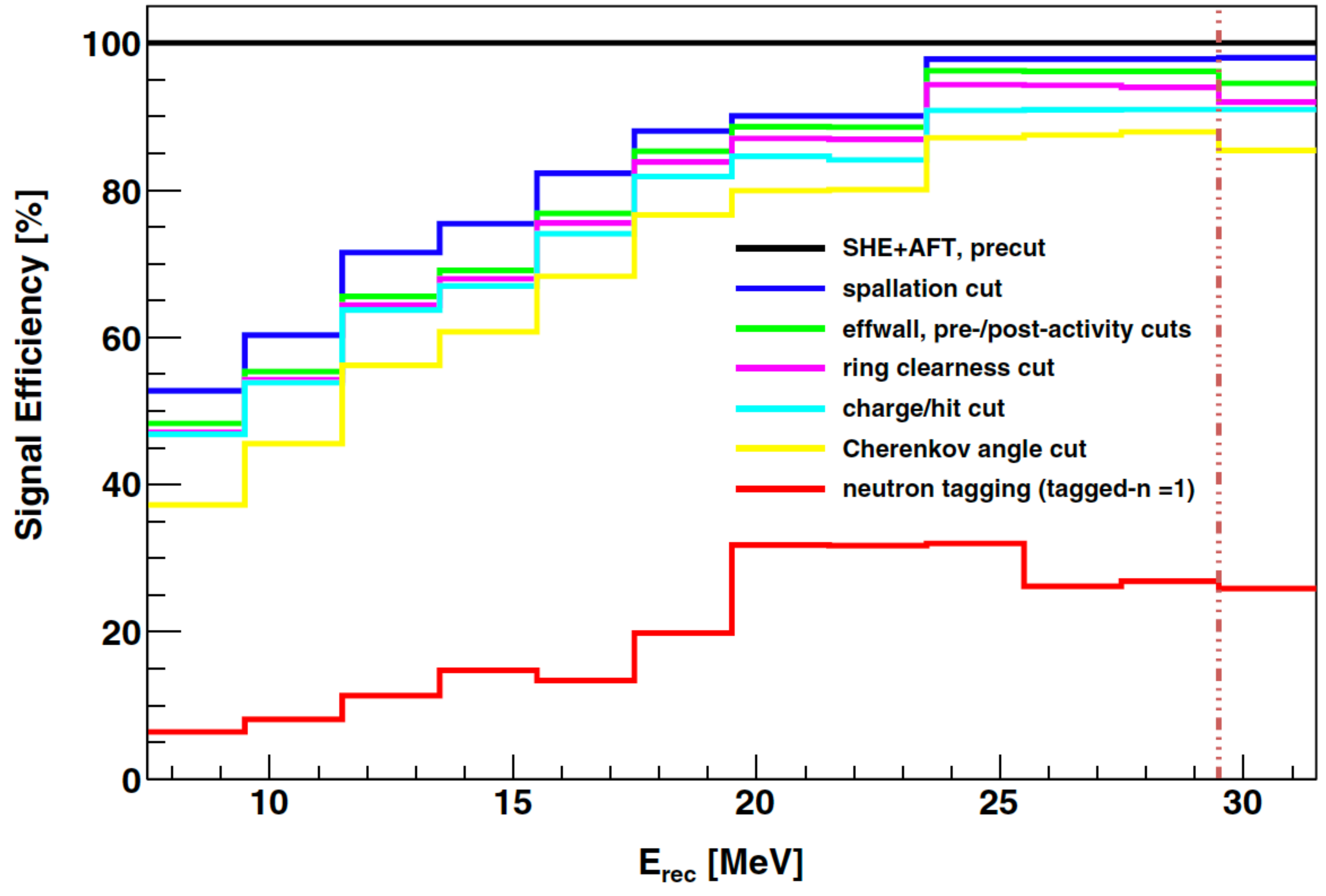

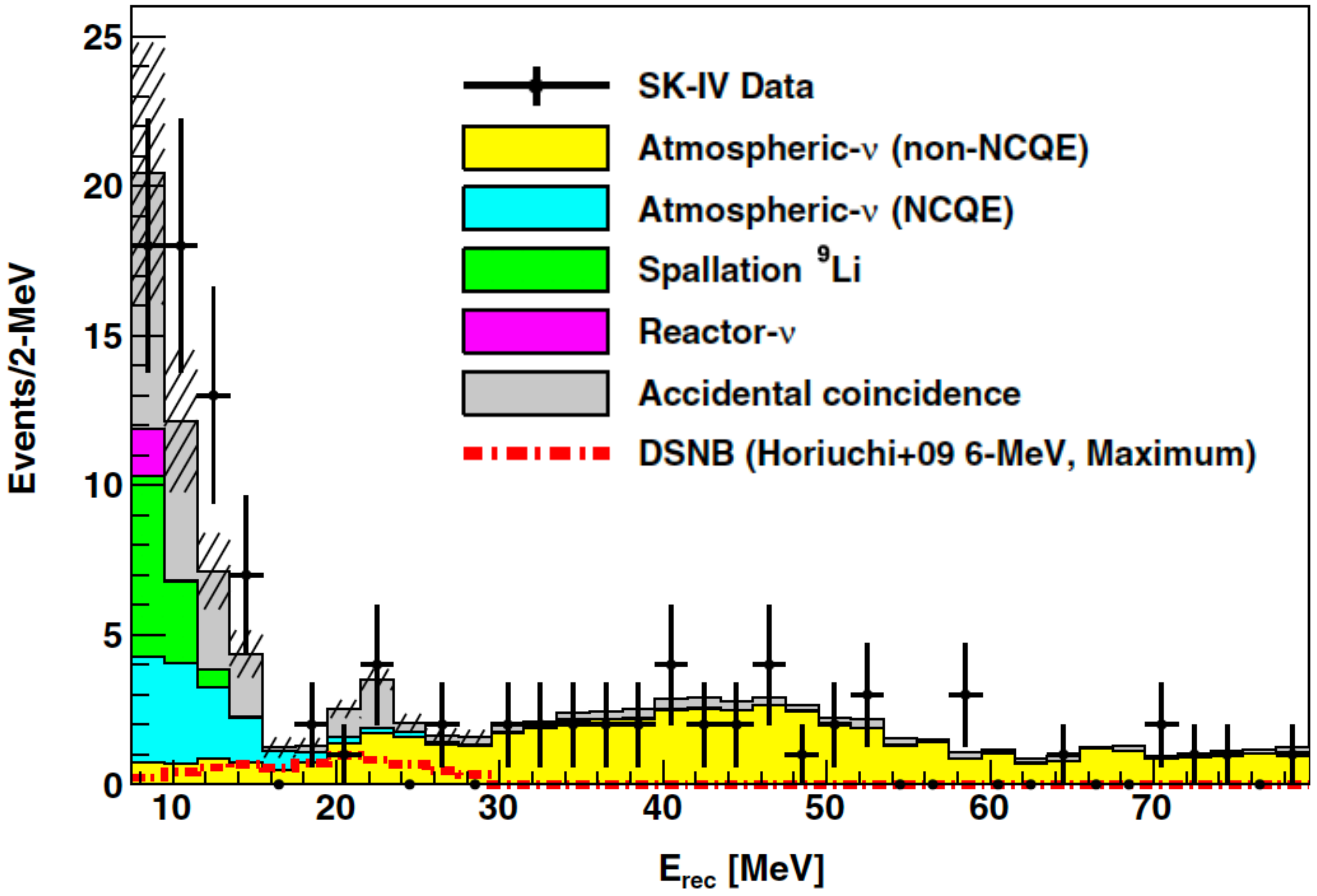

Model-Independent Differential Upper Limit

- Expected sensitivity reaches most optimistic model predictions.
- First search result below 13.3 MeV is achieved for improvements on bkg reduction.
- Observed upper limits are world most stringent above ~10 MeV.

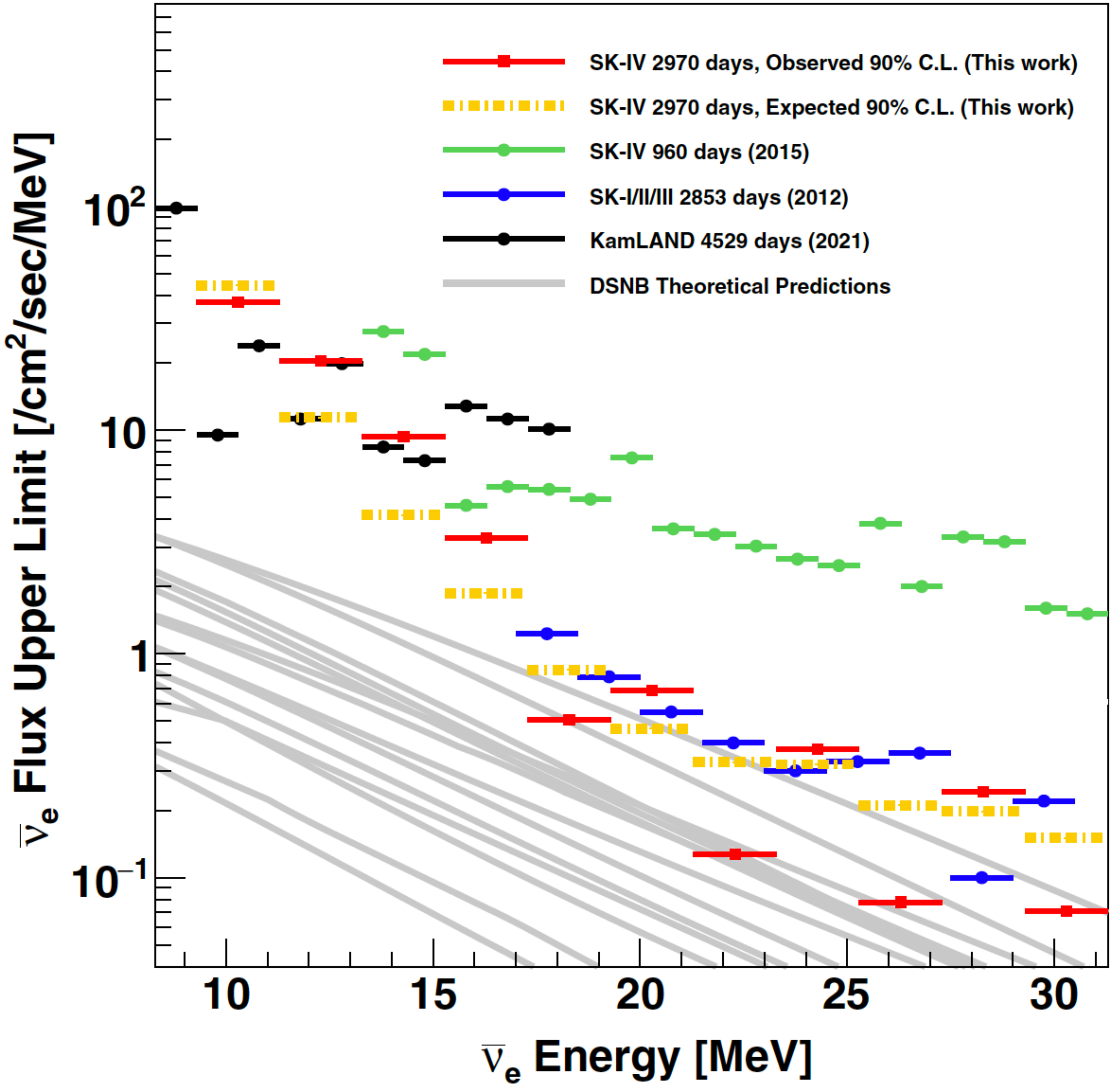

Spectral Fitting

- An unbinned maximum likelihood fitting is performed for $E_\nu > 17.3$ MeV with signal and background PDFs.
  - **DSNB** signal (models from introduction tested)
  - **Muon spallation** bkg
  - Atmospheric bkg: **NCQE**, **ν_e CC**, **decay-e**, **μ/π production**
  - Normalization of each to be fitted.
- Not only best signal window ($38 < \theta_C < 50$ deg, $N_n = 1$), but others are also used to constrain bkg (separation along N_n =1 or ≠1 is new for this analysis).

$$\mathcal{L}(\{N_j\}) = e^{-\sum_{j=0}^{5} N_j} \prod_{i=1}^{N_{\mathrm{events}}} \sum_{j=0}^{5} N_j \mathrm{PDF}_j^{(r)}(E_i).$$

Likelihood function with 6 PDFs

	μ/π window	signal window	NCQE window
N_n \ θ_C	20–38 deg	38–50 deg	78–90 deg
=1		used for bin-by-bin analysis	
≠1			

used for spectral fitting

Spectral Fitting

$N_n \neq 1$

Likelihood function with 6 PDFs

$$\mathcal{L}(\{N_j\}) = e^{-\sum_{j=0}^{5} N_j} \prod_{i=1}^{N_{\text{events}}} \sum_{j=0}^{5} N_j \text{PDF}_j^{(r)}(E_i).$$

$N_n = 1$

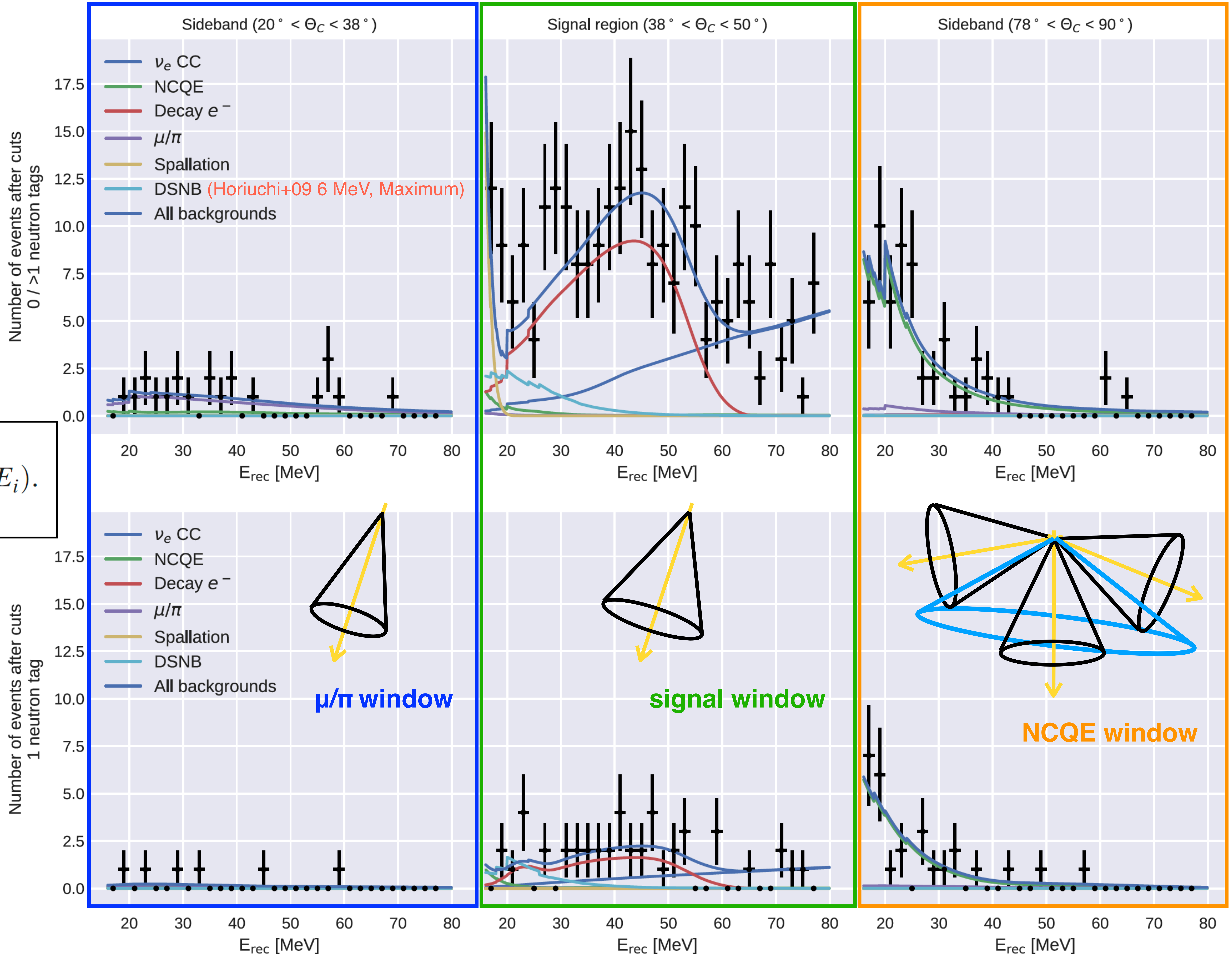

SK-I Best-fit (1497 days)

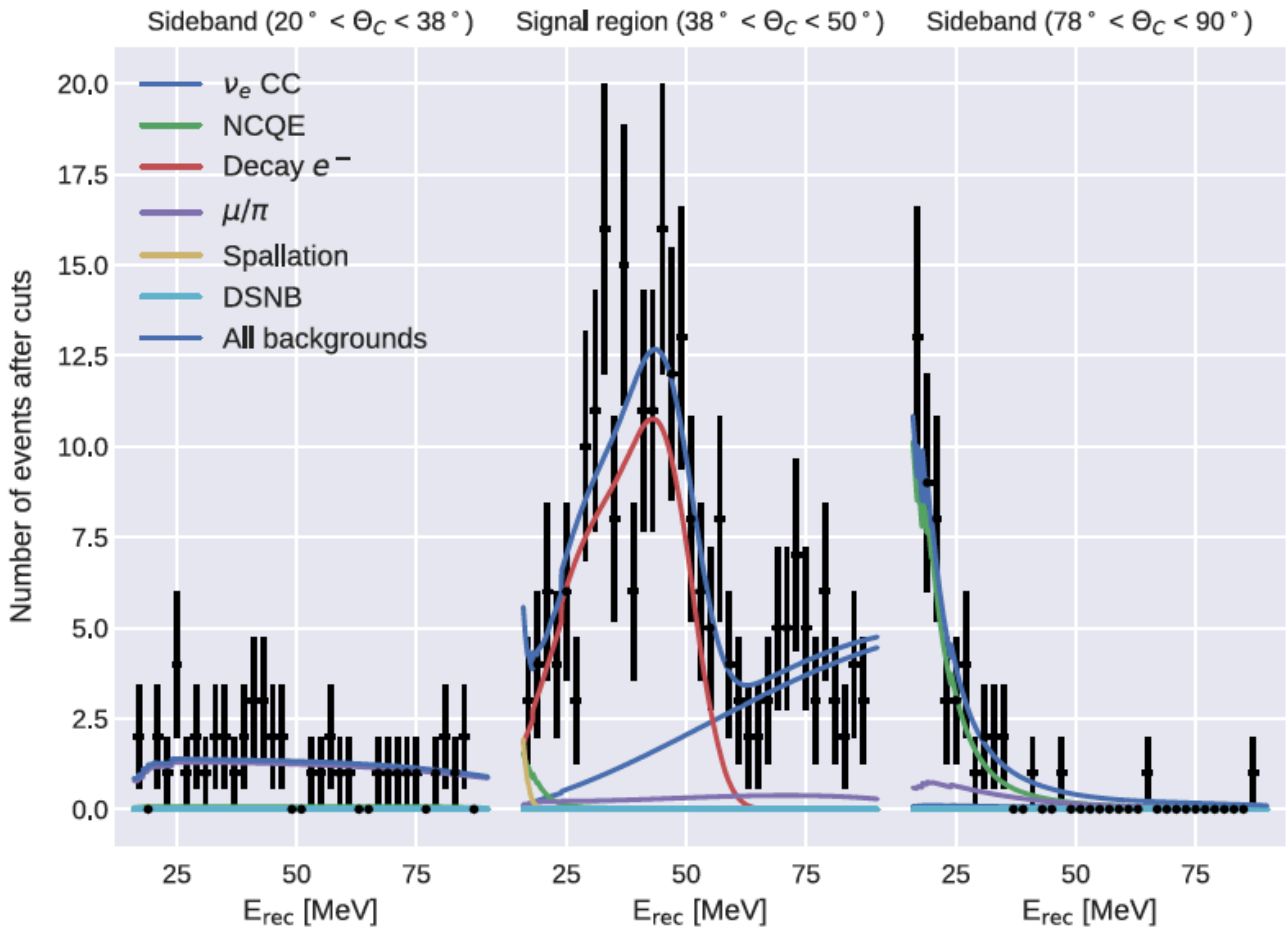

SK-II Best-fit (794 days)

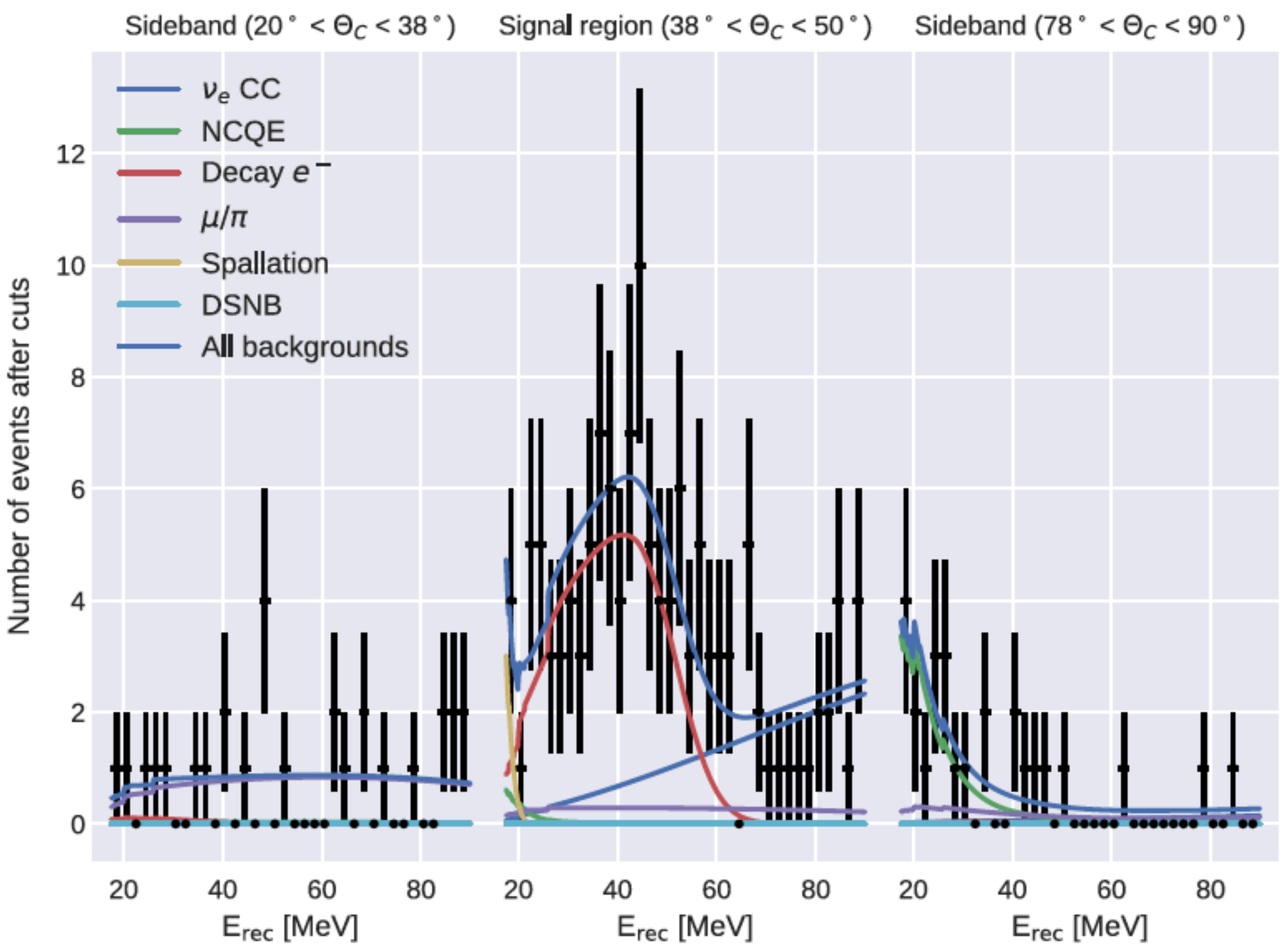

SK-III Best-fit (562 days)

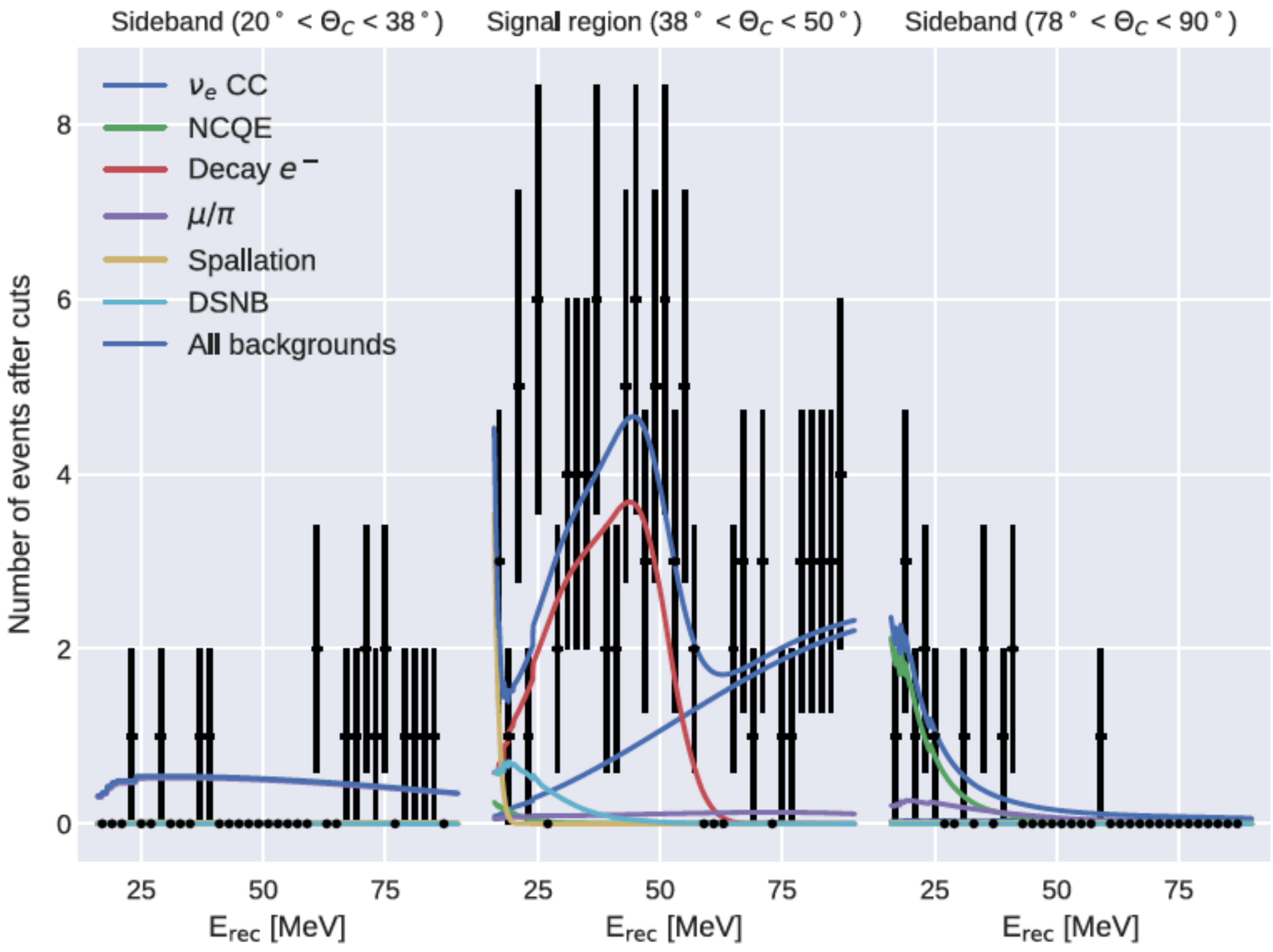

Combined Results with SK-I/II/III

- SK-I to IV results are statistically combined.
- Expected sensitivity reaches some models.
- Observed limits exclude optimistic models and lie within a factor to other models.

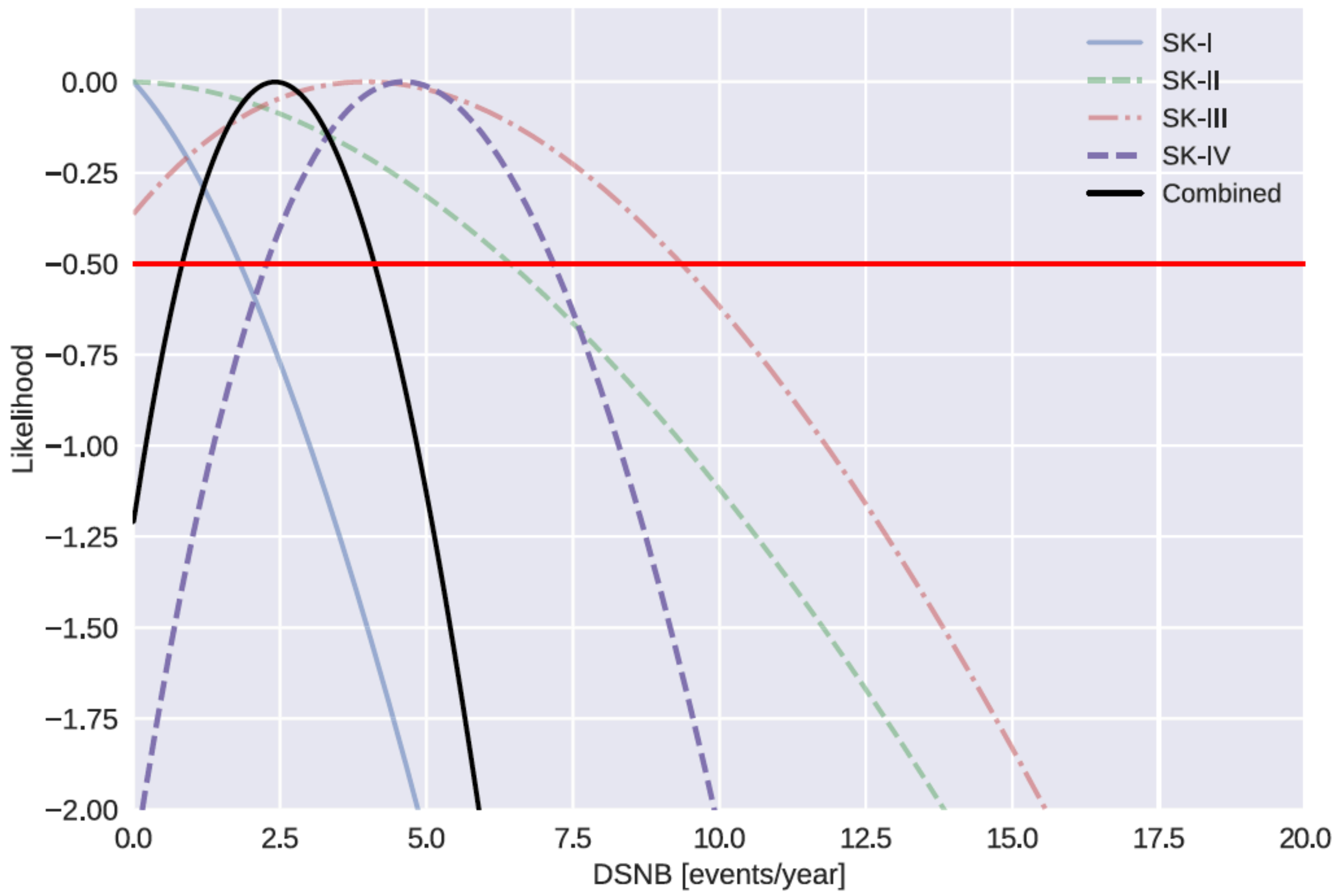

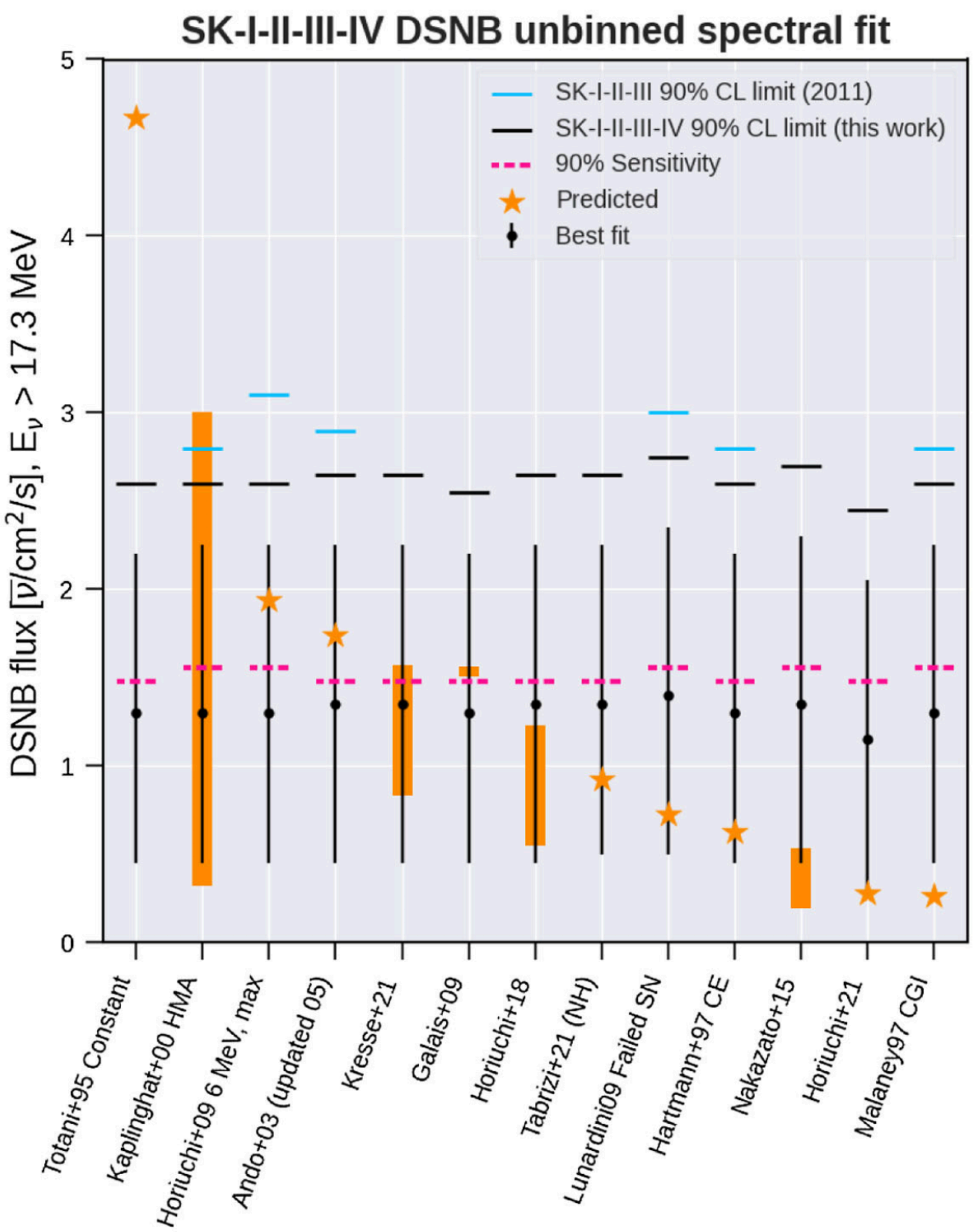

TABLE VIII. Best-fit values and the 90% CL upper limits on the DSNB fluxes (in $cm^{-2} \cdot sec^{-1}$) for the theoretical models for phases SK-I to IV as well as for the combined analysis. Here the upper limits are given for $E_\nu > 17.3$ MeV. For the Kresse + 21 models, the "High," "Fid," and "Low" predictions correspond to the "W20-BH2.7-α2.0," "W18-BH2.7-α2.0," and "W18-BH2.7-α2.0-He33" models from Ref. [12], respectively.

	Best-fit		90% CL limit					
Model	SK4	All	SK1	SK2	SK3	SK4	All	Pred.
Totani + 95 Constant	$2.5^{+1.4}_{-1.3}$	$1.3^{+0.9}_{-0.9}$	2.3	6.3	7.0	4.5	2.6	4.67
Kaplinghat + 00 HMA (max)	$2.6^{+1.5}_{-1.3}$	$1.3^{+0.9}_{-0.9}$	2.3	6.7	7.1	4.7	2.6	3.00
Horiuchi + 09 6 MeV, max	$2.6^{+1.4}_{-1.3}$	$1.3^{+0.9}_{-0.9}$	2.4	6.0	7.0	4.6	2.6	1.94
Ando + 03 (updated 05)	$2.7^{+1.5}_{-1.4}$	$1.4^{+0.9}_{-0.9}$	2.3	6.6	7.2	4.7	2.7	1.74
Kresse + 21 (High, NO)	$2.7^{+1.5}_{-1.3}$	$1.4^{+0.9}_{-0.9}$	2.3	6.7	7.2	4.7	2.7	1.57
Galais + 09 (NO)	$2.5^{+1.4}_{-1.3}$	$1.3^{+0.9}_{-0.9}$	2.3	6.3	7.0	4.5	2.6	1.56
Galais + 09 (IO)	$2.6^{+1.4}_{-1.3}$	$1.3^{+0.9}_{-0.9}$	2.3	6.4	7.0	4.5	2.6	1.50
Horiuchi + 18 $\xi_{2.5} = 0.1$	$2.6^{+1.4}_{-1.3}$	$1.4^{+0.9}_{-0.9}$	2.4	6.1	7.1	4.6	2.7	1.23
Kresse + 21 (High, IO)	$2.7^{+1.5}_{-1.3}$	$1.4^{+0.9}_{-0.9}$	2.3	6.7	7.1	4.7	2.7	1.21
Kresse + 21 (Fid, NO)	$2.7^{+1.5}_{-1.3}$	$1.4^{+0.9}_{-0.9}$	2.3	6.8	7.2	4.7	2.7	1.20
Kresse + 21 (Fid, IO)	$2.7^{+1.5}_{-1.3}$	$1.4^{+0.9}_{-0.9}$	2.3	6.8	7.2	4.7	2.7	1.02
Kresse + 21 (Low, NO)	$2.7^{+1.5}_{-1.4}$	$1.4^{+0.9}_{-0.9}$	2.3	6.8	7.2	4.8	2.7	0.96
Tabrizi + 21 (NO)	$2.7^{+1.5}_{-1.3}$	$1.4^{+0.9}_{-0.9}$	2.4	6.6	7.1	4.7	2.7	0.92
Kresse + 21 (Low, IO)	$2.7^{+1.5}_{-1.4}$	$1.4^{+0.9}_{-0.9}$	2.3	6.8	7.2	4.8	2.7	0.84
Lunardini09 Failed SN	$2.8^{+1.5}_{-1.4}$	$1.4^{+0.9}_{-0.9}$	2.4	6.8	7.3	4.8	2.8	0.73
Hartmann + 97 CE	$2.6^{+1.4}_{-1.3}$	$1.3^{+0.9}_{-0.9}$	2.3	6.5	7.1	4.6	2.6	0.63
Nakazato + 15 (max, IO)	$2.7^{+1.5}_{-1.4}$	$1.4^{+1.0}_{-0.9}$	2.4	6.5	7.2	4.8	2.7	0.53
Horiuchi + 18 $\xi_{2.5} = 0.5$	$2.7^{+1.5}_{-1.4}$	$1.3^{+0.9}_{-0.9}$	2.2	7.1	7.1	4.8	2.6	0.55
Horiuchi + 21	$2.1^{+1.3}_{-1.2}$	$1.2^{+0.9}_{-0.9}$	3.4	4.3	5.9	3.9	2.5	0.28
Malaney97 CGI	$2.7^{+1.5}_{-1.3}$	$1.3^{+0.9}_{-0.9}$	2.3	6.8	7.1	4.7	2.6	0.26
Nakazato + 15 (min, NO)	$2.8^{+1.5}_{-1.4}$	$1.4^{+1.0}_{-0.9}$	2.3	6.8	7.2	4.8	2.7	0.19

Successors to Super-K

J. Beacom and M. Vagins, Phys. Rev. Lett. 93, 171101 (2004)
K. Abe et al. (Hyper-Kamiokande Proto-Collaboration), arXiv:1109.3262

H: ~0.3 barn, a 2.2 MeV γ-ray
Gd: ~50 kbarn, ~8 MeV γ-rays

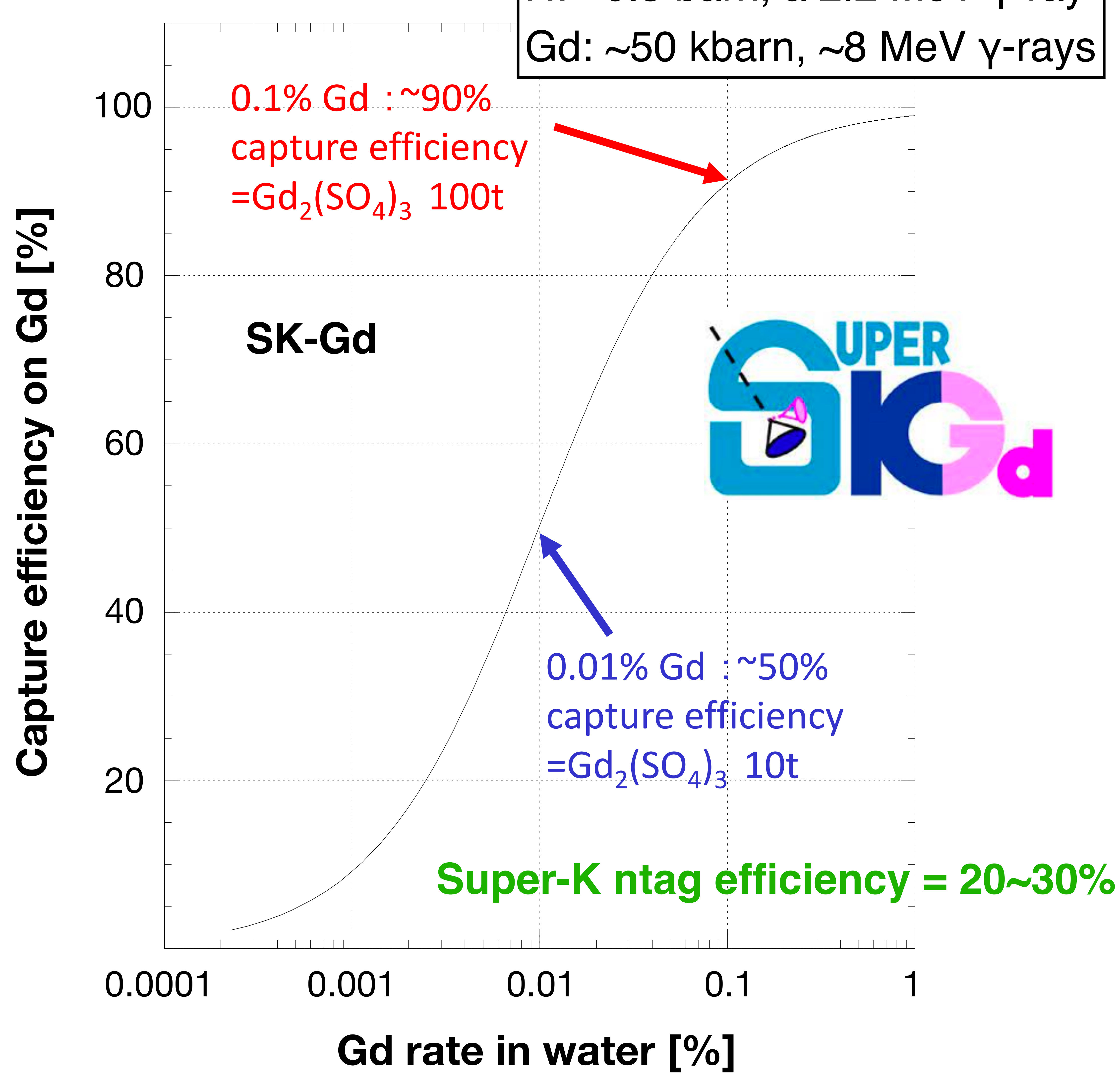

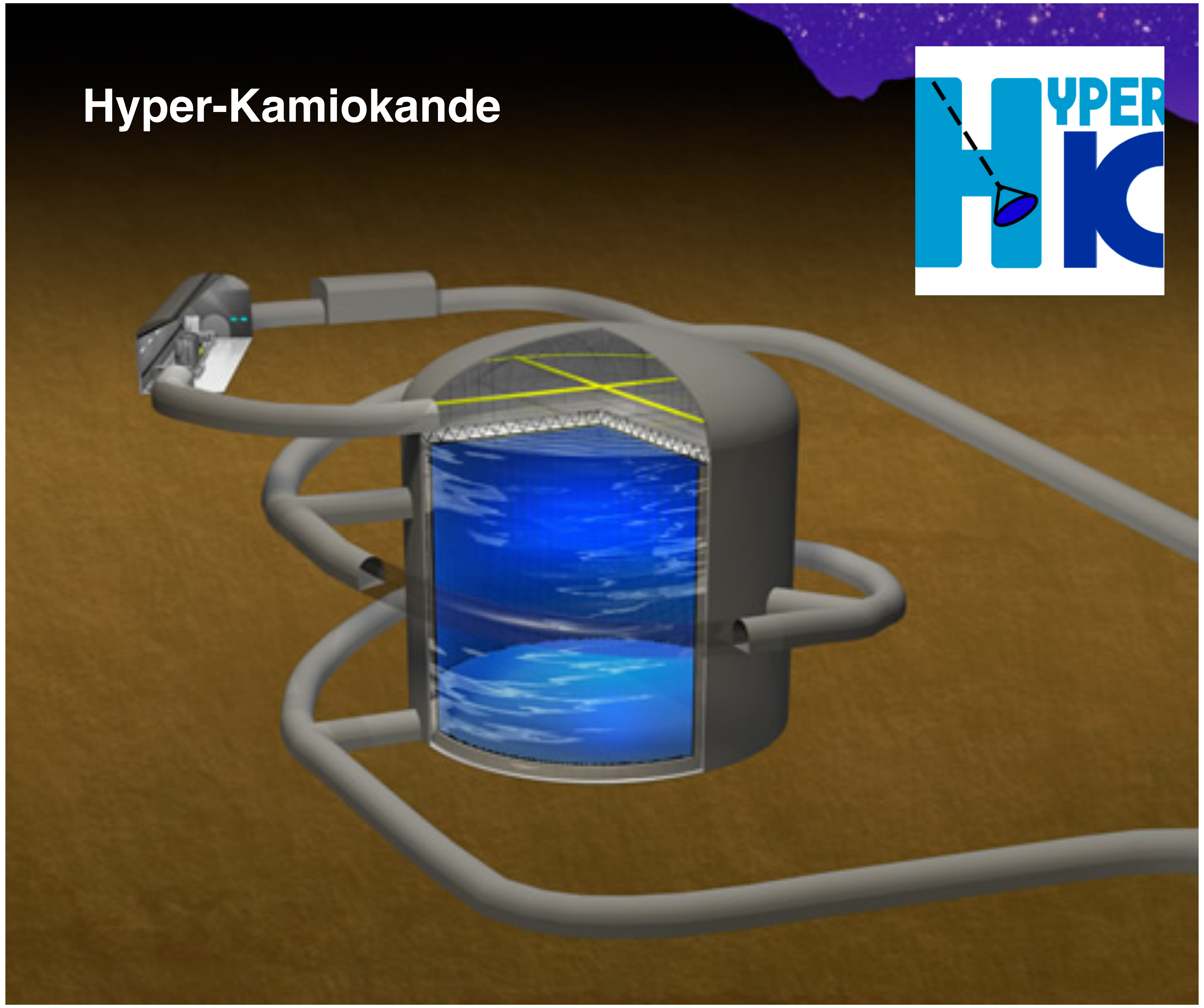

Detector mass: ~8.4 times larger than Super-K
Better PMTs: potentially higher ntag efficiency